Nematode assemblages in a nature reserve with historical pollution

Wim Bert[1]**, Joeri Manhout**[1,2]**, Carl Van Colen**[3]**, Gaetan Borgonie**[1] **& Wilfrida Decraemer**[1,2]

[1] **Department of Biology, Ghent University, K.L. Ledeganckstraat 35, B-9000, Ghent, Belgium**
[2] **Department of Recent Invertebrates, Royal Belgian Institute of Natural Sciences (RBINSc), Vautierstraat 29, B-1000 Brussels, Belgium**
[3] **Ghent University, Department of Biology, Marine Biology Section, Krijgslaan 281/S8, B-9000 Ghent, Belgium**

Corresponding author : email: wim.bert@UGent.be, Tel: ++32(0)92645223, Fax: ++32(0)9265344

ABSTRACT. Nematodes, and especially nematode communities, have significant potential as bio-indicators. The present study aimed to assess the nematode community structure of several sites with different historical pollution. Long-term polluted municipal waste-, tar- and sludge- sites were compared with less disturbed annex sites. At each site heavy metal and PAHs concentrations were measured together with soil texture classes, pH and total organic matter. Identification of three hundred nematodes at each location resulted in the discrimination of 63 genera from 32 different families of which the Cephalobidae, Belonolaimidae, Tylenchidae, Hoplolaimidae, Belonolaimidae and Plectidae were the most abundant families. The sampling sites harbour significantly different nematode communities and significant differences of life-strategy-related parameters (cp-groups, MI indexes) were observed. The significant augmentation of the proportion of the cp 2 nematodes in historically-polluted sites was especially informative. Omitting the cp 1 group from the MI (=MI2-5) better reflects putative historical pollution-induced community changes. However, the current study did not reveal significant relationships between historical pollution and the feeding type composition, or the Shannon-Wiener diversity. The observed results are critically assessed in the light of possible flaws such as sampling and analyzing limitations.

KEY WORDS : bio-indicator, diversity, heavy metals, life strategy, MI, pollution, feeding types

INTRODUCTION

Nematodes, and especially nematode communities, have significant potential as bio-indicators (BONGERS, 1990; RITZ & TRUDGILL, 1999; NEHER, 2001), which makes information on these communities especially useful for soil characterization and assessment of soil conditions. Generally, nematodes are among the most abundant multicellular organisms and often occur in large numbers even at heavily polluted sites. Their life cycle varies from a few days to years making them very sensitive to short term as well as long-term environmental changes. Furthermore, they are represented in nearly all trophic and functional groups in soil food webs (NEHER, 2001). The short and long-term effects of pollution and disturbances in different habitats have been studied on many occasions (WEISS & LARINK, 1991; WASILEWSKA, 1996; HOHBERG, 2003). In all of these studies the nematode communities underwent significant changes in relation to disturbances. In general, species diversity declined due to stress factors while the dominance of r-strategists increased, and the larger and longer living K-strategists were usually eliminated from the soil ecosystem (BONGERS, 1990). Changes in nematode communities, therefore, can be used to assess disturbances of the soil ecosystem including organic pollution and heavy metal pollution.

More specific studies that included long term effects of heavy metals on nematode assemblages were reported by NAGY, 1999; NAGY et al., 2004; GEORGIEVA et al., 2002; YEATES et al., 2003; BAKONYI et al., 2003; in particular, the analysis of the c-p group composition turned out to be a valuable tool to detect heavy metal pollution. Some studies of the effect of low-level pollution on soil invertebrates (ERSTFELD & SNOW-ASHBROOK, 1999) and nematode communities (SNOW-ASHBROOK & ERSTFELD, 1998) investigated polycyclic aromatic hydrocarbon contamination (PAH). The effect of PAH contamination on soil food webs and ecological processes was further investigated by BLAKELY et al. (2002).

However, with the exception of some specific pollution elements, the relation of nematode assemblages to a wide range of historical pollutants resulting in chronic low-level contamination over long periods has received relatively little attention. The present study aimed to assess the community structure of several sites with different historical pollution, where the chemical concentrations were expected to exceed background concentrations, but without extreme pollution. More particularly, nematode community characteristics of long-term polluted locations were compared with less disturbed annex sites.

MATERIALS AND METHODS

The study area

The study sites are located in and around the nature reserve Bourgoyen-Ossemeersen near Ghent (Belgium). This reserve is located on an alluvial plain of the river Leie and was used as a dumping site for a variety of waste products up to the 1970s. Three easily accessible areas, characterized by different types of relatively mild industrial and municipal pollution, were sampled in November 2002. In addition to each polluted site, an annex site was sampled. The annex sites are not considered true reference sites since it is simply impossible to find two soils exactly the same with only a difference in degree of pollution.

(1) An old municipal waste site was subdivided into two zones: the municipal bush, a site with a vegetation of trees and bushes (*Fraxinus excelsior, Galium aparine, Sambucus nigra, Tilia cordata, Urtica dioica*) and another zone (municipal grass) with a dominance of grasses and weeds (*Arrhenatherum elatius, Cirsium arvense, Holcus lanatus, Medicago lupulina, Poa trivialis*). Additionally, a non-polluted site (municipal annex) at 20m separation, was chosen as an annex site with the following vegetation: *Anthtiscus sylvestris, Lolium perenne, Poa trivialis, Rumex acetosella, Trifolium pratense.*

(2) The second site investigated was an old tar dumping site (tar) with very dense vegetation. Its non-polluted annex site (tar annex) was 5m away, possessing a similar vegetation (*Alnus glutinosa, Arrhenatherum elatius, Fraxinus excelsior, Rumex acetosa, Urtica dioica*) and soil texture.

(3) The third sampled site, currently used as a pasture, is a sludge site (sludge) with sludge originating from the nearby river Leie. The annex site (sludge annex) is situated 20m away and has the same vegetation (*Alopecurus pratensis, Dactylis glomerata, Lolium perenne, Poa trivialis, Rumex acetosa*) and soil texture.

The exact composition of the dumped materials, the historical behaviour of the pollutants and possible treatments were unknown.

At each site bulk samples were taken in November 2002; each sample consisted of 15 cores (diameter 5cm, sampling depth 25cm) within a radius of 20cm. Five cores were manually mixed and used for nematode sampling and ten cores for chemical analysis. This procedure was replicated, to a total of three replicates. Total soil Pb, Cd, Cu, Zn, Hg, As, Cr(III) and Cr(VI) were determined after *aqua regia* digestion (VAN RANST et al., 1999). Analyses were subsequently performed, using Inductively Coupled Plasma Optical Emission Spectrometry (ICP-OES) (Varian Liberty Series II, Varian, Palo Alto, CA). Although reduction of Cr(VI) was as much as possibly avoided by preliminary sample treatment and an appropriate rapid analysis (VITO reference procedure soil inspection, 2006a), Cr(VI) was nevertheless excluded from further analysis. The metal concentrations (mg/kg) for each site are presented in Table 1. The sites were also examined for a variety of polycyclic aromatic hydrocarbons (PAHs) (Table 1). Extractable Organic halogens (EOX) and mineral oils were extracted by a soxhlet extraction (VITO, reference procedure soil inspection, 2006b). EOX was further analyzed by colourimetric titration (EUROGLAS BV, 1998; VITO reference procedure soil inspection, 2006c) and mineral oil was determined by capillary column gas chromatography (Varian CP-3800, Palo Alto, CA; VITO (2006b) reference procedure soil inspection: mineral oil). Accuracy, reproducibility and yield of the applied methods was confirmed with blanks and certified reference material of similar structure to the analysed samples (VITO reference procedure soil inspection, 2006d).

The organic matter content was also determined by loss of mass after ignition. To determine soil pH, 50ml of deionised water were added to 10g of air dried soil and allowed to stand for 24h. Acidity of the supernatant fluid was then measured using a pH electrode (Model 520A, Orion, Boston, MA, USA). Soil structure was analysed with a particle size analyzer (Beckman Coulter LS 100, Fullerton, CA,

USA) (BUCHANAN, 1984) and allocated to a texture class in a texture triangle (GERAKIS & BAER, 1999) (Table 1). Finally, the most abundant vegetation types were identified.

Sampling strategy and nematode analysis

The five "nematode" cores (196cm³) of each bulk sample were fixed with 204ml 4%-formaldehyde (60°C); nematodes were extracted from 100ml of this mixture by the centrifugal-flotation technique (CAVENESS & JENSEN, 1955); the sediment was centrifuged twice with Ludox HS-40 (DuPont Chemicals, Wilmington, USA) and kaolin for 5 minutes at 3500 rotations/minute and the supernatant was rinsed over a 38μm sieve. Nematodes were counted, 100 individuals were picked out randomly using a stereomicroscope (50X magnification). Formaldehyde (4% with 1% glycerol) was heated to 70°C and 4-5ml were quickly added to the specimens to fix and kill the nematodes in one process. The fixed nematodes were processed in anhydrous glycerol following the glycerol-ethanol method (SEINHORST, 1959) and mounted on aluminium slides with double coverslips.

The nematodes were identified to family and genus level and assigned to their feeding type (YEATES et al., 1993a). However, the feeding habits of the so-called "facultative plant parasites" or "plant associates" is unclear (OKADA & HARADA, 2007; BERT et al., 2008). Therefore, a distinction was made between "real" plant-parasitic species (endo- and ectoparasites) dependant on higher plants (=plant-parasites) and those tylenchs that feed on algae, lichens, mosses, epidermal cells or root hairs, apparently without causing damage, of which the exact feeding behaviour is unknown (="plant associated nematodes", see also YEATES et al., 1993b). Except for the plant-feeding nematodes all individuals were classified according to their colonizer-persister value (cp 1, cp 2, cp 3, cp 4, cp 5 and the combined group cp 3-5). The maturity indices MI and MI2-5 were calculated following BONGERS (1990) and KORTHALS et al. (1996).

Data analysis

Data were analyzed using a combination of multivariate and univariate methods. The correlation structure among the environmental variables was explored by means of Spearman rank correlations. Differences between groups of sites and within a group of sites (*i.e.* all polluted *vs.* all annex sites and the polluted *vs.* the annex site of one site type) of total densities, diversity, maturity indices, the relative abundance of feeding- and cp-groups were analyzed by a one-way ANOVA in SAS v. 9.1.3; this after square root and arcsine transformations for proportional data. Bartlett's and Cochran's tests were used to verify homogeneity of variances prior to the analysis.

Differences in nematode communities among groups of sites were analysed by permutational multivariate analyses of variance (PerMANOVA; ANDERSON, 2001) on square root transformed data, followed by pair-wise comparisons between groups of sites. Site was treated as a fixed factor and the Bray-Curtis dissimilarity measure was applied for all analyses. Each term in the analyses was calculated using 9999 permutations of the appropriate units. Since PerMANOVA is sensitive to differences in multivariate dispersion between groups, possibly increasing the Type I

error, the same model was tested for differences in multivariate dispersion (PERMDISP; ANDERSON, 2004). Furthermore, species indicative for each group of sites were identified by Indicator Species Analysis (INDVAL) (DUFRÊNE & LEGENDRE, 1997) and their statistical significance was tested by a Monte Carlo Test.

Multivariate patterns were visualised through non-metric Multi-Dimensional Scaling (MDS ordination) applying the Euclidean distance similarity measure (KRUSKAL, 1964) after normalisation of the environmental data and the Bray-Curtis dissimilarity measure on square root transformed nematode data. The correlation between the multivariate nematode and environmental pattern was examined using the BIOSTEP routine (CLARKE & GORLEY, 2001). Finally, in order to allow better visualization between sites and variables, the environmental parameters that best explain the nematode community pattern, indicative genera and certain community characteristics (feeding types groups, cp-groups, diversity, MI) were superimposed on MDS ordination diagrams as circles whose sizes reflect the magnitude of these variables. Multivariate analyses were performed using the PRIMER v5.0 software package (CLARKE & GORLEY, 2001).

RESULTS

The environmental variables

Detailed results of the analyzed soil parameters for each location are shown in Table 1. Comparison with quality standard values extracted from literature data (after correction for clay and organic matter content) give an indication of the severity of the analysed pollutants (Table 1). The municipal bush and municipal grass, the sludge and the tar were more polluted sites (for organic as well as heavy metal pollution) than their corresponding annex sites. However, as this study is of an observational type, a thorough inspection of the correlation structure among the explanatory variables is a prerequisite for understanding the observed relationships.

TABLE 1

Soil parameters (soiltype, pH, clay percentage, organic matter, total heavy metal concentrations and organic pollutants) in the sampled locations in the Bourgoyen-Ossemeersen. Values expressed as average and standard error.

		Municipal bush	Municipal grass	Municipal annex	Sludge	Sludge annex	Tar	Tar annex
Soil structure		sandy-clay-loam	sandy-clay-loam	clay	clay	clay	sandy-clay-loam	sandy-clay-loam
pH		7.3 (±0.1)	6.9 (±0.2)	6.4 (±0.4)	7.3 (±0.1)	6.4 (±0.1)	7.4 (±0.2)	6.6 (±0.3)
Clay	%	28.2	23.4	64.1	80.5	70.8	26.2	34.8
Organic matter	% C	4.9 (±2)	6.4 (±1.6)	5.9 (±2.3)	17.9 (±1.6)	7.4 (±0.2)	6.6 (±1.2)	6 (±2.3)
As	mg/kg	-	-	-	**110**[II] (±25)	-	-	-
Cd	mg/kg	-	1.6 (±0.9)	-	50 (±0.7)	-	2.0 (±1.1)	-
Cr^{3+}	mg/kg	17.6 (±7.1)	-	-	196 (±12)	22 (±8.3)	20.3 (±4.9)	27.6 (±7.7)
Cu	mg/kg	50 (±19)	44 (±18)	-	300 (±24)	57 (±14)	67 (±19)	-
Hg	mg/kg	-	-	-	4.7 (±0.3)	-	-	-
Pb	mg/kg	158 (±67)	203 (±84)	-	**759**[III] (±50)	**220**[I] (±74)	**346**[II] (±31)	-
Zn	mg/kg	171 (±68)	378 (±121)	138 (±59)	**1787**[IV] (±97)	221 (±24)	571 (±126)	115 (±42)
Naftalene	mg/kg	0.5 (±0.2)	-	0.4 (±0.1)	-	-	2.9 (±0.4)	-
Aceanftylene	mg/kg	-	-	-	-	-	-	-
Fluorine	mg/kg	-	-	-	-	-	-	-
Fenantrene	mg/kg	-	-	-	-	-	0.4 (±0.3)	-
Antracene	mg/kg	0.2 (±0.1)	-	-	0.3 (±0)	-	2.1 (±0.1)	0.1 (±0)
Fluorantene	mg/kg	0.1 (±0.1)	-	-	-	-	0.5 (±0.2)	-
Pyrene	mg/kg	-	-	-	1.2 (±0.4)	-	2.0 (±0.1)	-
benzo(a)antracene	mg/kg	-	-	-	1.0 (±0.4)	-	1.2 (±0.1)	-
Chrysene	mg/kg	-	-	-	0.9 (±0.6)	-	0.8 (±0.2)	-
benzo(b)fluorantene	mg/kg	-	-	-	1.3 (±0.9)	-	1.1 (±0.1)	-
benzo(k)fluorantene	mg/kg	-	-	-	2.0 (±0.2)	-	1.5 (±0.1)	-
benzo(a)pyrene	mg/kg	-	-	-	0.5 (±0.2)	-	0.5 (±0.1)	-
indeno(1.2.3-cd)pyrene	mg/kg	-	-	-	0.6 (±0.4)	-	0.6 (±0.1)	-
dibenzo(a.h)antracene	mg/kg	-	-	-	0.8 (±0.2)	-	0.7 (±0)	-
benzo(ghi)perylene	mg/kg	-	-	-	0.3 (±0.4)	-	0.2 (±0.1)	-

-: below detection level; **Bold:** exceeding legislated clean-up values, Latin numbers reflect increasing exceeding of norm values (from stringent to less stringent: [I]nature and forest area; [II]: rural area; [III]: residential area; [IV]: recreation area, [V]: industrial area). Values are corrected for clay and organic matter and compared according to VLAREBO (the Flemisch environmental legislation concerning soil cleanup) as described in VAN GEHUCHTE et al. (1997).

Several environmental data appeared highly correlated. Nearly all metal concentrations of Cd, Pb, Cu, Hg and Zn were significantly positively correlated with each other and with carbon content. Cr(III) and As formed a second group of significantly positively correlated metal concentrations. Evidently, nearly all analyzed PAK's were significantly positively correlated with each other and total PAK.

Ordination of the environmental variables by an MDS analysis (stress: 0.10) did show a clear separation between replicated annex and polluted sites for Tar and Sludge. The municipal sites did not form a unequivocal pattern (Fig. 1).
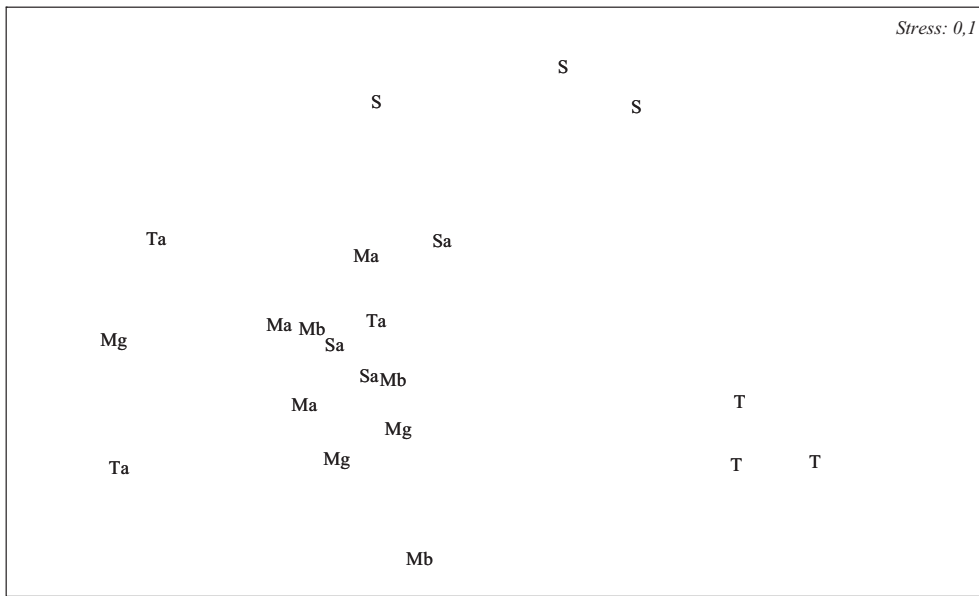
Fig. 1. – Output of non-metric Multi Dimensional Scaling (MDS) on fourth root transformed normalization of the environmental data from seven sampled sites (three replicates) in the Bourgoyen-Ossemeersen (Ghent, Belgium). (Mb): Municipal bush, (Mg): Municipal grass, (Ma): Municipal annex, (S): Sludge, (Sa): Sludge annex, (T): Tar, (Ta): Tar annex.
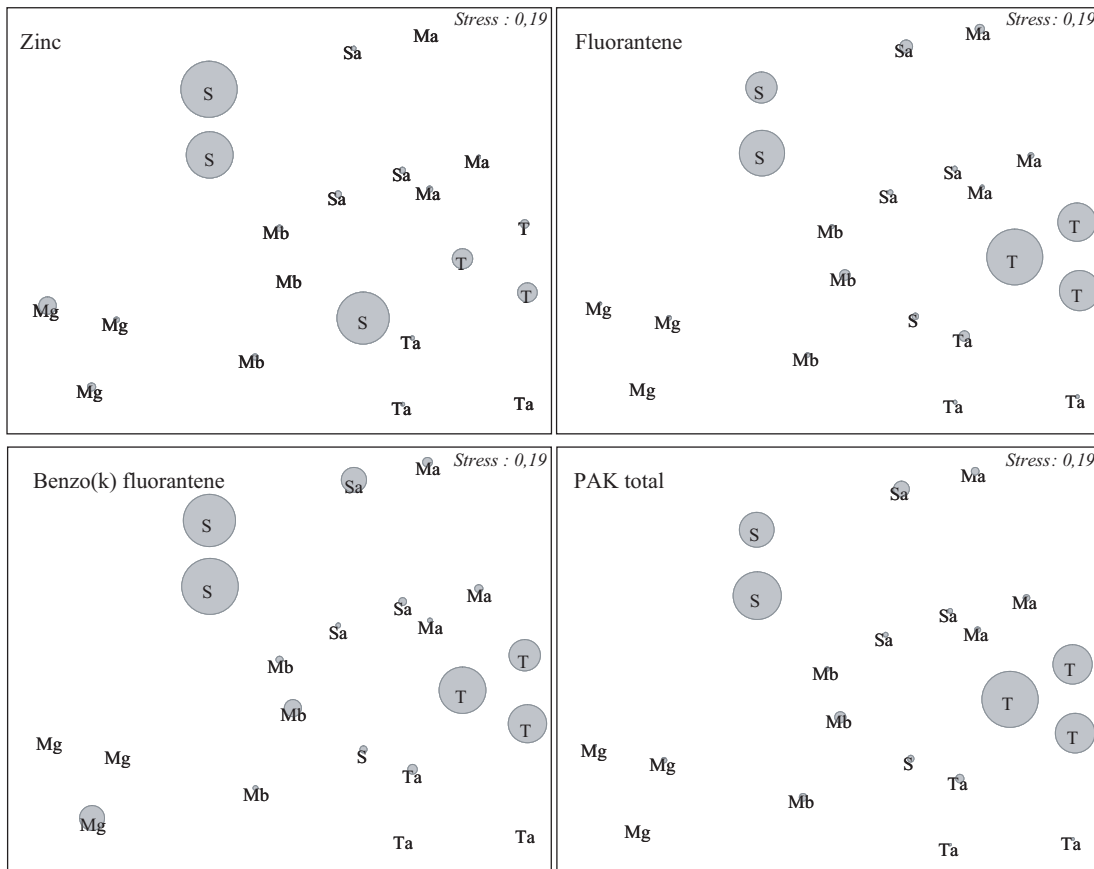
Fig. 2. – Most discriminative environmental parameters superimposed on Non-metric Multi Dimensional Scaling (MDS) biological ordination diagrams. Sizes of shaded circles reflect the relative magnitude of the superimposed variables. MDS output based on square-root-transformed genus abundances from seven sampled sites (three replicates) in the Bourgoyen-Ossemeersen (Ghent, Belgium). (Mb): Municipal bush, (Mg): Municipal grass, (Ma): Municipal annex, (S): Sludge, (Sa): Sludge annex, (T): Tar, (Ta): Tar annex.

Nematode communities and relation with the environment

Sixty-three genera from 32 different families were identified in this study (Table 2). The Cephalobidae, Belonolaimidae, Tylenchidae, Hoplolaimidae, Belonolaimidae and Plectidae were the most abundant families.

TABLE 2

An overview of the identified nematode genera families and genera ordered by feeding type in the sampled locations in the Bourgoyen-Ossemeersen (Ghent, Belgium)

Bacteriovores		Fungal-feeders	Omnivores	Predators	"plant associated nematodes"	Plant-parasites
Alaimidae	Monhysteridae	Aphelenchoididae	Dorylaimidae	Aporcelaimidae	Tylenchidae	Belonolaimidae
Alaimus	*Eumonhystera*	*Aphelenchoides*	*Laimydorus*	*Aporcelaimellus*	*Aglenchus*	*Geocenamus*
Amphidelus	*Monhystera*	Aphelenchidae	Nordiidae	Mononchidae	*Basiria*	*Tylenchorhynchus*
Bunonematidae	*Monhystrella*	*Aphelenchus*	*Longidorella*	*Clarkus*	*Coslenchus*	Criconematidae
Bunonema	Panagrolaimidae	Diphtherophoridae	*Thornia*	*Mononchus*	*Filenchus*	*Mesocriconema*
Bastianiidae	*Panagrolaimus*	*Diphtherophora*	Qudsianematidae	*Mylonchulus*	*Tylenchus*	*Criconema*
Bastiania	Plectidae	Tylencholaimidae	*Epidorylaimus*	*Prionchulus*		*Crossonema*
Cephalobidae	*Anaplectus*	*Tylencholaimellus*	*Eudorylaimus*	Qudsianematidae		Hoplolaimidae
Acrobeles	*Plectus*		*Microdorylaimus*	*Labronema*		*Helicotylenchus*
Acrobeloides	*Wilsonema*		*Prodorylaimus*	*Thonus*		*Rotylenchus*
Cephalobus	Prismatolaimidae		Thornenematidae	Nygolaimidae		Nordiidae
Cervidellus	*Prismatolaimus*		*Mesodorylaimus*	*Nygolaimus*		*Pungentus*
Chiloplacus	Rhabditidae		*Opisthodorylaimus*	Tripylidae		Pratylenchidae
Eucephalobus	*Mesorhabditis*			*Paratrypila*		*Pratylenchus*
Heterocephalobus	Rhabdolaimidae			*Tripyla*		Trichodoridae
Desmodoridae	*Rhabdolaimus*					*Trichodorus*
Prodesmodora	Teratocephalidae					
Diplopeltidae	*Teratocephalus*					
Cylindrolaimus	Tylopharyngidae					
	Tylopharynx					

TABLE 3

One-way permutational analyis of variance (Permanova) and one-way permutational test of mulivariate dispersion (Permdisp) based on Bray-Curtis square root transformed nematode community data

Source	df	Permanova				Permdisp			
		SS	MS	F	P	SS	MS	F	p
Site	6	16064.0	2677.3	3.16	0.0001	726.2	121.0	1.90	0.1564
Residual	14	11876.3	848.3			891.6	63.7		
Total	20	27940.4				1617.8			

Initial examination by an MDS analysis (stress: 0.19) did show six, not clear cut, groups representing the sampling sites, except for the sludge replicates, which are not grouped (Figs 2-5). However, the MDS plot did not show a clear pattern related to pollution, *i.e.* polluted and non-polluted or annex samples are irregularly grouped on the plot. Nevertheless, a permutational multivariate analyses of variance (PermANOVA) could demonstrate that the sampling sites harbour significantly different nematode communities. Multivariate dispersions did not differ significantly for the factor Site (Table 3), which indicates that the significant site effect, revealed by the PerMANOVA, is not due to artefacts as a result of variable dispersions. However, *a posteriori* pairwise comparisons showed that the nematode communities from Sludge and Sludge annex were not significantly different from all the other sites. Sludge annex harboured only a significantly different community as compared to the Tar site, while differences between the communities of the Sludge site and other sampling sites could not be considered significant – most likely because of the considerable community composition differences between the replicates. Indicative species for the seven sampling localities are shown in Table 4 and Fig. 3. Only the species of *Bastiana* and *Ogma* were significantly indicative (Monto Carlo permutation test) for the Municipal bush site and the Tar-annex site respectively. Matching the pattern found in environmental characteristics with that found in nematode communities (BIOSTEP) revealed a relatively small Spearman rank correlation coefficient for any combination of pollutants ($\rho=0.433$). Maximal matching between nematode assemblages and pollutants was explained by Zinc, benzo(k)fluoranteen and PAK total. A combination of Zinc, benzo(k)fluoranteen and fluoranteen resulted in a slightly lower correlation coefficient ($\rho=0.430$).

TABLE 4

Total nematode abundance, genus abundance, indicative genera, Shannon-Wiener index (H'), Maturity Indices, relative abundance of feeding types and cp-groups in the sampled locations in the Bourgoyen-Ossemeersen (Ghent, Belgium). Results ± standard deviation and with indication of significance differences (one-way ANOVA; *=p<0.05; dotted line: significant differences between all polluted and all annex sites; underlined and ↔: significant differences between the polluted and annex site of a single site)

	Municipal bush	Municipal grass	Municipal annex	Sludge	Sludge annex	Tar	Tar annex
Abundance(±SD)							
per 50cm³ soil	3920 (±53)	3297 (±62)	3980 (±333)	2971 (±241)	3008 (±171)	3289 (±81)	3701 (±268)
# Genera (±SD)	18 (±3)	18 (±2)	21 (±2)	17 (±2)	20 (±5)	23 (±5)	25 (±2)
Diversity (H')	2.63 (±0.16)	2.54 (±0.12)	2.74 (±0.01)	2.51 (±0.17)	2.87 (±0.32)	2.89 (±0.14)	2.98 (±0.13)
Top 3 density	*Prismatolaimus*	*Plectus*	*Filenchus*	*Helicotylenchus*	*Mesodorylai-mus*	*Filenchus*	*Ogma*
	Mesocriconema	*Mesocriconema*	*Helicotylen-chus*	*Eucephalobus*	*Rotylenchus*	*Helicotylen-chus*	*Eudorylaimus*
	Eumonhystera	*Tylenchorhynchus*	*Mesocri-conema*	*Tylenchorhyn-chus*	*Mesocri-conema*	*Alaimus*	*Eumonhystera*
Indicative genera (and indicator value)	*Bastiana** (41)	*Teratocephalus* (78)		*Eucephalobus* (25)	*Mesodorylai-mus* (33)		*Ogma** (66)
	Prismatolaimus (28)	*Wilsonema* (75)					
MI	2.79 (±0.11)	**2.58 (±0.25)*** ↔	3.22 (±0.37)*	2.68 (±0.06)	3.24 (±0.46)	2.86 (±0.14)	2.84 (±0.23)
MI (2-5)	2.81 (±0.15)	**2.64 (±0.27)*** ↔	3.25 (±0.38)*	**2.71 (±0.03)*** ↔	3.43 (±0.17)*	2.94 (±0.14)	3.02 (±0.14)
Trophic groups %							
Bacteriovores	46.7 (±13.6)	52.8 (±16.8)	20.2 (±7.4)	30.9 (±15.7)	31.7 (±6.0)	36.2 (±4.6)	43.6 (±4.6)
fungal-feeders	1.0 (±1.7)	6.6 (±2.1)	1.9 (±2.5)	0.6 (±1.1)	15.9 (±1.6)	3.7 (±2.5)	1.7 (±2.1)
"plant associates"	4 (±1.7)	0 (±0)	29.5 (±8.3)	9.8 (±6.8)	8.2 (±0.4)	29.2 (±2.7)	11.6 (±2.3)
plant-parasites	35.7 (±16)	25.7 (±12.6)	29 (±4.8)	45.7 (±18.4)	24.5 (±12.1)	21.5 (±6.1)	28.7 (±2.6)
Omnivores	9.6 (±4.5)	6.2 (±1.6)	12.7 (±12.3)	10.3 (±2.8)	20.6 (±11.4)	9.1 (±1.0)	11.2 (±4.1)
Predators	3.0 (±1.0)	8.7 (±6.5)	6.7 (±4.6)	2.7 (±1.6)	9.1 (±8.5)	0.3 (±0.6)	3.3 (±4.1)
Cp-groups %							
cp-1	1.3 (±2.3)	3.2 (±1.8)	1.0 (±1.8)	1.4 (±2.4)	8.4 (±14.7)	4.0 (±0.22)	9.1 (±5.6)
cp-2	44.4 (±8.3)*	56.4 (±9.2)*	27.2 (±11.7)*	60.4 (±5.7)* ↔	25.0 (±4.5)*	42.2 (±6.2)* ↔	29.1 (±4.2)*
cp-3	33.2 (±10.5)	19.4 (±4.8)	29.5 (±2.6)	9.3 (±9.02)	17.8 (±6.02)	22.6 (±2.0)	31.9 (±14.5)
cp-4	16.4 (±4.3)	20.5 (±12.0)	32.9 (±20.5)	26.4 (±1.6)	31.7 (±8.1)	25.8 (±4.8)	28.3 (±5.3)
cp-5	4.7 (±1.9)	0.38 (±0.7)	9.4 (±5.91)	2.5 (±1.16)	17.0 (±7.55)	5.3 (±0.91)	1.5 (±1.3)
cp-(3-5)	54.2 (±8.2)*	40.3 (±7.4)* ↔	71.8 (±13.4)*	38.2(±6.7)* ↔	66.5 (±10.4)*	53.8 (±7.4)*	61.7 (±13.8)*

Nematode abundance & diversity

The average nematode density ranged from 2971ind./100cm³ (sludge site) to 3980 ind./100cm³ (municipal annex site), with no significant differences between the sites (Table 4). Disturbed sites were generally less diverse compared to the annex sites, but this difference could not be considered significant (p>0.05). The highest average total number of genera (25) and average value of the Shannon-Wiener diversity index (2.98) was recorded from the tar annex site. Sludge was characterized by lowest total average number of genera (17) and the lowest (2.51) Shannon-Wiener diversity index. (Table 4; Fig. 4).

Feeding types, "colonizer-persister"-groups and MI

Generally, numbers of bacteriovores and plant-parasites are more than twice the numbers of predators, omnivores, fungal-feeders, and "plant associated nematodes" (=amalgam of tylenchid nematodes that feed on algae, lichens, mosses, epidermal cells or root hairs but of which the exact feeding behaviour is largely unknown). The dis-turbed sites contained relatively fewer omnivores and predators as compared to the annex sites, however, differences were not significant (Table 4 and Fig. 5). There was also no significant correlation found between any pollutant and the composition of feeding types. Table 4 and Fig. 4 show the relative distribution of the different cp-groups. The disturbed sites contained significantly more colonizers of type cp 2 (p=0.0003) and less persisters (cp 3-5) (p=0.0022) compared to their annex site. Also a direct contrast of individual polluted sites in relation to their respective annex sites with respect to the distribution of the cp groups showed significant differences; sludge (p=0.006) and tar (p=0.049) had significantly more cp 2 colonizers, while municipal grass (0.049) and sludge (0.023) had significantly fewer cp 3-5 persisters. Furthermore, the cp 2/cp 3-5 nematodes were significantly positively/negatively correlated with both groups of intercorrelated metal correlations and PAK's content (r-values and p-values of individual correlations are not given because of the high intercorrelated structure of pollutants related to pollution).
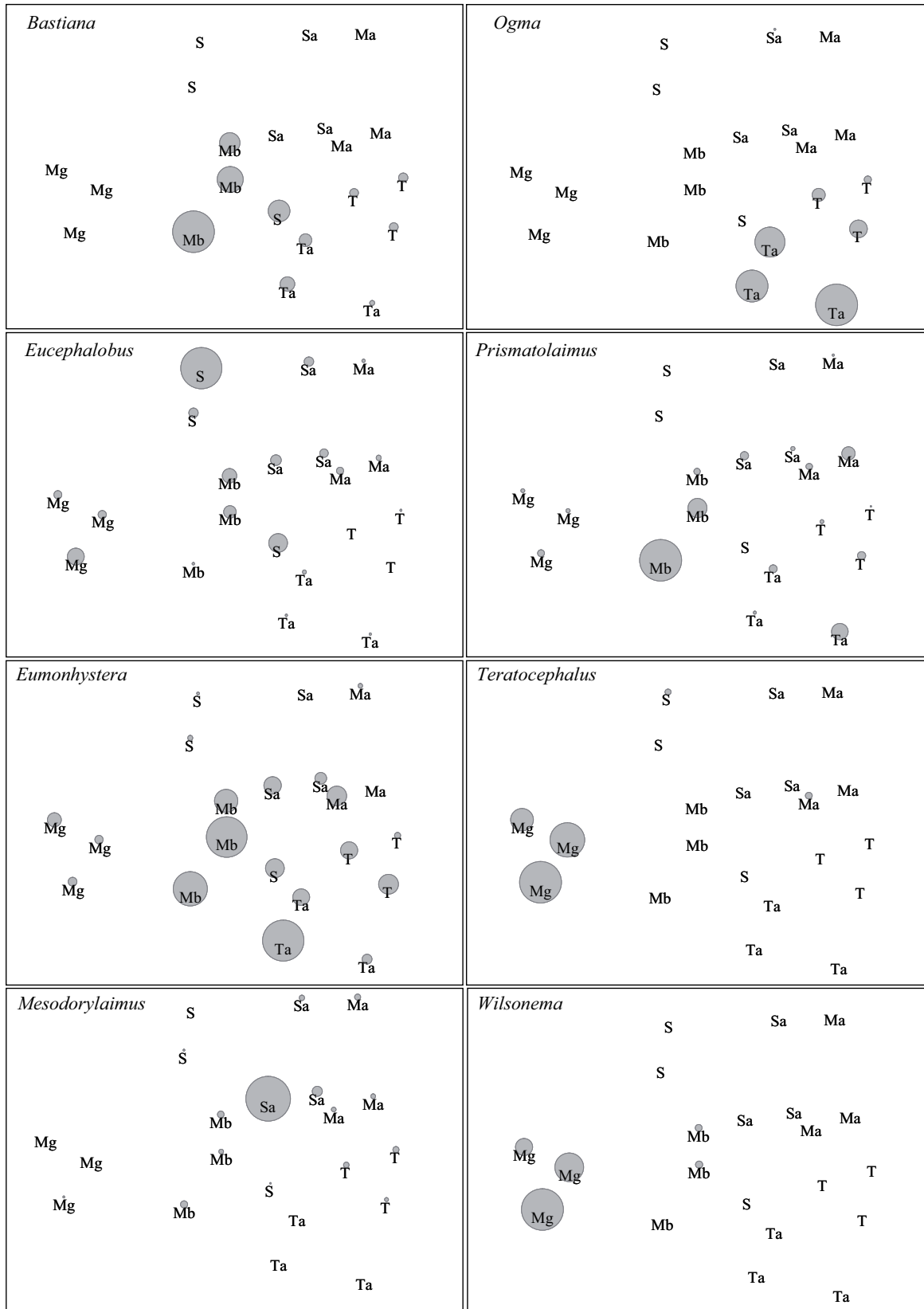
Fig. 3. – Indicative species for the seven sampling localities superimposed on Non-metric Multi Dimensional Scaling (MDS) ordination diagrams. Sizes of shaded circles reflect the relative magnitude of the superimposed variables. MDS output based on square-root-transformed genus abundances from seven sampled sites (three replicates) in the Bourgoyen-Ossemeersen (Ghent, Belgium). (Mb): Municipal bush, (Mg): Municipal grass, (Ma): Municipal annex, (S): Sludge, (Sa): Sludge annex, (T): Tar, (Ta): Tar annex.
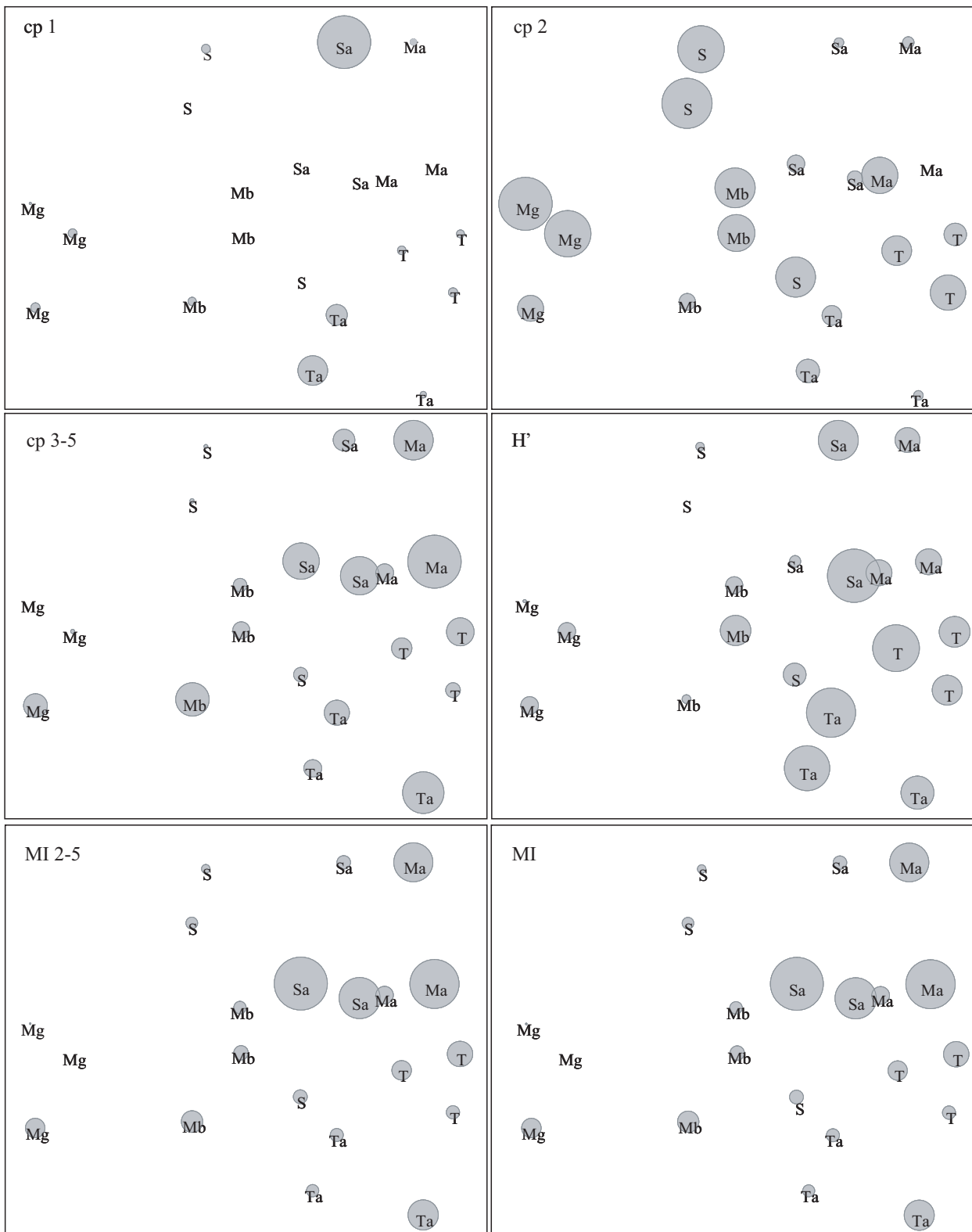
Fig. 4. – Nematode community characteristics ("colonizer-persister"-groups: cp 1, cp 2 and cp3-5; Shannon-Wiener diversity: h'; Maturity Indexes: MI, MI2-5) superimposed on Non-metric Multi Dimensional Scaling (MDS) ordination diagrams. Sizes of shaded circles reflect the relative magnitude of the superimposed variables. MDS output based on square-root-transformed genus abundances from seven sampled sites (three replicates) in the Bourgoyen-Ossemeersen (Ghent, Belgium). (Mb): Municipal bush, (Mg): Municipal grass, (Ma): Municipal annex, (S): Sludge, (Sa): Sludge annex, (T): Tar, (Ta): Tar annex.
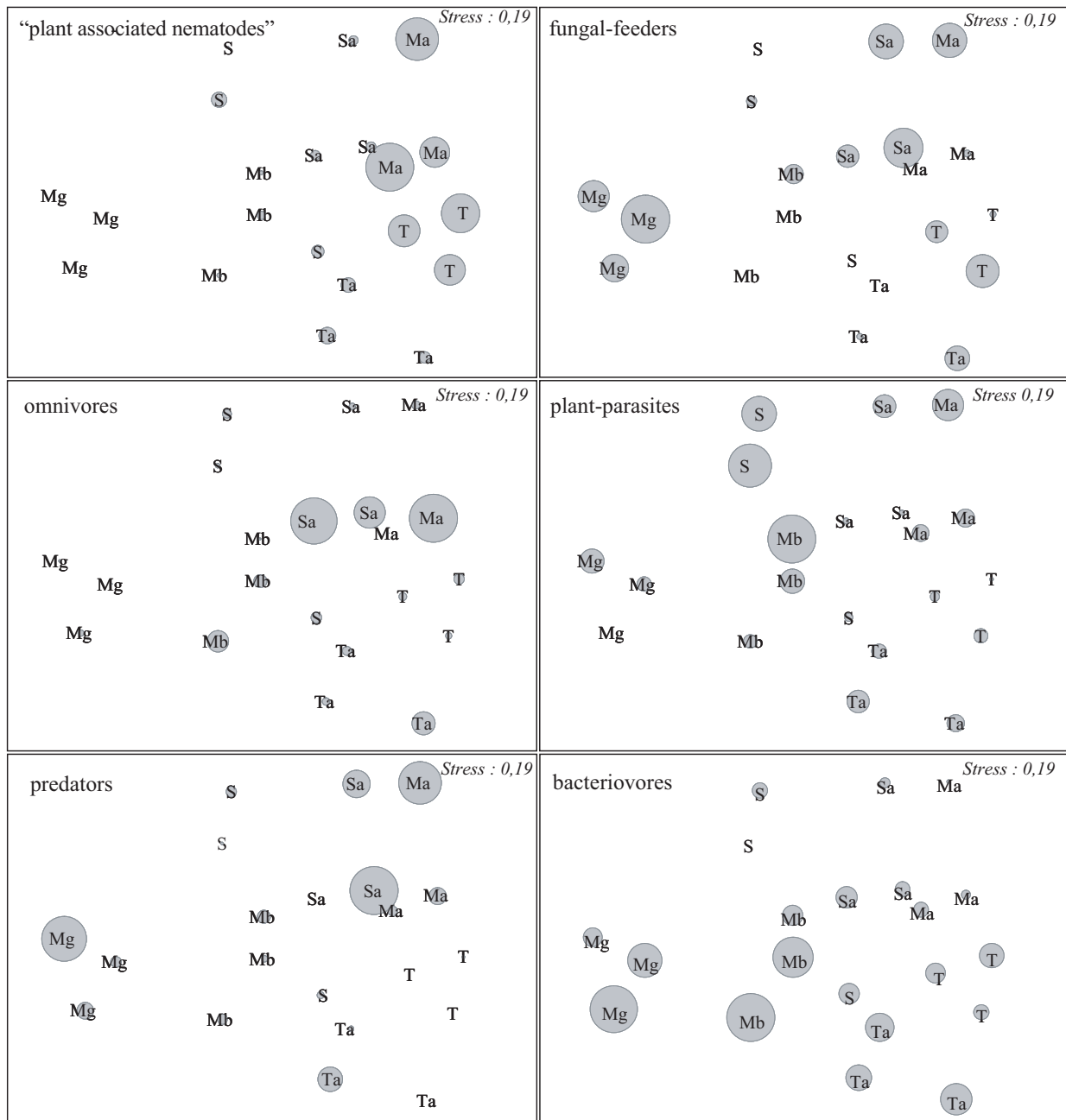
Fig. 5. – Feeding types (bacteriovores, plant-parasites, predators, omnivores, fungal-feeders, and "plant associated nematodes") superimposed on Non-metric Multi Dimensional Scaling (MDS) ordination diagrams. Sizes of shaded circles reflect the relative magnitude of the superimposed variables. MDS output based on square-root-transformed genus abundances from seven sampled sites (three replicates) in the Bourgoyen-Ossemeersen (Ghent, Belgium). (Mb): Municipal bush, (Mg): Municipal grass, (Ma): Municipal annex, (S): Sludge, (Sa): Sludge annex, (T): Tar, (Ta): Tar annex.

The average maturity indices (MI/MI2-5) respectively ranged from 2.79/2.81 (Municipal bush) to 3.24/3.43 (Sludge annex) (Table 4; Fig. 4). The total average MI/ MI2-5 were higher for the annex sites (3.10/3.24) compared with the polluted sites (2.74/2.79). However, only the MI/ MI2-5 of the municipal grass were significantly higher compared to their respective annex site (p=0.003/ 0.004); while for the sludge site differences in life strategy could only be significantly (p=0.0007) appointed with the MI2-5 index. Thus, differences related to historical pollution were slightly more pronounced for the MI2-5 values compared to the original MI (absolute differences as well as significance levels).

DISCUSSION

Genera: analyses and diversity

The total number of genera (63) found in this study is high for the latitude 50°-60° where the mean number of species is only 58 (BOAG & YEATES, 1998). In comparison, only 141 genera were recorded from 200 different locations in the Netherlands that were selected to cover the maximal habitat diversity (MULDER et al., 2005). Furthermore, in another period of the year, Manhout et al. (unpublished results) recovered a further 50 genera in our study area that were not recovered in this study. This further points to the remarkably high nematode diversity in the examined alluvial plain. In disparity to the known adverse effect of several heavy metals on nematode diversity (e.g. GEORGIEVA et al., 2002; YEATES et al., 2003), no relationship between pollution and decreasing nematode diversity could be discerned. Possibly, the historical nature of the pollution and time elapsed could have allowed a build-up of the nematofauna to a high diversity. On the other hand, several studies have shown that other, more recent, disturbances did not have a significant effect on nematode diversity (e.g.: urbanization: PAVAO-ZUCKERMAN & COLEMAN, 2007; agricultural management practices: PORAZINSKA et al., 1999). Furthermore, the underlying assumption that larger, more diverse assemblages reflect "more healthy" soils and are thus "desirable" is still under debate (YEATES, 2003). Especially there is no unambiguous evidence to support the view that diversity or complexity predictably affect the stability of ecosystem properties or processes (CRAGG & BARDGETT, 2001).

"Colonizer-persister"-groups and MI

Like other organisms, soil nematodes can be ranked along a gradient referring to their reproductive strategies, from larger (persistent) K-strategists adapted to stable environments because of their long life cycles, towards colonizing r-strategists that respond quickly to favourable conditions (BONGERS, 1990; BONGERS & FERRIS, 1999; FERRIS et al., 2001).

This study did not show any relation of enrichment opportunists (cp 1) and historical pollution. The cp 1 group consists of bacteriovores that grow rapidly upon an increase in microbial activity caused by an organic input either biological or anthropogenic (WASILEWSKA & BIENKOWSKI, 1985; FERRIS et al., 1996; YEATES et al., 1997). The cp 1 group can thus show very different sensitivities and reactions to disturbances and therefore are of limited use as bioindicators (GEORGIEVA et al., 2002).

Conversely, the contribution of colonizers of type cp 2 and persisters (cp 3-5) was significantly different between the polluted sites and their annex site. Regarding comparisons of individual sites, the significant augmentation of cp 2 nematodes in the tar samples is especially informative. This because explorative analyses of the environmental variables (irregular scattering of environmental variables of the municipal sites) and the communities (sludge community not significantly different from other sites) reveals that the insight in the relation of the nematode community and pollution within a single site can be best explored for the tar samples. A higher abundance of general opportunists (cp 2) is an indication of pollution-induced stress (KORTHALS, 1997; BONGERS & FERRIS, 1999). Especially the Cephalobidae are known to increase in proportion as a result of resource limitation such as heavy metal addition (YEATES, 2003). Conversely, omnivores and predators (mostly K-strategist mononchs and dorylaims from the cp 3-5 groups) are well known to be negatively related to pollution or disturbance. Their abundance is negatively affected by heavy metals, especially Pb, Zn and Cu (BARDGETT et al., 1994; YEATES et al., 1994; BAKONYI et al., 2003; GEORGIEVA et al., 2002; NAGY et al., 2004) or by a mixture of pollutants (WRIGHT & COLEMAN, 1988; RUESS et al., 1993; WASILEWSKA, 1996; GEORGIEVA et al., 2002). Thus taxa with higher cp values (3-5) indicate a more stable undisturbed ecosystem (RUESS et al., 1993; KORTHALS et al., 1996). Indirect evidence of a relation between historical pollution and a shift in the relative contribution of the cp 2/cp 3-5 nematodes is corroborated with significant positive/negative correlations with both groups of intercorrelated metal correlations and PAK's content.

Thus, this study showed significant relations between the relative contribution of colonizer/persister and historical pollution, though only for the relative contribution of cp 2 and cp 3-5 nematodes and not for cp 1 nematodes. Logically, omitting the cp 1 group from the MI (=MI2-5) (KORTHALS, 1997) should better reflect (historical) pollution-induced community changes. The average MI and MI2-5 are clearly lower for the polluted sites compared to the annex sites (2.74/2.79 vs. 3.10/3.23) but significance levels are not met because of the relatively high variation within a limited number of replicates. Differences between the minimum and maximum MI/MI2-5 (2.42/ 2.48 in historically disturbed site vs. 3.63/3.63 in annex site) is also not pronounced as compared to several other MI studies. For example, according to BONGERS & FERRIS (1999) the value of the MI varies from below 2 (for nutrient enriched sites) to about 4 in undisturbed sites. Since the disturbed sites contained significantly more colonizers of type cp 2 and less persisters (cp 3-5) the difference between MI2-5 values is on average more pronounced than the MI range, despite the fact that the latter is composed of a wider array of cp-groups. Furthermore, some differences in life strategy could only be significantly appointed with the MI2-5 index and not with the "overall" MI (see e.g. the sludge analyses).

Critical evaluation of the obtained nematode community characteristics

The current study did not show any significant relation between historical pollution and feeding type composition and the Shannon-Wiener diversity. Only limited, but significant effects were observed on life-strategy-related parameters (cp-groups, MI indexes). Although nematodes are known to reflect long term effects (NAGY, 1999; NAGY et al., 2004; GEORGIEVA et al., 2002; YEATES et al., 2003; BAKONYI et al., 2003), it is experimentally indicated that the nematode assemblages as represented in c-p groups can partly recover after a few years (BAKONYI et al., 2003). Nevertheless, despite nematodes in the current study having had possibly more than thirty years to adapt physiologically and genetically to the contaminants, puta-

tive remaining effects on the community structure were still observed. The supposed relations are here merely based on assessing nematode assemblages as a whole based on genus or family level. But, it has been suggested that several ecological insights should be investigated by addressing diversity within individual functional groups, and species-level identification can provide pivotal information (YEATES, 2003). Furthermore, despite the fact that the nematode community structure is generally acknowledged as an excellent bio-indicator (BONGERS & FERRIS, 1999), future research challenges should include other biological data in order to fully understand the effects of historical pollution.

In the current study there were considerable differences between the replicates, which definitely reduced the statistical power and complicated interpretation of the results. Albeit the analyses were based on bulk samples, compounded of a mixture of 15 cores, several replicates of a single sampling spot were remarkably different. The observed large dissimilarity suggests high spatial differences that are possibly related to high micro-habitat variability. The latter presumably partly explains the observed remarkably high generic variability in a geographically small sampling area. However, patchiness and micro-habitat variability have rarely been considered in ecotoxicological investigations although such variability is certainly not a negligible factor in the interpretation of the results. Insufficient insight into the micro-habitat variability in the current study could possibly have led to the flawed community structure pattern within the sludge samples, and the environmental variables structure within the municipal samples. In order to effectively cope with a high species and habitat diversity, the use of comprehensive mathematical models to obtain the appropriate sample size is possibly the way forward. Such approaches are already common practice in agro-nematology (for an overview, see BEEN & SCHOMAKER, 2006). Thus, future sampling could include systematically more and smaller cores to obtain a bulk sample of a certain optimal size (see BEEN & SCHOMAKER, 2006).

Finally, the possibility of differences in bio-availability and measured pollution content (KORTHALS et al., 1996) dictates caution in interpretations, especially for the current study, which deals with substances that were deposited a long time ago. Biological effects are due to the activity of heavy metals in solution; any bound, inert inactive metal components will not have a direct effect on soil processes. Furthermore, buffered conditions in soil differ markedly from *in vitro* conditions. Thus, although some significant relations between the nematode community and historical pollution were observed in the current study, any assessment of the direct impact of heavy metals, and extension to all pollutants, should be based on their activity rather than total concentration (e.g. YEATES et al., 2003). Use of the cotton strip decomposition method (YEATES et al., 1994; LATTER et al., 1998) is proposed as an example of such an effect-based measurement.

Thus, studies such as the present investigation do not permit elucidation of causal relationships between nematodes and environmental factors. The observed significant relationships between historical pollution and nematode

life strategy characteristics remain to be further analysed with more experimental approaches, though, the obvious constraints associated with studies that cover such a long time-span remain a restricting factor.

ACKNOWLEDGMENTS

REFERENCES

ANDERSON MJ (2001). A new method for non-parametric multivariate analysis of variance. Austral Ecology, 26:32-46.

ANDERSON MJ (2004). PERMDISP: a FORTRAN computer program for permutational analysis of multivariate dispersions (for any two-factor ANOVA design) using permutation tests. Department of Statistics, Unversity of Auckland, New Zealand.

BAKONYI G, NAGY P & KADAR I (2003). Long-term effects of heavy metals and microelements on nematode assemblage. Toxicology Letters, 140:391-401.

BARDGETT RD, SPEIR TW, ROSS DJ, YEATES GW & KETTLES HA (1994). Impact of pasture contamination by copper, chromium and arsenic timber preservative on soil microbial properties and nematodes. Biology and Fertility of Soils, 18:71-79.

BEEN TH & SCHOMAKER CH (2006). Distribution Patterns and Sampling. In: PERRY RN & MOENS M (eds), Plant Nematology. CABI Publishing, Wallingford: 302-326.

BERT W, LELIAERT F, VIERSTRAETE AR, VANFLETEREN JR & BORGONIE G (2008). Molecular phylogeny of the Tylenchina and evolution of the female gonoduct (Nematoda: Rhabditida). Molecular Phylogenetics and Evolution, 48:728-744.

BLAKELY JK, NEHER DA & SPONGBERG AL (2002). Soil invertebrate and microbial communities, and decomposition as indicators of polycyclic aromatic hydrocarbon contamination. Applied Soil Ecology, 21:71-88.

BOAG B & YEATES GW (1998). Soil nematode biodiversity in terrestrial ecosystems. Biodiversity and Conservation, 7:617-630.

BONGERS T (1990). The maturity index: an ecological measure of environmental disturbance based on nematode species composition. Oecologia, 83:14-19.

BONGERS T & FERRIS H (1999). Nematode community structure as a bioindicator in environmental monitoring. Trends in Ecology & Evolution, 14:224-228.

BUCHANAN JB (1984). Sediment analysis. In: HOLME NA & MCINTYRE AD (eds), Methods for the Study of Marine Benthos, Blackwell Scientific Publications, Oxford: 41-65.

CAVENESS FE & JENSEN HJ (1955). Modification of the centrifugal-flotation technique for the isolation and concentration of nematodes and their eggs from soil and plant tissue. Proceedings of the Helminthological Society of Washington, 22:87-89.

CLARKE KR & GORLEY RN (2001). Primer v5: User manual/tutorial. Primer-E, Plymouth Marine Laboratory, Plymouth, U.K.

CRAGG RG & BARDGETT RD (2001). How changes in soil faunal diversity and composition within a trophic group influence decomposition processes. Soil Biology & Biochemistry, 33:2073-2081.

DUFRÊNE M & LEGENDRE P (1997). Species assemblages and indicator species: The need for a flexible asymmetrical approach. Ecological Monographs, 67:345-366.

ERSTFELD KM & SNOW-ASHBROOK J (1999). Effects of chronic low-level PAH contamination on soil invertebrate communities. Chemosphere, 39:2117-2139.

EUROGLAS (1998). Manual for determination of AOX, POX and EOX, Euroglas BV, Delft.

FERRIS H, BONGERS T & DE GOEDE RGM (2001). A framework for soil food web diagnostics: extension of the nematode faunal analysis concept. Applied Soil Ecology, 18:13-29.

FERRIS H, VENETTE RC & LAU SS (1996). Dynamics of nematode communities in tomatoes grown in conventional and organic farming systems & their impact on soil fertility. Applied Soil Ecology, 3:161-175.

GEORGIEVA SS, MCGRATH SP, HOOPER DJ & CHAMBERS BS (2002). Nematode communities under stress: the long-term effects of heavy metals in soil treated with sewage sludge. Applied Soil Ecology, 20:27-42.

GERAKIS A & BAER B (1999). A computer program for soil textural classification. Soil Science Society of America journal, 63:807-808.

HOHBERG K (2003). Soil nematode fauna of afforested mine sites: genera, distribution, trophic structure and functional guilds. Applied Soil Ecology, 26:113-126.

KORTHALS GW (1997). Pollutant induced changes in terrestrial nematode communities. Ph.D. Thesis, Wageningen Agricultural University.

KORTHALS GW, ALEXIEV AD, LEXMOND TM, KAMMENGA JE & BONGERS T (1996). Long-term effects of copper and pH on the nematode community of an agroecosystem. Environmental Toxicology and Chemistry, 15:979-985.

KRUSKAL JB (1964). Multidimensional scaling by optimizing goodness of fit to a nonmetric hypothesis. Psychometrika, 29:1-27.

LATTER PM, BANCROFT G & GILLESPIE J (1988). Technical aspects of the cotton strip assay in soils. International Biodeterioration, 24:25-47.

MULDER C, SCHOUTEN AJ, HUND-RINKE K & BREURE AM (2005). The use of nematodes in ecological soil classification and assessment concepts. Ecotoxicology and Environmental Safety, 62:278-89.

NAGY P (1999). Effect of an artificial metal pollution on nematode assemblage of a calcareous loamy chernozem soil. Plant and Soil, 212:35-43.

NAGY P, BAKONYI G, BONGERS T, KADAR I, FABIAN M & KISS I (2004). Effects of microelements on soil nematode assemblages seven years after contaminating an agricultural field. Science of the Total Environment, 320:131-143.

NEHER DA (2001). Role of nematodes in soil health and their use as indicators. Journal of Nematology, 33:161-168.

OKADA H & HARADA H (2007). Effects of tillage and fertilizer on nematode communities in a Japanese soybean field. Applied Soil Ecology, 35:582-98.

PAVAO-ZUCKERMAN MA & COLEMAN DC (2007). Urbanization alters the functional composition, but not taxonomic diversity, of the soil nematode community. Applied Soil Ecology, 35:329-39.

PORAZINSKA DL, DUNCAN LW, MCSORLEY R & GRAHAM JH (1999). Nematode communities as indicators of status and processes of a soil ecosystem influenced by agricultural management practices. Applied Soil Ecology, 13:69-86.

RITZ K & TRUDGILL DL (1999). Utility of nematode community analysis as an integrated measure of the functional state of soils: perspectives and challenges. Plant and Soil, 212:1-11.

RUESS L, FUNKE W & BREUNIG A (1993). Influence of experimental acidification on nematodes bacteria and fungi: Soil microcosms and field experiments. Zoologischen Jahrbuch (Systematik), 120:189-199.

SEINHORST J.W (1959). A rapid method for the transfer of nematodes from fixative to anhydrous glycerin. Nematologica, 4:67-69.

SNOW-ASHBROOK J & ERSTFELD KM (1998). Soil nematode communities as indicators of the effects of environmental contamination with polycyclic aromatic hydrocarbons. Ecotoxicology, 7:363-70.

VAN GEHUCHTE D, CORNELIS D, PLOVIE P & VAN DER VEKEN H (1997). Het bodemsaneringsdecreet en VLAREBO: handleiding voor de notariële praktijk en de vastgoedsektor. Roularta Books, Roeselare.

VAN RANST E, VERLOO M & DEMEYER AP (1999). Manual for the soil chemistry and fertility laboratory. Faculty Agricultural and Applied Biological Sciences, Ghent University.

VITO (2006a). Reference procedure soil inspection: inorganic analysis methods, Chroom (VI). http://www.emis.vito.be/EMIS/Media/referentielabo_bodem_CMA_2006_2-I-C7.pdf

VITO (2006b). Reference procedure soil inspection: mineral oil. http://www.emis.vito.be/EMIS/Media/referentielabo_bodem_CMA_2002_3_R1.pdf

VITO (2006c). Reference procedure soil inspection: EOX. http://www.emis.vito.be/EMIS/Media/referentielabo_bodem_CMA_2006_3-N.pdf

VITO (2006d). Reference procedure soil inspection: inorganic analysis methods. http://www.emis.vito.be/EMIS/Media/referentielabo_bodem_CMA_2006_2-II-A3.pdf

WASILEWSKA L (1996). The influence of acid rain on soil nematode communities: a comparison of contaminated habitats in the belt of the Karkofnosze and Izerskie mountains (southwest Poland) with uncontaminated areas in other regions of Poland. Ekologia Polska, 44:73-110.

WASILEWSKA L & BIENKOWSKI P (1985). Experimental study on the occurrence and activity of soil nematodes in decomposition of plant material. Pedobiologia, 28:41-57.

WEISS B & LARINK O (1991). Influence of sewage sludge and heavy metals on nematodes in an arable soil. Biology and Fertility of Soils, 12:5-9.

WRIGHT DH & COLEMAN DC (1988). Soil fauna versus fertilization effects on plant nutrition: results of a biocide experiment. Biology and Fertility of Soils, 7:46-52.

YEATES GW (2003). Nematodes as soil indicators: functional and biodiversity aspects. Biology and Fertility of Soils, 37:199-210.

YEATES GW, PERCIVAL HJ & PARSHOTAM A (2003). Soil nematode responses to year-to-year variation of low levels of heavy metals. Australian Journal of Soil Research, 41:613-25.

YEATES GW, WARDLE DA & WATSON RN (1993b). Relationships between nematodes, soil microbiological biomass and weed management strategies in maize and asparagus cropping systems. Soil Biology & Biochemistry, 25:869-876.

YEATES GW, BONGERS T, DE GOEDE RGM, FRECKMAN DW & GEORGIEVA SS (1993a). Feeding-habits in soil nematode families and genera - an outline for soil ecologists. Journal of Nematology, 25:315-331.

YEATES GW, ORCHARD VA, SPEIR TW, HUNT JL & HERMANS MCC (1994). Impact of pasture contamination by copper, chromium, arsenic timber preservative on soil biological-activity. Biology and Fertility of Soils, 18:200-208.

YEATES GW, BARDGETT RD, COOK R, HOBBS PJ, BOWLING PJ & POTTER JF (1997). Faunal and microbial diversity in three Welsh grassland soils under conventional and organic management regimes. Journal of Applied Ecology, 34:453-470.

Introgressive hybridization and population genetic diversity between rusty-necklaced partridge and chukar partridge in northwestern China

Zuhao Huang[1,2], Zhisong Yang[2], Jiao Zhang[2] & Naifa Liu[2]

[1] **School of Life Sciences, Jinggangshan University, Ji'an, Jiangxi Province, 343009, China.**
[2] **School of Life Sciences, Lanzhou University, Lanzhou, Gansu Province, 730000, China.**
Corresponding author : Naifa Liu, School of Life Sciences, Lanzhou University, Lanzhou, Gansu Province, 730000, China.
E-mail: naifaliu@sohu.com.

ABSTRACT. Introgressive hybridization is a common feature of the contact zone between divergent partridges of the genus *Alectoris*. The rusty-necklaced partridge (*Alectoris magna*) is paralleled with the chukar partridge (*A. chukar*) along the Liupan Mountain in northwestern China, and hybridization between the two species has been detected in the contact zone within this region. We examined nine populations of rusty-necklaced partridge and eight populations of chukar partridge to determine the extent and nature of the hybridization between them. A total of 458 nucleotides of mitochondrial DNA control-region were sequenced, revealing a strong asymmetry in introgression between the two taxa. The hybrids, morphologically identified as *A. magna*, were partly introgressed with genetic material from *A. chukar*. The haplotype diversity and nucleotide diversity decreased with increasing hybrid ratio among hybrid populations. The genetic integrity of the rusty-necklaced partridge is shown to be at risk from the introgressive hybridization.

KEY WORDS : *Alectoris magna*, *Alectoris chukar*, introgressive hybridization, genetic diversity, genetic assimilation

INTRODUCTION

Hybridization and introgression are increasingly recognized as important factors in the diversification of plants, and provide an excellent opportunity to study evolutionary processes (ARNOLD, 1997; KLINGENBERG et al., 2000). Speciation caused by introgressive hybridization occurs frequently in plants (ELLSTRAND & SCHIERENBECK, 2000), but its importance in animal evolution remains controversial. The importance of introgressive hybridization is increasingly supported by recent molecular and ecological studies (ROQUES et al., 2001). Hybridization is relatively common in birds (GRANT & GRANT, 1992), and many avian parapatric distributions have been described (e.g. RISING, 1983) that apparently represent stable zones of overlap and hybridization.

In some cases, hybrids may constitute a large part of the natural populations (CRESPIN et al., 1999). Also, serious problems for the conservation of rare native species can occur because of hybridization (LEARY et al., 1995). Natural hybridization is expected to increase genetic diversity and fitness (ROELKE et al., 1993), such as in plant species of hybrid origin, and in genetic exchange among microorganisms. Empirical evidence supporting this hypothesis remains ambiguous. Hybridization can result in genetic assimilation and hybrid depression (RISING, 1983; RYMAN et al., 1995). Hybridization can also compromise the genetic integrity of existing species to the point of causing genetic extinctions (GILL, 1994; ABERNETHY, 1994). Hybridizing avian populations often show low geographic variation and absence of diagnostic alleles at both nuclear and mitochondrial loci (RANDI & BERNARD-LAURENT, 1999). We are not yet able to make a priori judgments about when the "positive" or "negative" effects of hybridization will dominate. There is thus a practical need for advanced studies.

Two closely related species of *Alectoris* partridge, namely, rusty-necklaced partridge (*Alectoris magna*) and chukar partridge (*A. chukar*), are distributed in northern China. The former is limited to small areas in Ningxia, Gansu and Qinghai, while the latter is found in the broad Palearctic region. They live parapatrically along the Liupan Mountain (LIU, 1984; Fig. 1). The Liupan Mountain represents a barrier to dispersal and an area of secondary contact among many western and eastern taxa (WANG, 1988). Hybridization between the two species was detected in the contact zone (CHEN et al., 1999; LIU et al., 2006), and provided an interesting case to illustrate the consequences of asymmetrical introgression on genetic diversity. We thus undertook to clarify the genetic status of rusty-necklaced partridge in the parapatric region based on mitochondrial DNA (mtDNA) control-region. Our general aims were: (1) to infer the extent of introgressive hybridization between the two species, (2) to discuss the causes of the hybridization, and (3) to assess the effects of the introgressive hybridization on rusty-necklaced partridge.

MATERIALS AND METHODS

Sample collection and DNA extractions

A total of 106 birds from nine populations of rusty-necklaced partridge were collected along the Liupan Mountain from the following localities: Lanzhou (LZ, n=17), Dingxi (DX, n=10), Jingyuan (JY, n=10), Haiyuan (HY, n=22), Huining (HN, n=10), Beidao (BD, n=9),

Zhuanglang (ZL, n=10), Lixian (LX, n=10) and Wushan (WS, n=8) (Table 1, Fig. 1). Eighty-four birds from eight populations of chukar partridge were collected from the following localities: Tianshui (TS, n=10), Xichuan (XC, n=10), Quzi (QZ, n=10), Tongchuan (TC, n=10), Panke (PK, n=10), Gaoping (GP, n=14), Honghui (HH, n=10) and Wangxia (WX, n=10) (Fig.1). Wild birds were collected during three consecutive hunting seasons (2001, 2002 and 2003). Liver samples were dissected from birds and stored in 95% ethanol immediately after removal. Total DNA was extracted from liver by the ethanol sedimentation procedure as described by RANDI & LUCCHINI (1998).

TABLE 1

Number of hybrids and hybrid ratio in the nine populations of rusty-necklaced partridge

Population	N	Numbers of hybrid	Hybrid ration (%)
Huining	10	1	10.00
Wushan	8	0	0
Beidao	9	2	22.22
Haiyuan	22	9	40.91
Jingyuan	10	0	0
Lanzhou	17	0	0
Dingxi	10	0	0
Lixian	10	2	20.00
Zhuanglang	10	8	80.00
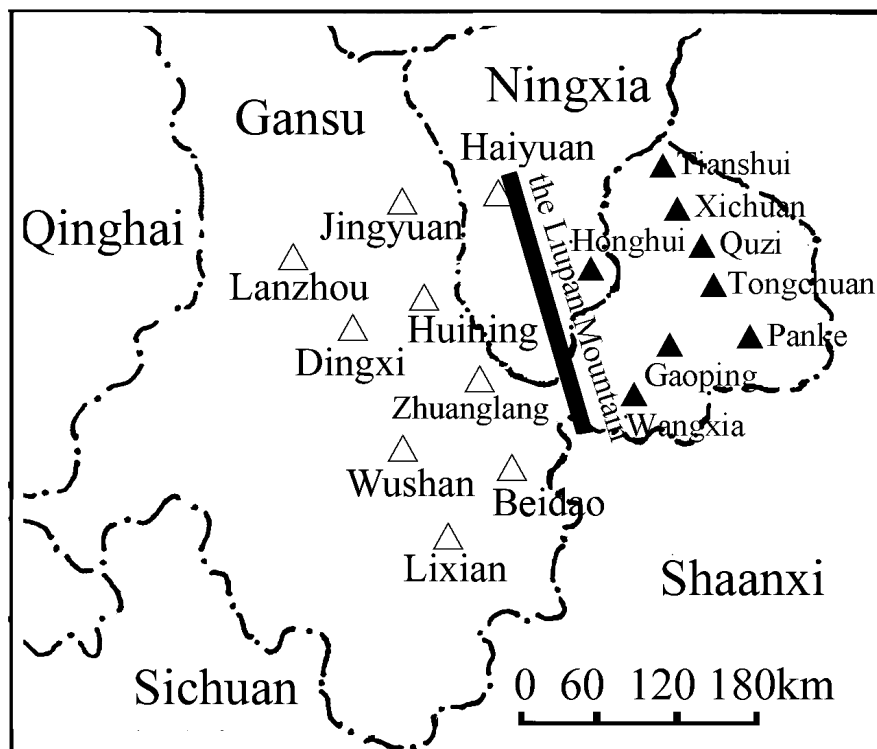
Fig. 1. – Map showing the sampling sites. △: *Alectoris magna*, ▲: *A. chukar*.

Laboratory methods

Two oligonucleotide primers, PHDL (5-AGGAC-TACGGCTTGAAAAGC-3) and PH1H (5-TTATGT-GCTTGACCGAGGAACCAG-3) (RANDI & LUCCHINI, 1998), were used to amplify and sequence 458bp mitochondrial DNA control-region segment. There was 1 unit of Taq DNA polymerase in 35μL reactions. The final concentrations were 10mmol/L Tris-HCl (pH 8.3), 50mmol/L KCl, 1.5mmol/L MgCl$_2$, 150μmol/L dNTP, 10pmol/L primers and about 100ng DNA templates. PCR conditions were as follows: 95°C 4min; 35 cycles of 95°C 40sec, 55–58°C 40sec, 72°C 60sec; followed by 72°C 10min in PE2400 thermocycler. After examination by 1% agarose gel electrophoresis, PCR products were purified with Wizard^{TM} PCR Preps DNA purification box (Promega Inc. USA). Sequences were obtained by the double-stranded DNA cycle sequencing with each of the primers used in the amplifications on an ABI 373 automated sequencer. All individuals were sequenced in both directions. The sequences were deposited in GenBank and the accession numbers are from DQ157593 to DQ157619 (*A. magna*), and from AY190634 to AY190659 (*A. chukar*).

Sequence analysis

Sequences were aligned by Clustal X Procedure (THOMPSON et al., 1997) and refined manually. Arlequin 2.0 (SCHNEIDER et al., 2002) was used to define the haplotypes. DnaSP4.0 (ROZAS et al., 2003) was used to estimate population haplotype diversity (h), mean number of pairwise differences (k), nucleotide diversity (π). The difference of haplotype and nucleotide diversity between the hybridized populations and the pure ones was compared

statistically using a randomization test. The individuals were pooled and then randomly assigned to the two groups. The difference between these random values was stored and this procedure was repeated 1000 times. The observed differences were compared with this random distribution: the P value (p*) is given by the proportion of random values greater than the observed one (using absolute values because the test is two-tailed).

The population differentiation was determined using the Arlequin 2.0 analysis of molecular variance (AMOVA) (SCHNEIDER et al., 2002). Unrooted haplotype networks were obtained using TCS1.21 Procedure (TEMPLETON et al., 1992). A Mantel test (MANTEL, 1967) was performed to estimate the relationship between two independent dissimilarity matrices: the genetic diversity and hybrid ratio.

RESULTS

Introgressive hybridization and hybrid ratio

Of all the samples, a total of 458 nucleotides of the mtDNA control region genes were sequenced. Twenty-eight samples of rusty-necklaced partridge from five populations (Zhuanglang, Lixian, Haiyuan, Beidao and Huining) had chukar partridge mtDNA genotype. The hybrids were morphologically similar to *A. magna*. However, there were no samples of chukar partridge with rusty-necklaced partridge genotype. We thus confirmed that the hybridization between the two species was asymmetrical introgression, gene flow being only from chukar partridge into rusty-necklaced partridge. The hybrid ratio ranged from 10.00% (Huining) to 80.00% (Zhuanglang) in the

five hybrid populations (Table 1). The total hybrid ratio was 20.75% in rusty-necklaced partridge.

Mitochondrial DNA haplotype

The mtDNA control-region sequence alignment showed 50 different haplotypes, defined by 67 polymorphic sites including 65 substitutions (40 transitions and 15 transversions) and two deletes (187, *chukar*; 246, *magna*) (Table 2). There were 17 haplotypes (C1-C17) belonging to chukar partridge, among which C1 was the most common haplotype, with 41 individuals from all the sampling sites of chukar partridge (Table 2). The number of observed haplotypes within populations of chukar partridge ranged from three in Honghui to six in Gaoping. Twenty-five haplotypes (M1-M25) were found in rusty-necklaced partridge. The number of observed haplotypes within populations varied from one in Zhuanglang to seven in Lanzhou (Table 3). The most common haplotype M2 was geographically widespread, in 32 individuals of rusty-necklaced partridge. The hybrids had 12 haplotypes, among which four haplotypes (C1, C2, C3 and C12) were shared with chukar partridge and the others (H1-H8) were unique haplotypes. As in the chukar partridge, haplotype C1 was the most common haplotype with 16 hybrids.

The haplotype network showed that haplotypes of chukar partridge and hybrids grouped together, stemming from C1, which was at the centre of a star-like topology (Fig. 2). The haplotypes of rusty-necklaced partridge constituted the other group, stemming from M2, which was at the other centre of a star-like toplogy (Fig. 2). The pairwise percentage sequence divergence between chukar partridge and rusty-necklaced partridge was 0.0599.

TABLE 2

Haplotyes and variable sites of chukar partridge (C1~C15), rusty-necklaced partridge (M1~M25) and hybrids (C1~C3, C12, H1~H8)

Haplotype	Variable positions in sequences	Sampling location (sample size)
	0000000000000001111111122222222222222222222222222222222233333333333333444	
	0001111122255670005689900111112222333344444557889990001113478999445	
	1350578978905493482170602012683458567812456388890194560145813479064	
C1	ACCTCAAAACCCGCTATACA-	*
	CCTTGGTAAGCTCTCACTCTCTCGCACTCTTACACCGACTCTACCC	
C2	....................-....................A....................T..	**
C3	................T.-.....................	TS(1),HH(1)
C4	....................-..C..........................	TS(1), HY(1)
C5	....................-....................T....................	TS(1),QZ(2)
C6	....................-.................A..T.............	XC(1),QZ(1)
C7	....................-T.................A..T.............	XC(1)
C8	....................-............................T..........	QZ(1)
C9	....................-........T......A....................T..	TC(3)
C10	....................-........G.......................T..	TC(1)
C11	....................-..........C.........A.....................	PK(5)
C12	....................-..................................T..	PK(2),WX(1),GP(1), LX(1)
C13	.........G........-.......................T..	WX(1)
C14	.............C.....-.T....................A............	WX(1)
C15	..T...............-...................A.................T..	GP(1)
C16	C.................-....................A.................T..	GP(1)
C17	....................-.G.......................T..	GP(1)
M1	............T..CG.GT...AA.AG....T.TG.C..T...T...TC.GTC.T..G.T.CT..	LZ(1),LX (1)
M2	............T..CG.GT...AA.AG....T.TG.C..T-..T...TC.GTC.T..G.T.CT..	***
M3	............T..CG.GT...AA.AG....T.TG.C..T-..T...TC.GTC.T..G.T.CT..	LX(3)
M4	............T..CG.GT...AA.AG.A.T.TG.C...T.T.T...TC.GTC.T..G.T.CT..	LX(1)
M5	............T..CG.GT...AA.AG.A..T.TG.C..T.T.T..CTC.GTC.T..G...CT..	BD(5)

TABLE 2

Haplotyes and variable sites of chukar partridge (C1~C15), rusty-necklaced partridge (M1~M25) and hybrids (C1~C3, C12, H1~H8)

Haplotype	Variable positions in sequences	Sampling location (sample size)
M6	............T..CG.GT...AA.AG....T.TG.C..T.T.T...TC.GTC.T..G..CT..	BD(1)
M7	............T..CG.GT...AA.AG....T.TG.C..T-..T...TC.GTC.TA.G.T.CT..	WS(2)
M8	.......G.....T..CG.GT...AA.AG.A..T.TG.C..T.T.T...TC.GTC.TA.G.T.CT..	WS(1)
M9	............T..CG.GT...AA.AG....T.TG.C.CT.T.T..CTC.GTC.T..G...CT..	WS(1)
M10	............T..CG.GT...AA.AG....T.TG.C..T...T...TC.GTC.T..G...CT..	LZ(3),JY(1),HY(1), WS(3)
M11	............T..CG.GT...AA.AG....TCTG.C...-..T...TC.GTC.T..G.T.CT..	DX(5)
M12	............T..CG.GT...AA.AG....T..G.C..T-..T...TC.GTC.T..G.T.CT..	DX(1)
M13	............T..CG.GT...AA.AG....T.TG.C..T-..T...TC.GTC.T.GGCT.CT..	DX(1),HN(1)
M14	............T.GCG.GT...AA.AG....T.TG.CT.T-..T...TC.GTC.T..G.T.CT..	HN(1)
M15	.....G.......T..CG.GT...AA.AG....TCTG.C..T-..T...TC.GTC.T..G.T.CT..	HN(1)
M16	............T..CG.GT...AA.AG....T.TG.CT.T-..T...TC.GTC.T..G.T.CT..	HN(1),HY(1)
M17	............T..CG.GT...AA.AG....T.TG.C..T-..T...TC.GTC.T..G.TCCT..	HY(1)
M18	............T..CG.GT...AA.AG....T.TG.C..T-..T...TC.GTC.T..G.T.CTGG	HY(1)
M19	............T..CG.GT...AA.AG....T.TG.C..T-..T...TC.GTC.T..G.T.CT.G	HY(2)
M20	............T..CG.GT...AA.AG....TCTG.C......T...TC.GTC.T..G.T.CT.G	JY(3)
M21	............T..CG.GT...AA.AG....T.TG.C..T-..T...TC.GTC.T..G.T.CTG.	JY(2)
M22	............T..CG.GT...AA.AG....T.TG.C..T-..T...TCCGTC.T..G.T..T..	LZ(2)
M23	............T..CG.GT...AA.AG....T.TG.C..T-..T...TCCGTC.T..G.T..T..	LZ(2),DX(1)
M24	.......G...T..CG.GTT...AA.AG....T.TG.C......T...TC.GTC.T..G.T.CT..	LZ(2)
M25	............T..CG.GT...AA.AG....T.TG.C...-..T...TC.GTC.T..G.T.CT..	LZ(1)
H1	...................-......................T...................	BD(1)
H2	...C..............-....................A..................T..	ZL(1)
H3	C..................-.......................................	ZL(1)
H4	....A...........T.-..	HY(1)
H5	.A................-..	LX(1)
H6	......G..A........T.-..	HY(1)
H7	...................-....................A...................	HY(1)
H8	...................-....................T................	HY(1)

*: TS(5),XC(7),QZ(5),TC(5),PK(3),WX(5),GP(4),HH(7), BD(1),HY(3),ZL(6)
**: TS(2),XC(1),QZ(1),TC(1),WX(2),GP(6),HH(2), HN(1)
***: HN(5),BD(1),HY(7),LZ(6),DX(2),WS(1),LX(3),JY(4), ZL(2).

TABLE 3

Total number of haplotypes and number of unique haplotypes found within each population, mean pairwise differences (K) and nucleotide diversity (π) and haplotype diversity (h) of *Alectoris chukar*, *A. magna* and hybrids.

Population	Sample size	Total haplotypes	Unique haplotypes	K	π (x±SD)	h (x±SD)
Alectoris magna						
Huining	9	5	2	2.17	0.0047±0.0018	0.73±0.16
Wushan	8	5	3	3.14	0.0057±0.0011	0.86±0.11
Beidao	7	3	2	1.81	0.0039±0.0018	0.52±0.04
Haiyuan	13	6	3	0.85	0.0028±0.0008	0.72±0.13
Jingyuan	10	4	2	2.47	0.0054±0.0009	0.78±0.09
Lanzhou	17	7	3	2.60	0.0057±0.0009	0.85±0.06
Dingxi	10	5	2	3.18	0.0069±0.0012	0.76±0.13
Lixian	8	4	2	1.03	0.0023±0.0005	0.78±0.12
Zhuanglang	2	1	0	0.33	0.0000	0.00
Total	88	25	19	2.33	0.0051±0.0005	0.83±0.04
Alectoris chukar						
Tianshui	10	5	1	1.31	0.0029±0.0007	0.76±0.13
Xichuan	10	4	1	0.96	0.0027±0.0009	0.53±0.18
Quzi	10	5	1	1.11	0.0027±0.0007	0.76±0.13
Tongchuan	10	4	2	1.93	0.0042±0.0008	0.71±0.12
Panke	10	3	1	1.47	0.0032±0.0005	0.69±0.10
Gaoping	14	6	3	1.62	0.0036±0.0006	0.77±0.09
Wangxia	10	5	2	1.53	0.0035±0.0009	0.76±0.13
Honghui	10	3	0	0.91	0.0020±0.0007	0.51±0.16
Total	84	17	11	1.49	0.0033±0.0003	0.73±0.05
hybrids	22	12	8	1.28	0.0035±0.0007	0.80±0.09
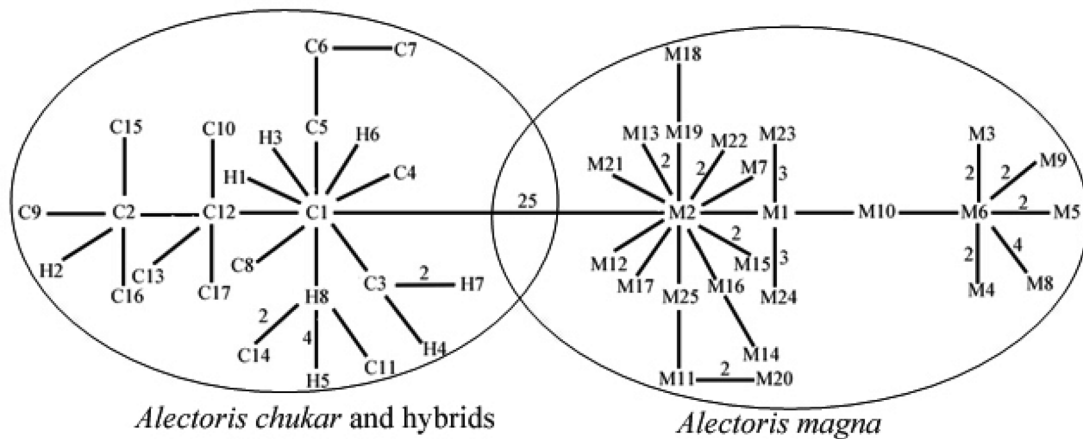
Fig. 2. – Haplotype network using the number of different mutations among 50 mtDNA haplotpyes of *Alectoris chukar*, *A. magna* and hybrids. Distances between linked haplotypes correspond to one mutation, except when shown by numbers.

Genetic diversity

Nucleotide diversity among the nine populations varied from 0.0000 (Zhuanglang) to 0.0069 (Dingxi); at the same time, haplotype diversity ranged from 0.00 (Zhuanglang) to 0.86 (Wushan) in rusty-necklaced partridge (Table 3). The pairwise divergence between haplotypes of rusty-necklaced partridge was lowest in Zhuanglang (k=0.00) and highest in Dingxi (k=3.18). Nucleotide diversity ranged from 0.0020 (Honghui) to 0.0042 (Tongchuan), and haplotype diversity varied from 0.51 (Honghui) to 0.76 (Tianshui, Quzi and Wangxia) among the eight populations of chukar partridge (Table 3). Nucleotide diversity and haplotype diversity of hybrids were 0.0035 and 0.80, respectively (Table 3).

The average nucleotide diversity and haplotype diversity in the five hybrid populations of rusty-necklaced par-

tridge (Huining, Baidao, Haiyuan, Zhuanglang and Lixian) were 0.0027 and 0.55, respectively, while those of the other populations (Lanzhou, Dingxi, Jingyuan and Wushan) were 0.0059 and 0.81. Statistically insignificant differences in haplotype diversity and nucleotide diversity were observed between five hybridized populations and the pure ones (p>0.05) based on randomization tests. The Mantel test indicated that the haplotype diversity and nucleotide diversity showed negative correlation with hybrid ratio (r=-0.847, p>0.05, n=5; r=-0.905, p<0.05, n=5) among the five hybrid populations (Fig. 3). The results of AMOVA showed significant genetic differentiation ($\chi 2$=32.06, p<0.01, n=9) between the five hybrid populations and the other four non-hybrid population of rusty-necklaced partridge.
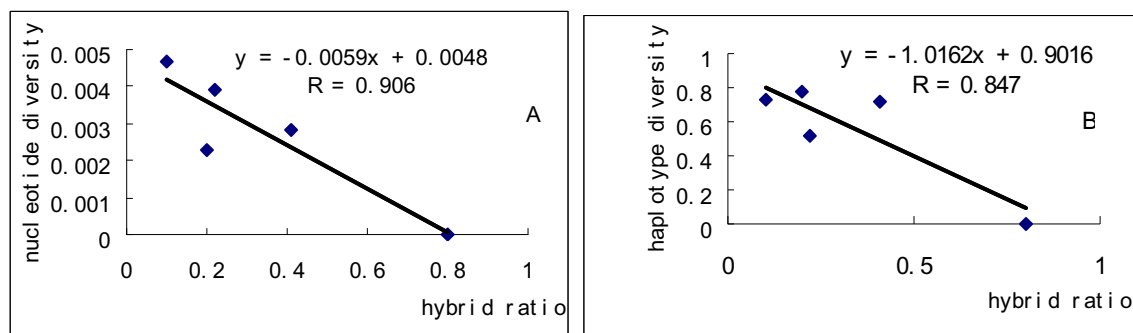
Fig. 3. – The relationship between genetic diversity and hybrid rate. A: nucleotide diversity, B: haplotype diversity. Regression equation and correlation coefficient (r) are given. Each dot represents one population.

DISCUSSION

A general difficulty in studies of hybridization in the wild is to assess the degree of hybridization of individuals (CRESPIN et al., 1999). Historically, morphological markers such as counts, measurements and colour patterns

were first used to describe hybridization. More recently, molecular tools have provided very informative genetic markers. Mitochondrial DNA data showed a strong asymmetry in introgression between rusty-necklaced partridge and chukar partridge. Some partridges from the contact zone, morphologically identified as *A. magna*, are actu-

ally partly introgressed with *A. chukar*. The introgression demonstrates that the natural hybridization does not affect both taxa in the same way (CRESPIN et al., 1999). Behavioural, ecological or genetic factors must act in the hybrid zone, either favouring the advance of chukar partridge alleles into the rusty-necklaced partridge genome or impeding that of the latter alleles into the former genome. From a theoretical viewpoint, this asymmetry may be the result of various factors (ENDLER, 1977). One possibility is asymmetrical selection caused by an asymmetrical hybrid breakdown, as demonstrated by MORAN (1979). An alternative possibility is asymmetrical gene flow (MAY et al., 1975), resulting from differences in generation time (BARTON, 1986), in mating behaviour (LAMP & AVISE, 1986; KONKLE & PHILIPP, 1992) or some other component of fitness (ABERNETHY, 1994) between the two parental taxa. Among all these hypotheses, differences in mating behaviour and generation time do not appear to be relevant because laboratory experiments have revealed no such evidence. By contrast, an alternative hypothesis is that gene flow from chukar partridge to rusty-necklaced partridge is more important than gene flow in the reverse direction, because of the different habitat distributions of the two taxa. Chukar partridge has wide ecological amplitude and niche variation. In terms of its widespread Palearctic distribution and varied habitat affinities, chukar partridge may be considered the most successful of the seven species of *Alectoris* (JOHNSGARD, 1988). Because of its considerable adaptability and tolerance of conditions, hybrids involving chukar partridge have been recorded in other locations also: *A. chukar × A. rufa* in Italy (BARATTI et al., 2004) and *A. chukar × A. graeca* in Greece (DRAGOEV, 1974).

The introgressive hybridization cloud takes place through secondary contact between *A. chukar* and *A. magna* in the Liupan Mountain region. Fossils of *Alectoris* were recorded in early Pleistocene deposits in China (WETMORE, 1934), which demonstrated that *Alectoris* partridges were widespread in northwestern China during the early Pleistocene. Biochemical and molecular data (RANDI & LUCCHINI, 1998) suggested the divergence time between the two species was 1.90 million years ago, corresponding to Donau glaciation. Because of its lower altitude and precipitation, the Chaidamu Basin experienced no glacier effect during the Pleistocene (LI & LI, 1991), and thus it acted as a refuge for rusty-necklaced partridge. The ancestors of *A. magna* could have evolved in the Basin (HUANG et al., 2007). After the last glaciation, natural changes (such as desertification), and, more recently, anthropogenic habitat alterations such as deforestation and agriculture, produced a rapid extension of the ecological conditions suitable for rusty-necklaced partridge, which, in turn, resulted in their increased hybridization with chukar partridge along the Liupan Mountain.

Some authors have found that introgressive hybridization results in local genetic extinction of birds, such as *Anas platyrhynchos × A. rubripes* (ANKNEY et al., 1987), *Icterus galbula× I. bullocki* (RISING, 1983), *Passerina cyanea× P. amoena* (RISING, 1983) and *Vermivora pinus× V. chrysoptera* (GILL, 1994). ABERNETHY (1994) observed that the genetic integrity of the Scottish mainland red deer (*Cervus elaphus*) was shown to be at risk from sika (*Cervus nippon*). Rusty-necklaced partridge was strongly introgressed with chukar partridge, which raises questions about its genetic integrity. The haplotype diversity and nucleotide diversity decreased with increasing hybrid ratio among hybrid population. The Zhuanglang population exhibited the lowest nucleotide diversity and haplotype diversity, with the highest hybrid ratio (80.00%) and the least haplotypes (M2). Asymmetrical introgression between the two species may eventually result in local genetic assimilation of rusty-necklaced partridge populations.

REFERENCES

ABERNETHY K (1994). The establishment of a hybrid zone between red and sika deer (genus *cervus*). Molecular Ecology, 3:551-562.

ANKNEY CD, DENNIS DG & BAILEY CR (1987). Increasing mallards, decreasing black ducks: Coincidence or cause and effect? Journal of Wildlife Management, 51:523-529.

ARNOLD ML (1997). Natural Hybridization and Evolution. Oxford University Press, New York.

BARATTI M, AMMANNATI M, MAGNELLI C & DESSÌ-FULGHERI F (2004). Introgression of chukar genes into a reintroduced red-legged partridge (*Alectoris rufa*) population in central Italy. Animal Genetics, 36:29-35.

BARTON NH (1986). The effect of linkage and density-dependent regulation on gene flow. Heredity, 57:415-426.

CHEN Q, CHANG C & LIU NF (1999). Mitochondrial DNA introgression between two parapatric species of *Alectoris*. Acta Zoologcia Sinica, 45:456-463.

CRESPIN L, BERREB D & LEBRETON J (1999). Asymmetrical introgression in a freshwater fish hybrid zone as revealed by a morphological index of hybridization. Biological Journal of Linnean Society, 67:57-72.

DRAGOEV V (1974). On the population of the Rock Partridge (*Alectorisg raeca* Meisner) in Bulgaria and methods of census. Acta Ornithologie, 14:251-255.

ELLSTRAND NC & SCHIERENBECK KA (2000). Hybridization as a stimulus for the evolution of invasiveness in plants? Proceedings of the National Academy of Sciences of the USA, 97:7043-7050.

ENDLER JA (1977). Geographic Variation, Speciation, and Clines. Princeton; Princeton University Press.

GILL FB (1994). Rapid, asymmetrical introgression of mitochondrial DNA in hybridizing populations of Blue-wringed and Golden-wringed warblers. Journal of Ornithology, 135:359-369.

GRANT PR & GRANT BR (1992). Hybridization of bird species. Science, 256:193-197.

HUANG ZH, LIU NF, LUO SX & LONG J (2007). Phylogeography of rusty-necklaced partridge (*Alectoris magna*) in northwestern China. Molecular Phylogenetics and Evolution, 43:379-385.

JOHNSGARD PA (1988). The quails, Partridges, and francolins of the World. Oxford Univ. Press, Oxford.

KLINGENBERG CP, SPENCE JR & MIRTH CK (2000). Introgressive hybridization between two species of waterstriders (Hemiptera: Gerridae: Limnoporus): geographical structure and temporal change of a hybrid zone. Journal of Evolutionary Biology, 13:756-765.

KONKLE BR & PHILIPP DP (1992). Asymmetric hybridization between two species of sunfishes (*Lepomis*: Centrarchidae). Molecular Ecology, 1:215-222.

LAMP T & AVISE JC (1986). Directional introgression of mitochondrial DNA in a hybrid population of tree frogs: The influence of mating behavior. Proceedings of the National Academy of Sciences USA, 83:2526-2530.

LEARY RF, ALLENDORF FW & SAGE GK (1995). Hybridization and Introgression between Introduced and Native Fish. American Fisheries Society Symposium, 15:91-101.

LI BY & LI JJ (1991). Quaternary Glacial Distribution of the Tibet Plateau. Science Press, Beijing.

LIU NF (1984). On the taxonomic status of *Alectoris magna*. Acta Zootaxonomica Sinica, 9:212-217.

LIU NF, WEN LY, HUANG ZH & HOU P (2006). Introgressive hybridization between *Alectoris magna* and *A. chukar* in the Liupan Mountain Region. Acta Zoologica Sinica, 52:153-159.

MANTEL N (1967). The detection of disease clustering and a generalized regression approach. Cancer Research, 27:209-220.

MAY RM, ENDLER JA & MCMURTRIE RE (1975). Gene frequency clines in the presence of selection opposed by gene flow. The American Naturalist, 109:659-676.

MORAN C (1979). The structure of Hybrid Zone in *Caledia captiva*. Heredity, 42:13-32.

RANDI E & BERNARD-LAURENT A (1999). Population genetic of a hybrid zone between the red-legged partridge and rock partridge. The Auk, 116:324-337.

RANDI E & LUCCHINI V (1998). Organization and evolution of the mitochondrial DNA control region in the avian genus *Alectoris*. Journal of Molecular Evolution, 47:449-462.

RISING JD (1983) .The great plains hybrid zones. Current Ornithology, 1:131-157.

ROELKE ME, MARTENSON JS & O'BREIN SJ (1993). The consequences of demographic reduction and genetic depletion in the endangered Florida Panther. Current Biology, 3:340-350.

ROQUES S, SEVIGNY JM & BERNATCHEZ L (2001). Evidence for broadscale introgressive hybridization between two redfish (genus *Sebastes*) in the North-west Atlantic: a rare marine example. Molecular Ecology, 10:149-165.

ROZAS J, SÁNCHEZ-DELBARRIO JC, MESSEGUER X & ROZAS R (2003). DnaSP, DNA polymorphism analyses by the coalescent and other methods. Bioinformatics, 19:2496-2497.

RYMAN N, UTTER F & HINDAR K (1995). Introgression, Supportive Breeding and Genetic Conservation Population Management for Survival and Recovery. New York: Columbia University Press, 341-365.

SCHNEIDER S, ROESSLI D & EXCOFFIER L (2002). Arlequin Version 2.0: A Software for Population Genetics Data Analysis. Genetics and Biometry Laboratory, Department of Anthropology and Ecology, University of Geneva, Geneva, Switzerland.

TEMPLETON AR, CRANDALL KA & SING CF (1992) A cladistic analysis of phenotypic associations with haplotypes inferred from restriction endonuclease mapping and DNA sequence data III Cladogram estimation. Genetics, 132:619-633.

THOMPSON JD, GIBSON TJ, PLEWNIAK F, JEANMOUGIN F & HIGGINS DG (1997). The Clustal X windows interface flexible strategies for multiple sequence alignment aided by quality analysis tool. Nucleic Acid Research, 24:4876-4882.

WANG XT (1988). Scientific investigation of Liupan Mountain Natural Reserve. Ningxia People Press, Yinchuan.

WETMORE A (1934). Fossil birds from Mongolia and China. American Museum Novitates, 711:1-16.

Immature stages of *Rabigus tenuis* (Fabricius, 1792) (Coleoptera, Staphylinidae, Staphylininae) with observations on its biology and taxonomic comments

Bernard Staniec & Ewa Pietrykowska-Tudruj

Department of Zoology, Maria-Curie Sklodowska University, Akademicka 19 Street, 20-033 Lublin, Poland

Corresponding author : Ewa Pietrykowska-Tudruj, e-mail:ewpiet@poczta.onet.pl

ABSTRACT. The paper describes and illustrates the morphology of all preimaginal stages of *Rabigus tenuis* (Fabricius, 1792), including a detailed account of chaetotaxy and porotaxy. This is the first description of the immature stages for the genus *Rabigus*. Morphological differences between the first (L_1) and next (L_2 and L_3) larval instars are to be found in the: chaetotaxy of head, profemur, protibia, tarsungulus, abdominal tergites, sternites and urogomphi; structure of antennae, maxillae and urogomphi; microstructure of abdominal tergites, proportions of the bodyparts, body colour and habitus. Diagnostic characters of egg, larva and pupa of this species are given. Some data on its distribution, environmental requirements and biology under laboratory conditions are also provided. All immature stages of *R. tenuis* were compared with those of related genera and the respective distinguishing characters are provided.

KEY WORDS : Staphylinidae, *Rabigus tenuis*, immature stages, morphology, chaetotaxy.

INTRODUCTION

Nineteen species of the genus *Rabigus* Mulsant & Rey, 1876 are currently known worldwide. Three occur in Europe, two of which are found in Poland: *R. pullus* (Nordmann, 1837) and *R. tenuis* (Fabricius, 1792). Until 1980 the taxon *Rabigus* was considered as a subgenus of the genus *Philonthus* Stephens, 1829 by most authors (SMETANA, 1959; LUCHT, 1987). In recent years, however, it is mostly considered as a genus of its own (LOHSE & LUCHT, 1989). The taxonomic history of the taxon clearly illustrates that it is closely related to *Philonthus*.

Nothing is known of the morphology and general biology of the preimaginal stages of the genus *Rabigus* (PAULIAN, 1941; POTOTSKAYA, 1967; KASULE, 1970; TOPP, 1978; HINTON, 1981; STANIEC & PIETRYKOWSKA-TUDRUJ, 2007b). Some information on the ecology of *R. tenuis* is provided in SMETANA (1958), BURAKOWSKI et al. (1980) and SZUJECKI (1980). The main goal of this study is to describe the immature stages (egg, all three larval instars and pupa) and to observe the biology of this species in captivity.

MATERIALS AND METHODS

All immature stages of *R. tenuis* (eggs, three larval instars and pupa) were obtained by rearing 37 adults (11 of them females). These adults were collected on April 27-29, 2006 in sunny places, free of vegetation, in Lublin, and on an exposed loess slope with xerothermic plants in Ciechanki Łańcuchowskie near Lublin, SE Poland.

The collected adults were divided in the laboratory into two groups. 1) In order to determine the life cycle, repro-ductive activity, fertility and mortality of this staphylinid, six pairs (female and male) were reared separately. 2) Specimens of the second group (25) were reared together. The immature stages obtained from these adults were used for the description of morphology.

All beetles were kept in plastic containers (10cm diameter x 7cm high), filled with soil. Two hundred eggs, coming from six pairs reared separately, were placed separately in plastic containers (7cm diameter x 4cm high) about 1/3 filled with moist soil. The insects were reared from egg to adult, at a temperature of 24±3ºC. Different larval instars were fed with ant larvae. The immature stages obtained from the adults reared together were preserved in a 1:3 solution of glycerine and alcohol. For microscopic studies, the punctured larvae were rinsed in distilled water, cleared in chloralphenol and in lactic acid. Drawings were made from the preparations in lactic acid. Habitus illustrations of larvae, pupae and adults were based on photos of freshly-killed individuals.

The material examined comprises: a) 10 eggs, 11 L_1, 12 L_2, 11 L_3 and 16 pupae used for the study of morphology; all immature stages were reared from the eggs laid by the collected adults; b) 27 adults (including 12 females), 200 eggs, 141 L_1, 91 L_2, 52 L_3, 32 prepupae and 26 pupae, used for the study of life history.

Chetotaxy of *R. tenuis* is generally named based on the principles used for description of some species of the subfamily Staphylininae by SOLODOVNIKOV & NEWTON (2005) and summarized in SOLODOVNIKOV (2007).

Setae of thoracic segments I-III (chaetotaxy in L_1, L_2, and L_3 is the same) and abdominal segment IX (it is unclear which setae of L_2, L_3 are homologous with those of L_1) were not coded here.

RESULTS

1. Description of the developmental stages

Egg (Figs 1A-F)

Length: 0.90-1.04mm (mean 0.95mm), width: 0.58-0.66mm (mean 0.61mm). Macroscopic aspect (Fig. 1): milky white, oval; with about 35 unbranched, clearly visible, longitudinal ridges, about 12 of which reach posterior pole. Posterior pole with projection slightly widened on the end (Fig. 1A); egg 2.8-5.6 times as long as projection. Openings of aeropyles clearly visible, arranged between ridges in at least 10 rows from 6 to 8 aeropyles each (Figs 1; 1B). Microscopic aspect: aeropyles openings, chorion microstructure and anterior pole as in Figs 1B-F.

Date of the beginning of rearing adults: 26.IV.2006. The period of egg observation in the laboratory: 29.V-27.VI.2006.

Third instar larva (L₃)

Body length (from anterior margin of nasale to the end of pygopod): 6.10-7.10mm (mean 6.85mm); head width (between stemmata): 0.65-0.68mm (mean 0.66mm); head length (from anterior margin of nasale to neck): 0.83-0.90mm (mean 0.87mm); pronotum width in broadest place: 0.69-0.79mm (mean 0.72mm). Colour: head brown, mandibles dark brown, antennae, maxillae, labium yellowish, pronotum yellowish-brown, meso- and metanotum yellowish-grey, legs light yellowish-brown with brown tarsungulus, abdominal tergites grey-white, body and urogomphi dirty white, thoracic sternite yellowish-brown, abdominal sternite yellowish-white. Macro and micro setae of head, thorax, some setae on abdominal segments simple (Fig. 4); most setae on abdominal segments and urogomphi rod-shaped and frayed apically (Figs 5-11). Body elongated, abdomen slightly widened to segment V and then gradually narrowed to the terminal segment of the body.

Head (Figs 13-15; 15B; 15D; 17-24; 26; 27): about 1.2 times as long as wide, side margins almost parallel; dorsal ecdysial lines bifurcate before half of head length (Fig. 13). Chaetotaxy of epicranial (E) part: with 32 setae (codes: 12-27), six pores (codes: a-c) and two glands (Gl); posterior (P) part with six micro setae (codes: 28-30) and two pores (code: d) (Fig. 13). Ventral side of head with about 14 setae, six pores and a pair of clearly visible tentorial pits (Figs 15; 15D). Apotome (Ap) (Figs 15; 21) in broad outline triangular, slightly extending beyond tentorial pits; with six setae, two pores and a pair of glandular pits (Gp). Each side of head with four stemmata (Figs 14; 14A) in a cluster, three stemmata almost of equal size, the fourth one clearly smaller than the others (Fig. 14A). Antenna (Figs 17; 18) 4-segmented, length ratio of segments I-IV 1.0:1.9:2.1:1.1. respectively; segment I 1.1 as wide at the base as long, with one pore ventro-apically; segment II 2.3 times as long as wide, with two pores (one dorsally, and one ventro-apically); segment III 2.5 times as long as wide in the widest place, with three macro setae (one ventro-laterally and two laterally), two sensory appendages (Sa) (one club-shaped and second tiny), two

solenidia (So) and one pore ventrally; segment IV 2.5 times as long as wide at the widest place, about 2.1 times as long as sensory appendage, with three setae and four solenidia (So) apically. Nasale (Na) (Figs 13; 19) with 22 setae (14 macro and eight micro), two pores medially, two olfactory organs (Og) anteriorly and two glandular pits (Gp) posterio-laterally. Anterior margin of nasale (Fig. 19) with nine teeth divided into three distinct clusters (one middle and two lateral), each cluster with three teeth, paramedian teeth (Pmt) about 2.1 times as long as median tooth (Mt). Epipharynx (Fig. 20) with four bunches of straight, long hairs each, two olfactory organs (Og) at the anterior margin and 14 cuticular processes posteriorly. Mandible (Fig. 22) with uneven inner margin, two setae on outer margin and two pores dorsally. Maxilla (Figs 23; 24): length ratio of cardo (Cd) and stipes (St) 1:1.5; cardo 1.3 times as long as wide at the base, bearing one seta ventro-laterally; stipes 2.8 times as long as wide with seven setae (two on outer margin, two ventrally, three at the inner margin) and one pore. Mala (Ma) (Fig. 23) finger-shaped, with two long and two short setae apically; length ratio of mala and segment I of maxillary palp: 1:1.4.

Palpifer (Pf) (Fig. 23) with one pore and two micro seta ventrally. Maxillary palp (Pm) 4-segmented; length ratio of segments I-IV: 1.5:1.9:1.7:1.0 respectively; segment I 1.8 times as long as wide, with two pores; segment II 2.4 times as long as wide, with two setae and two pores; segment III 3.9 times as long as wide, with one digitiform sensory appendage basally on outer margin; segment IV 3.4 times as long as wide, with two pores and a few microsensory appendages on the apex (Fig. 24).

Hypopharynx: dorsal side of labium membranous and densely pubescent (Fig. 26). Labium (Fig. 27): ventral side of prementum (Pmnt) sclerotized, with four setae (two macro and micro) and two pores laterally. Ligula (Lg) conical, 2.5 times as long as wide at base; almost as wide as segment I of labial palp at the base; ligula almost as long as segment I of labial palp; apex with a few (clearly visible 2) microsensory appendages. Labial palps (Pl) 3-segmented; length ratio of segments I-III 2.1:1.4:1.0 respectively; segment I with one pore laterally; segment III with one pore laterally and one microsensory appendage apically.

Thorax (Figs 3; 28-30): pro-, meso-, and metanotum with mid-longitudinal ecdysial line. Pronotum (Fig. 28) with 46 (23 x 2) setae and eight pores; meso- (Fig. 28) and metanotum with similar chaetotaxy, each with 44 (22 x 2) setae (ten micro), eight pores and a pair of coeloconic sensilla (Cs) probably (Fig. 28D). Microstructure the anterior part pro- and mesonotum as in Figs 28A, C. Cervicosternum (Cr) (Fig. 29) triangular with ten setae (two micro). Prosternal area with two sternites (Sn), each with one seta; membranous surface between sternites and coxal cavities (Cc) with two pair setae, and between cervicosternum (Cr) and sternites (Sn) with six setae. Meso- and metasternal areas membranous, each with 12 micro setae: four between legs, six at the base of legs and two anteriorly (Fig. 29). The area between pro- and mesothorax with a pair of functional spiracles (Sp), one macro seta in front of each spiracle (Fig. 29). Foreleg (Fig. 30): femur (Fe) with 24 setae (15 spine-shaped of different

length, nine micro, codes: 1-24) and two pores (codes: a, b); tibia (Tb) with 18 spine-shaped setae of different length (codes: 1-18) and one pore (code: a), tibial comb absent; tarsungulus (Tu) with three spine-shaped setae (codes: 1-3). Length ratio of profemur, protibia and protarsungulus 3.7:2.6:1 respectively.

Abdomen (Figs 3; 33; 34; 36; 37; 38; 40; 42): segments I-VIII each with tergite (Te) and sternite (St) divided into two parts by membranous area until segments VII, a pair of paratergites (Pt) and a pair of parasternites (Ps) laterally (Figs 33; 34; 36); on segment I paratergites and parasternites partly fused (Fig. 34). Segment I: tergite with 34 setae (20 macro and 14 micro, codes: 1-17) and eight pores (codes: a-d) (Fig. 33); sternite with 18 setae (four macro rod-shaped and frayed apically, 14 micro, codes: 1-9) and two pores (code: a) (Fig. 36); fused paratergites and parasternites each with seven setae (five macro rod-shaped and frayed apically, two micro). Segments II-VIII: tergites with about 40 setae (32-34 macro rod-shaped and frayed apically and 6-8 micro, codes: 1-20); sternites with 30-32 setae (22 macro rod-shaped and frayed apically, 8-10 micro, codes: 1-15); paratergites and parasternites each with four setae and six setae (1 micro) respectively. Tergites I-IX each with a pair of organs that are probably campaniform or coeloconic sensillae (Ca) antero-lateraly (Figs 33B, 34). Microstructure of tergites of segments I-VIII as in Figs 33A; C-F; tergite and sternite of segment IX with 18 setae (four micro) and 14 setae (four micro) respectively (Figs 37; 38; 40). Microstructure of tergite and sternite of segment IX as in Figs 37A; B; D; E. Segment IX with pair of two-segmented urogomphi (Figs 37; 38; 40; 42); segment I with 25 setae (codes: 4-28) and one pore (Fig. 42); segment II slightly curved with three setae, one long seta apically (codes: 1-3); length ratio of segments I and II of urogomphus and apical seta 3.5:1:2.0 respectively; segment I six times as long as wide, microstructure of urogomphi as in Figs 42A; B. Segment X (pygopod): dorsal side with about 26-30 setae (Fig. 37); ventral side with 30-35 setae (Fig. 38); microstructure as in Fig. 37F. Pygopod shorter than urogomphi (without seta apically) and only slightly longer than segments I of urogomphi, length ratio of pygopod and urogomphi (without seta apically) 1:1.2. Abdominal segments I-VIII, each with a pair of spiracles (Sp) located between tergite and paratergites at segment I and on lateral sides of tergites at segments II-VIII (Fig. 34).

Second instar larva (L_2)

Body length: 3.87-5.65mm (mean 4.93mm); head width (between stemmata): 0.52-0.56mm (mean 0.54mm); head length: 0.66-0.71mm (mean 0.69mm); pronotum width: 0.52-0.60mm (mean 0.56mm).

First instar larva (L_1)

Body length: 2.80-4.50mm (mean 3.45mm); head width (between stemmata): 0.46-0.48mm (mean 0.47mm); head length: 0.58-0.64mm (mean 0.60mm); pronotum width: 0.44-0.45mm (mean 0.45mm). Colour: head yellowish-brown, anterior part of head and mandibles light brown, tergites of pro-, meso-, and metanotum slightly darkened, antennae and legs light brownish,

abdominal sclerites colourless, setae brown, body, urogomphi dirty white. Head about 1.3 times as long as wide; chaetotaxy of epicranial (E) part with 28 pairs of setae (codes: 12-14, 16-25, 27) and two pair of pores (codes: a, c) (Fig. 12). Structure of tentorial pit and microstucture of basal part of head as in Figs 15A & 15C respectively. Antenna (Fig. 16): length ratio of segments I-IV: 1:2.2:3.0:2.1 respectively; segment I 1.8 times as wide as long; segment II 1.5 times as long as wide; segment III 1.8 times as long as its maximal width, without one solenidium occurring in L_3 (Figs 16-18). Maxilla (Fig. 25): length ratio of cardo (Cd) and stipes (St) 1:1.9; cardo 1.1 times as wide as long; stipes 2.1 times as long as wide with five macro setae (Fig. 25). Length ratio mala (Ma) and segment I of maxillary palp 1:1.1 respectively; maxillary palp (Fig. 25): length ratio of segments I-IV 1.1:1.6:1.5:1 respectively; segment I 1.2 times as long as wide; segment II about 2.1 times as long as wide.

Foreleg (Fig. 31): femur (Fe) with 11 setae (code: 1, 2, 4, 6-8, 10, 11, 13, 15, 18) and two pores (a, b); tibia (Tb) with nine spine-shaped setae (code: 1-3, 6, 7, 12-15); tarsungulus (Tu) with two spine-shaped setae (code: 1, 2).

Abdomen (Figs 32; 35; 39; 41). Segment I: tergite with 32 (2 x 16) setae (code: 1-10, 12-17) (Fig. 32); sternite with 16 setae – 14 micro simple, two macro rod-shaped and frayed (code: 1, 2, 4-9) (Fig. 35). Segments II-VIII: tergite and sternite of each segment with 30 setae (code: 2, 3, 5, 6, 8, 9, 11, 13-20) and 26 setae (code: 1-5, 7, 8, 10-15) respectively; microstructure of tergites I-VIII as in Figs 32A-C. Segment IX (Fig. 39): tergite and sternite each with 12 setae; microstructure as in Fig. 37C. Segment X: microstructure and chaetotaxy as in Figs 37G; 39 respectively. Urogomphus (Ug): segment I with 18 setae (codes: 4-9, 11-13, 15, 17-20, 25-28); length ratio of segments I, II of urogomphus and apical seta 1.8:1:1.6 respectively; segment I 4.6 as long as wide (Fig. 41); microstructure of segment I and II as in Figs 41A, B.

Pupa (Figs 44-60)

Before pupation, the mature larva constructs in the soil an oval cocoon about 5.0mm long (Fig. 43). Body length: 3.43-3.82mm (mean 3.59mm); maximal width (between hind knees): 1.51-1.72mm (mean 1.6mm); head width (between eyes): 0.73-0.82mm (mean 0.78mm); maximal width of pronotum: 0.90-1.00mm (mean 0.95mm). Colour: light yellow just after pupation, then orange with darker edges, projections on pronotum and abdomen light brown; shortly before metamorphosis pupa black except for orange pronotum. Head 1.3 times as long as wide; labrum relatively short and wide, 1.7 as wide at base as long. Antennae curved, lie on the knees of fore and middle legs, reaching almost two thirds of length of elytra (Figs 44; 45). Wings protruding beyond posterior margin of the first clearly visible abdominal sternite (Fig. 44). Pronotum 1.1 times as long as wide; anterior margin with 10-12 setiform projections (looking from ventral side 5/5, 5/6, 6/5, 6/6 projections on sides). Each fore and middle tibiae with three and seven clearly visible outlines of protuberances respectively. Hind tarsi slightly protruding posterior margin of segment IV (morphological segment VI) clearly visible abdominal segment (Fig. 44). Abdomen narrowed below segment IV (Fig. 46). Abdominal

tergite I twice as long as tergite II. Segments III-VIII, each bearing a pair of setiform projections on sides (all six pairs). Setiform projections on segments III-VI short, spine-shaped, a least three times shorter than length of segments (Fig. 47); setiform projections on segments VII, VIII long, always longer than segment, with tiny processes occurring on the greater part of projections (Figs 48; 49). Microstructure of the abdominal tergite as in Figs 50-53. The first abdominal tergite with unidentified cuticular structure (Fig. 54). Abdominal tergites I-IV with tuberculate, functional spiracles (Fsp), the first pair bigger and situated more laterally than the rest, moderately protruding (Figs 45; 46; 55), tergites V-VIII with externally visible, but apparently atrophied spiracles (Asp) (Figs 45; 46; 56; 57). Terminal sternite: with well-marked sexual dimorphism (Figs 58; 59) in female with two well-developed ventral prolongations (Vp) terminal prolongation (Tp) mostly with numerous, sharp cuticular processes (Fig. 60).

2. Remarks on the ecology and biology of *Rabigus tenuis* under laboratory conditions and on its distribution

Rabigus tenuis (adult habitus and aedeagus as in Figs 61-63) is Palearctic species known from almost the entire European region, as well as from the central part of Russia (Siberian), Caucasus, Turkey, Iran, Uzbekistan, Mongolia, China and Japan. In Poland it is recorded from about twenty localities, distributed in the central and southern part of the country (BURAKOWSKI et al., 1980; LUCHT, 1987; STANIEC, 1991; HERMAN, 2001; DERUNKOV & MELKE, 2001). It is defined as a eurytopic, psamophilous, ripicolous and phytodetriticolous species, inhabiting exposed, moist, sandy or clayey banks of rivers, streams, lakes, sunny clayey slopes and dirty roads. Under the climate of the south-eastern part of Poland *R. tenuis* distinctly prefers sunny, slightly moist places. It lives on clayey and loess soil sparsely covered by grasses or devoid of any vegetation. It also occurs very often in urban areas in exposed places, on pavement sides and in small rockeries (BURAKOWSKI et al., 1980; KOCH,1989; the first author's observation).

During the rearing, conducted from the 26th of April 2006, oviposition was observed for 50 days; from April 29 to June 27 (Fig. 64; Table 1). The highest intensity of oviposition was observed in May (Fig. 64). Eggs were laid separately, distributed in the soil in a rearing container. During the reproductive period, a single female laid from one to four eggs per day, exceptionally five eggs. Six females kept in the laboratory (each kept with a male) laid a total of 605 eggs, whereas a single female laid 116, 83, 75, 128, 103, 100 eggs respectively; on average about 101 eggs per female. The embryonic development at a temperature of 24°C±3 lasted on average about six days (Table 2), the mortality rate being about 30%.

Under laboratory conditions the larvae appeared from the beginning of May until the last ten days of June (Table 1). Development of each larval instar lasted on average four to six days. The highest mortality rate among different larval instars was recorded in L_2 (Table 2). Usually shortly before pupation mature larvae (L_3) made cocoons with wet soil on the bottom of the containers, where pupation took place (Fig. 43). The prepupa and pupa are motionless stages, and lasted on average about four and seven days, respectively. Both stages showed the lowest mortality rates; for prepupa about 19%, for pupa 11.5% (Table 2). The prepupal and pupal stages were observed in the laboratory from the last ten days of May until almost the end of June. Adults of the new generation appeared from the end of May to the end of June. Under field conditions this period probably extended until the end of July, because the latest laid eggs of this species were recorded at the end of June. Out of two hundred specimens kept in the laboratory, only 23 (11.5%) completed their development from egg to adult. At a temperature of 24°C (±3), it lasted from 23 to 41 days, on average 26 days. Under laboratory conditions the last adults of the old generation lived until the ten-day period of July, with females generally living longer than males (Table 1).
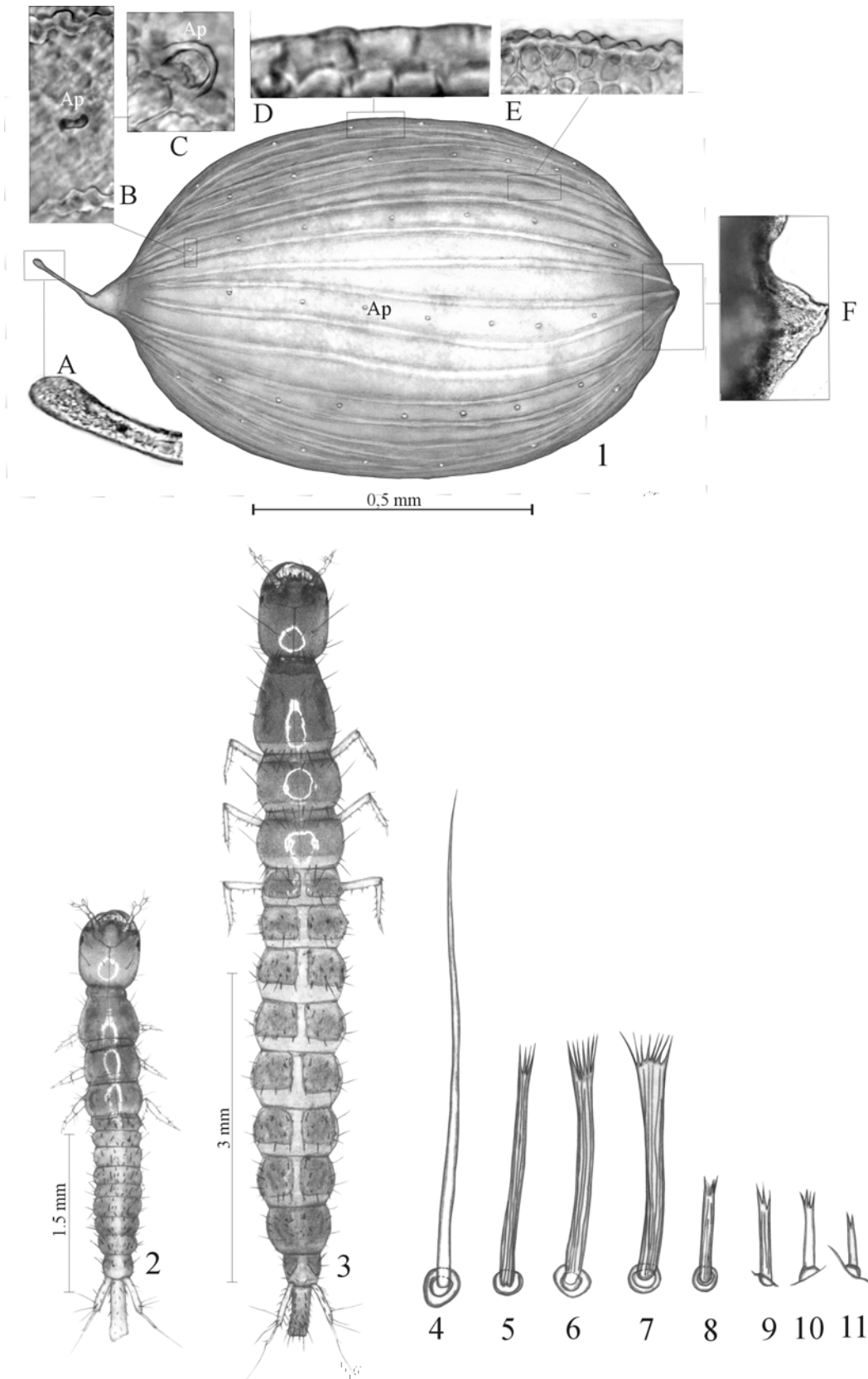
Figs 1-11. – *Rabigus tenuis*. 1, 1A-F – Egg; 2 – 1st larval instar; 3, 4-11 – mature larva. 1 – General view with aeropyles (Ap); 1A – distal end clubbed of posterior projection; 1B-E – microstructure with aeropyles (Ap); 1F – anterior pole; 2 – general view; 3 – general view; 4 – simple macro seta of pronotum; 5-10 – rod-shaped and frayed apically macro seta of abdominal tergite: I (5), IV (6), VI (7), X (8) and urogomphus (9-11).
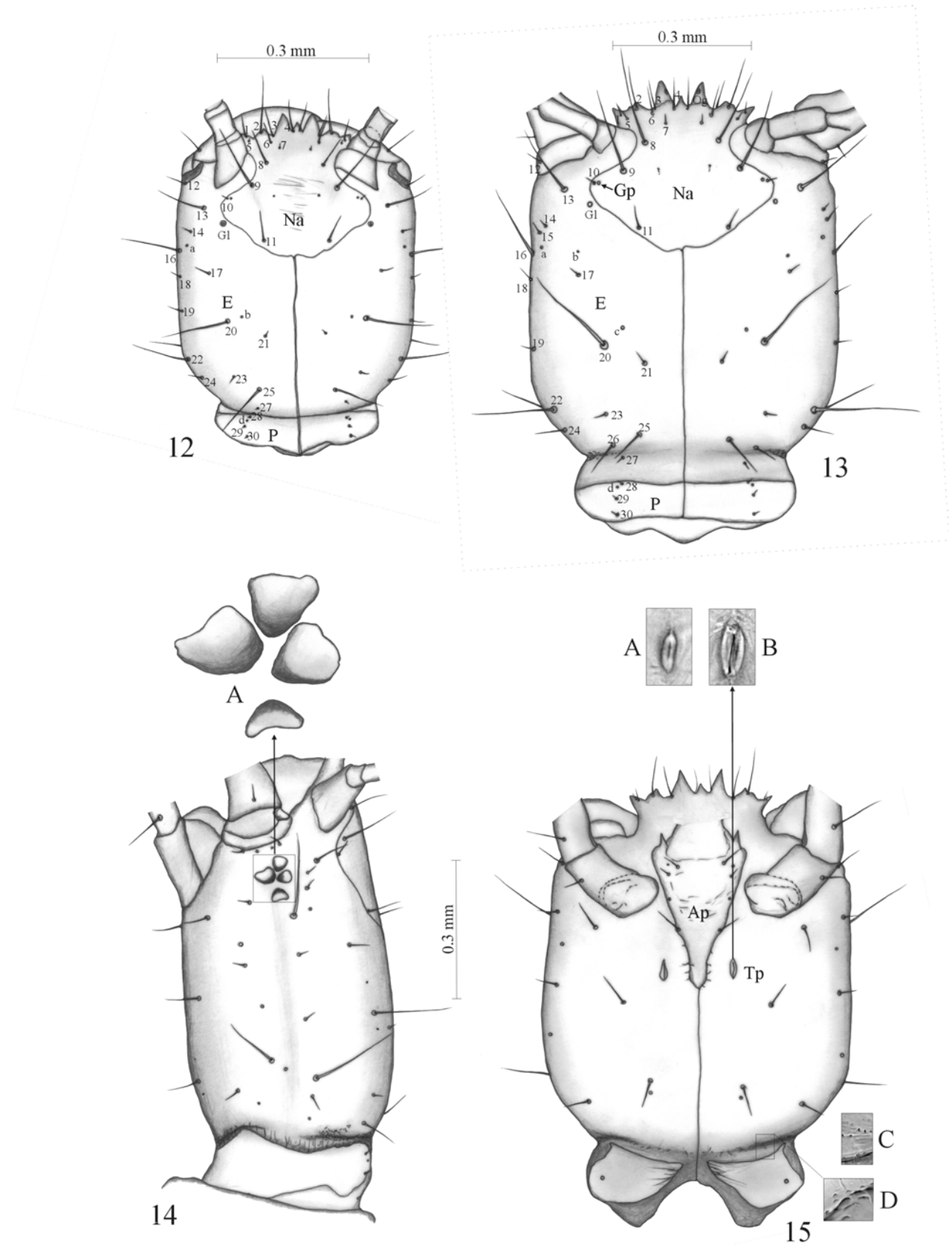
Figs 12-15. – *Rabigus tenuis*, head. 12, 15A, 15C – 1st instar larva; 13-15, 15B, 15D – mature larva. 12, 13 – Head in dorsal aspect (E – epicranial part, Gl – gland, Na – nasale, P – posterior part, 1, 2... – codes of setae); 14 – head in lateral aspect; 14A – stemmata; 15 – head in ventral aspect (Ap – apotome, Tp – tentorial pit); 15A, 15B - tentorial pit; 15C, 15D – microstructure of head.
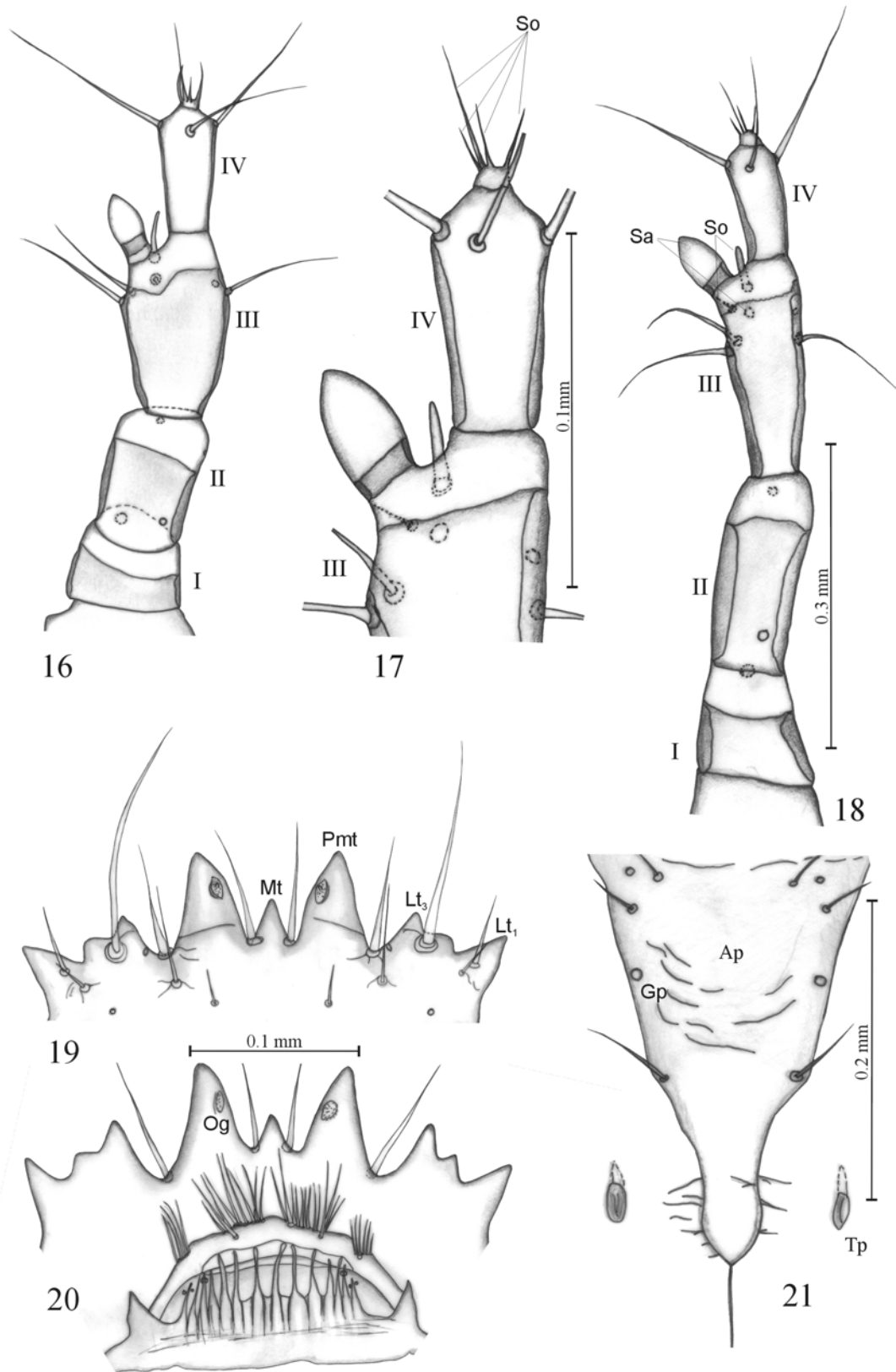
Figs 16-21. – *Rabigus tenuis*. 16 – 1st instar larva; 17-21 – mature larva. 16, 18 – Right antenna in dorsal aspect (I-IV – antennal segments); 17 – apical part of right antenna in dorsal aspect (Sa – sensory appendages, So – solenidia, III and IV – antennal segments); 19 – anterior part of nasale in dorsal aspect (Mt – median tooth, Pmt – paramedian tooth); 20 – epipharynx (Og – olfactory organ); 21 – apotome (Ap) and tentorial pits (Tp) (Gp - glandular pit).
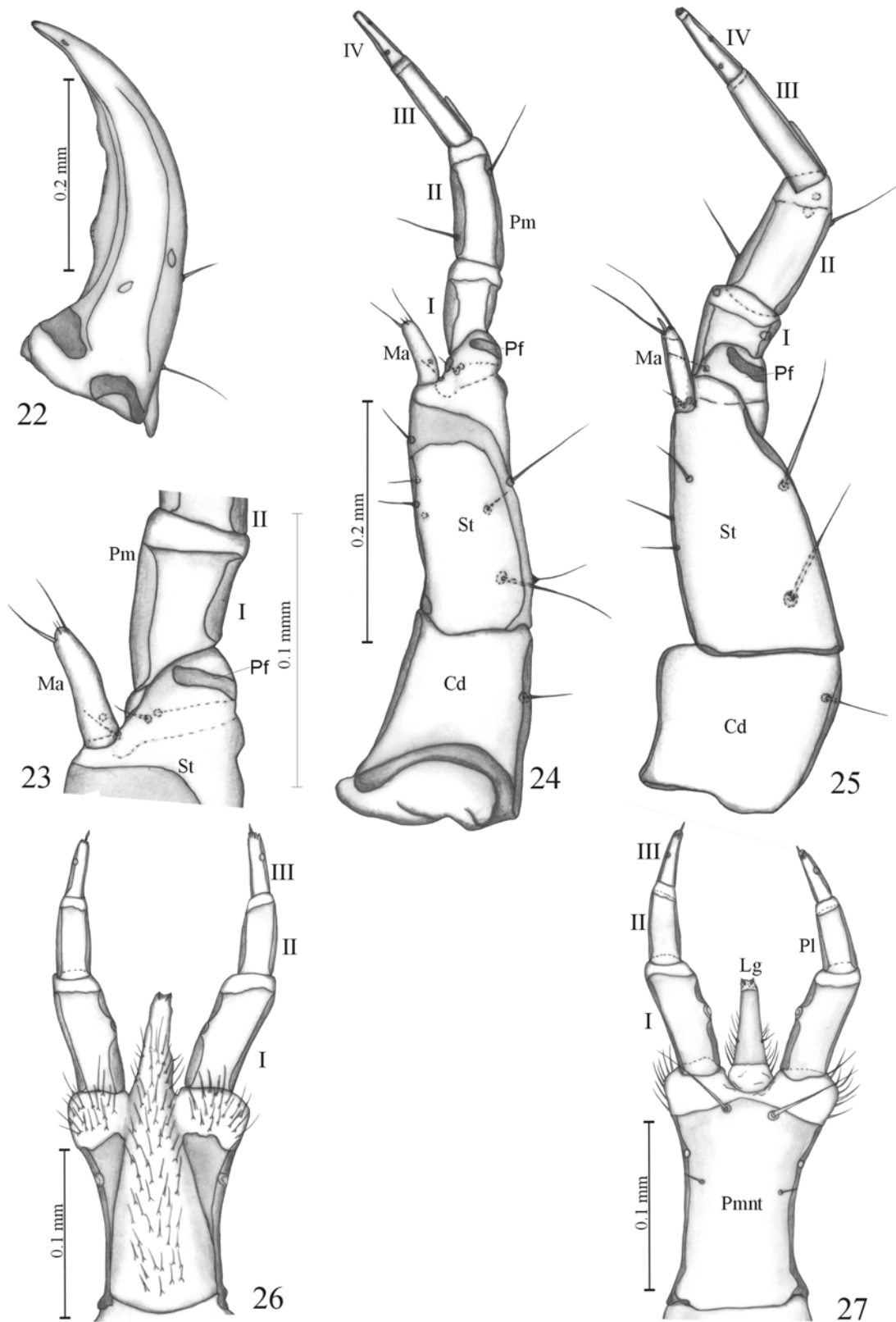
Figs 22-27. – *Rabigus tenuis*. 25 - 1st instar larva; 22-24, 26, 27 – mature larva. 22 – Right mandible in dorsal aspect; 23 - anterior part of stipes in dorsal aspect (Ma – mala, Pf – palpifer, Pm – maxillary palp, St – stipes); 24, 25 – right maxilla in dorsal aspect (Cd – cardo, Ma – mala, Pf – palpifer, Pm – maxillary palp, St – stipes); 26 - hypopharynx (I-III – segments of labial palp); 27 - labium in ventral aspect (Lg – ligula, Pl - labial palp, Pmnt – prementum, I-III – segments of labial palp).
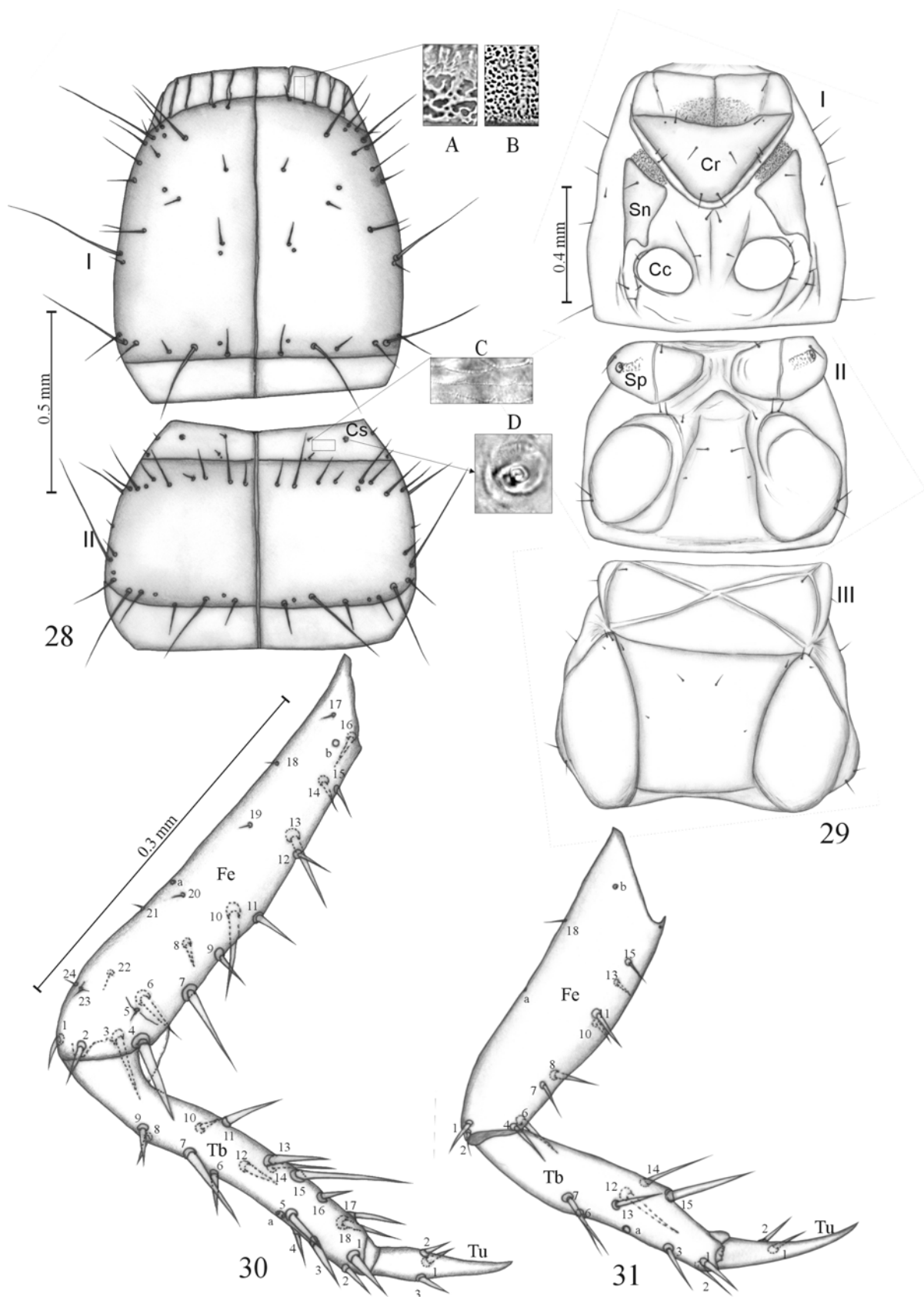
Figs 28-31. – *Rabigus tenuis*. 31 – 1st instar larva; 28-30 - mature larva. 28 - Prothorax (I) and mesothorax (II) in dorsal aspect (Cs – coeloconic sensillum); 29 – prothorax (I), mesothorax (II) and metathorax (III) in ventral aspect (Cr – cervicosternum, Sn – sternite, Cc – coxal cavity, Sp - spiracles); 30, 31 – fore leg in anterior aspect (a, b – codes of pores, Fe – femur, Tb – tibia, Tu – tarsungulus, 1, 2, … – codes of setae).
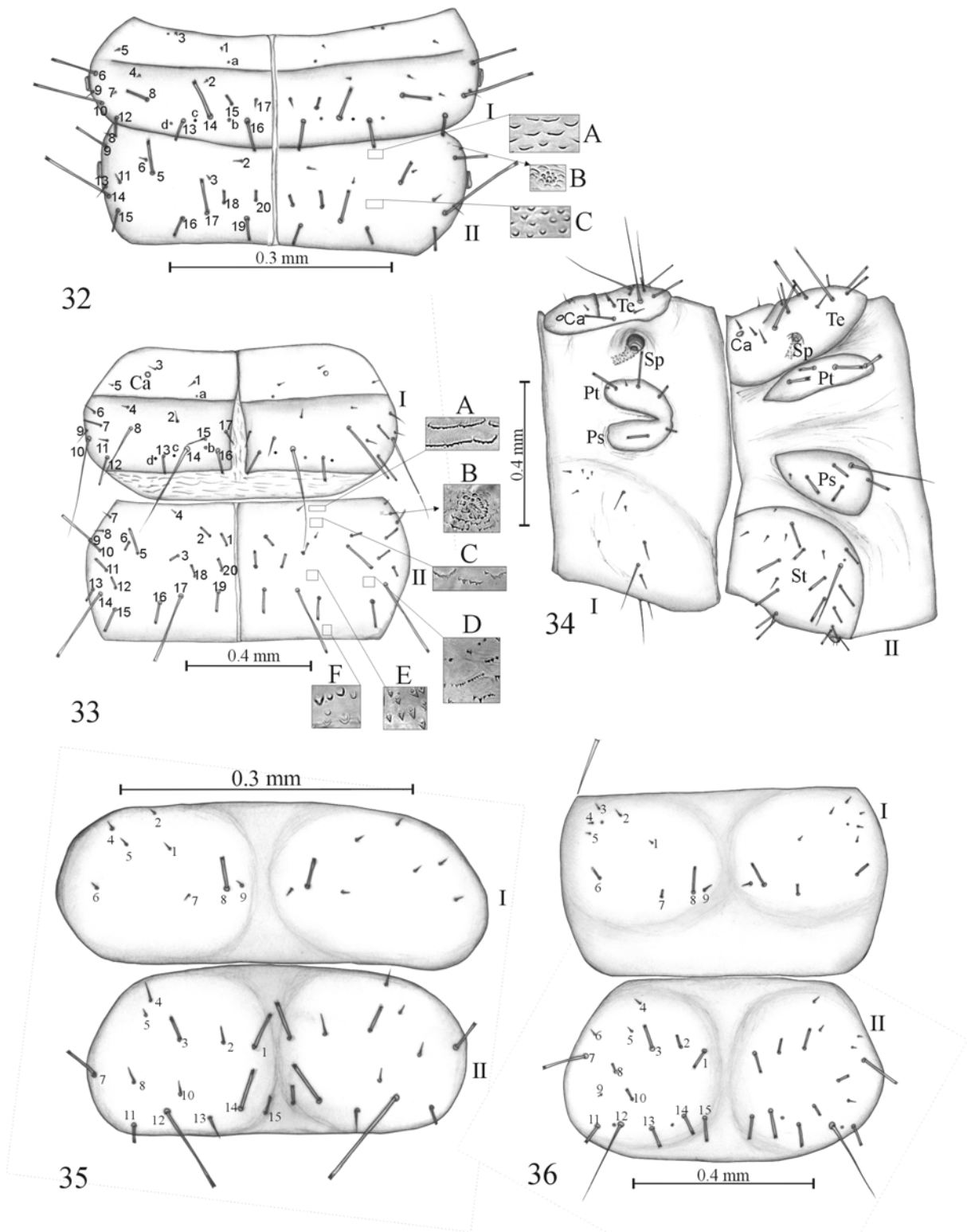
Figs 32-36. – *Rabigus tenuis*. 32, 32 A-C, 35 – 1st instar larva; 33, 33 A-F, 34, 36 – mature larva. 32, 33 – Abdominal tergites I and II (a, b … – codes of pores, Ca – coeloconic sensilla, 1, 2… – codes of setae); 32 A, C - microstructure of abdominal tergite II; 32 B – sensilla; 33 A, C, D-F - microstructure of abdominal tergite II; 33 C – sensilla; 34 – abdominal segments I and II in lateral aspect (Ca – coeloconic sensilla, Ps – parasternite, Pt – paratergite, Sp – spiracle, St – sternite, Te – tergite, 1, 2… – code of setae); 35, 36 – abdominal sternite I and II (1, 2… – codes of setae).
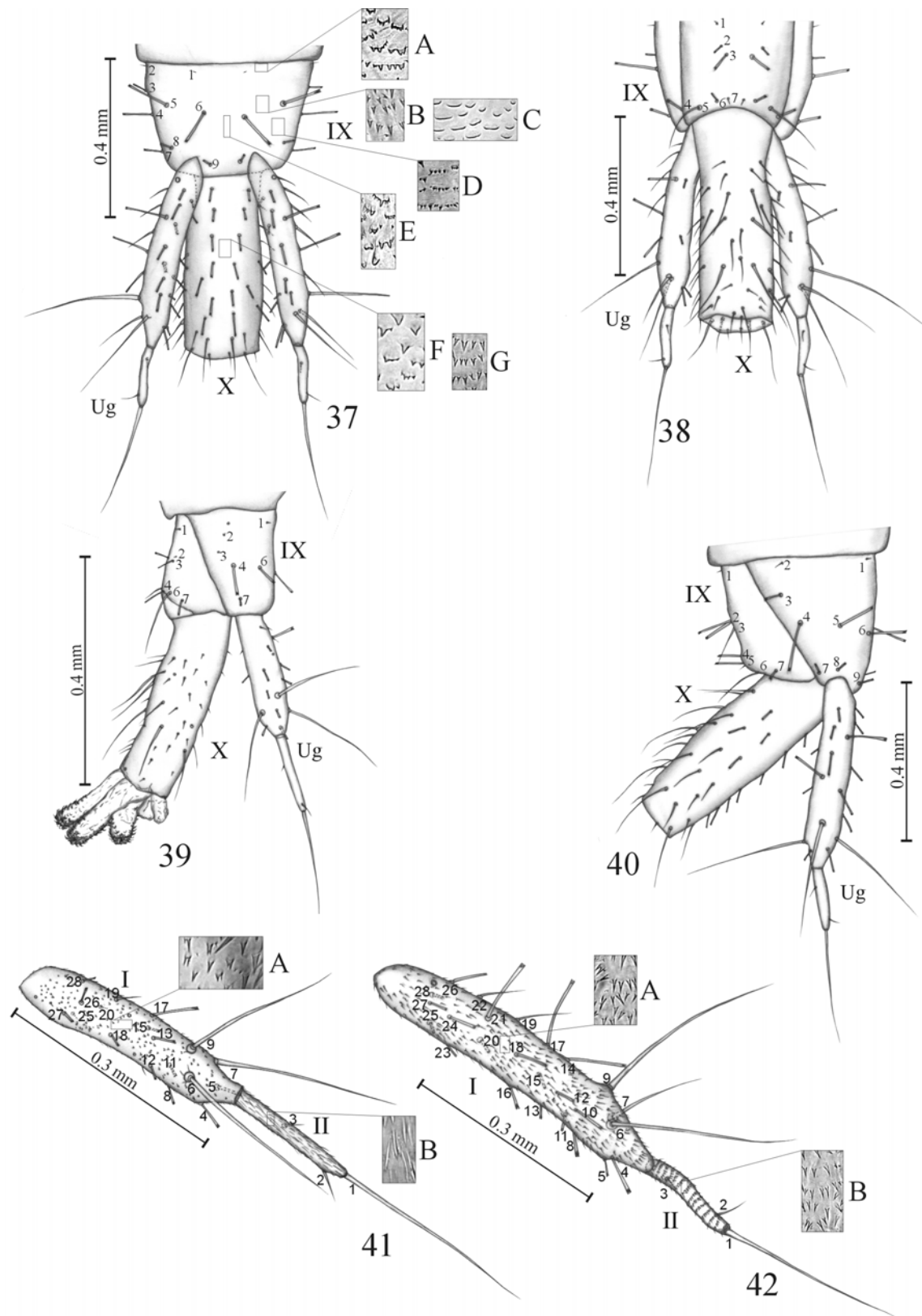
Figs 37-42. – *Rabigus tenuis*. 39, 37C, 37G, 41, 41A, 41B – 1st instar larva; 37, 37A, 37B, 37D-F, 38, 40, 42, 42A, 42B – mature larva. 37, 38 – Abdominal segment IX and X in dorsal aspect (37) and ventral aspect (38) (Ug – urogomphus); 37A-E – microstructure of abdominal segment IX; 37F-G – microstructure of abdominal segment X; 39, 40 – abdominal segment IX and X in lateral aspect (Ug – urogomphus, 1, 2… – codes of setae); 41, 42 – right urogomphus in dorsal aspect (I, II – segments of urogomphus, 1, 2… – codes of setae), 41A, 42A – microstructure of urogomphus of segment I; 41B, 42B – microstructure of urogomphus of segment II.
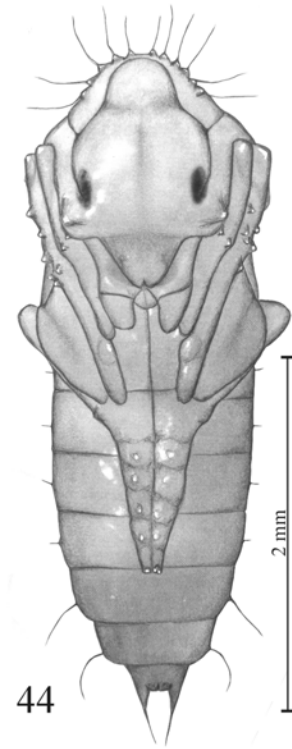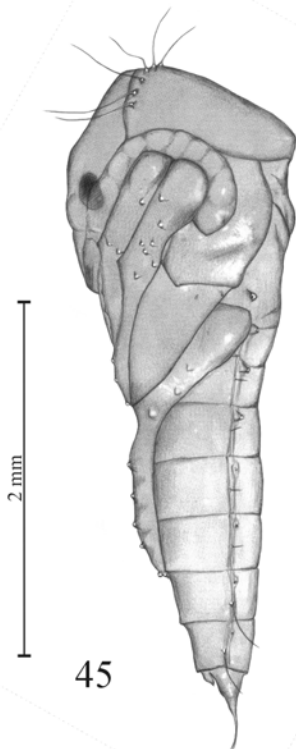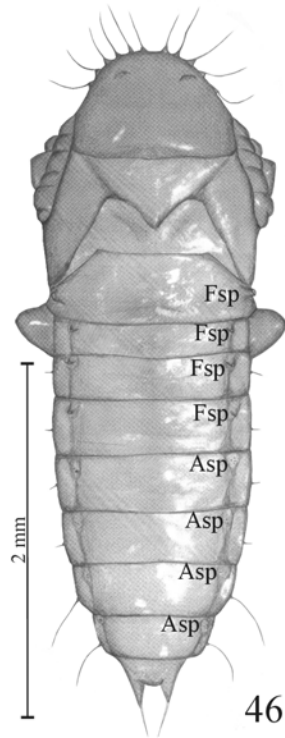
Figs 43-46. – *Rabigus tenuis*. 43 – cocoon; 44-46 – pupa in ventral aspect (44), lateral aspect (45), dorsal aspect (46) (Fsp – functional spiracles, Asp – atrophied spiracles).
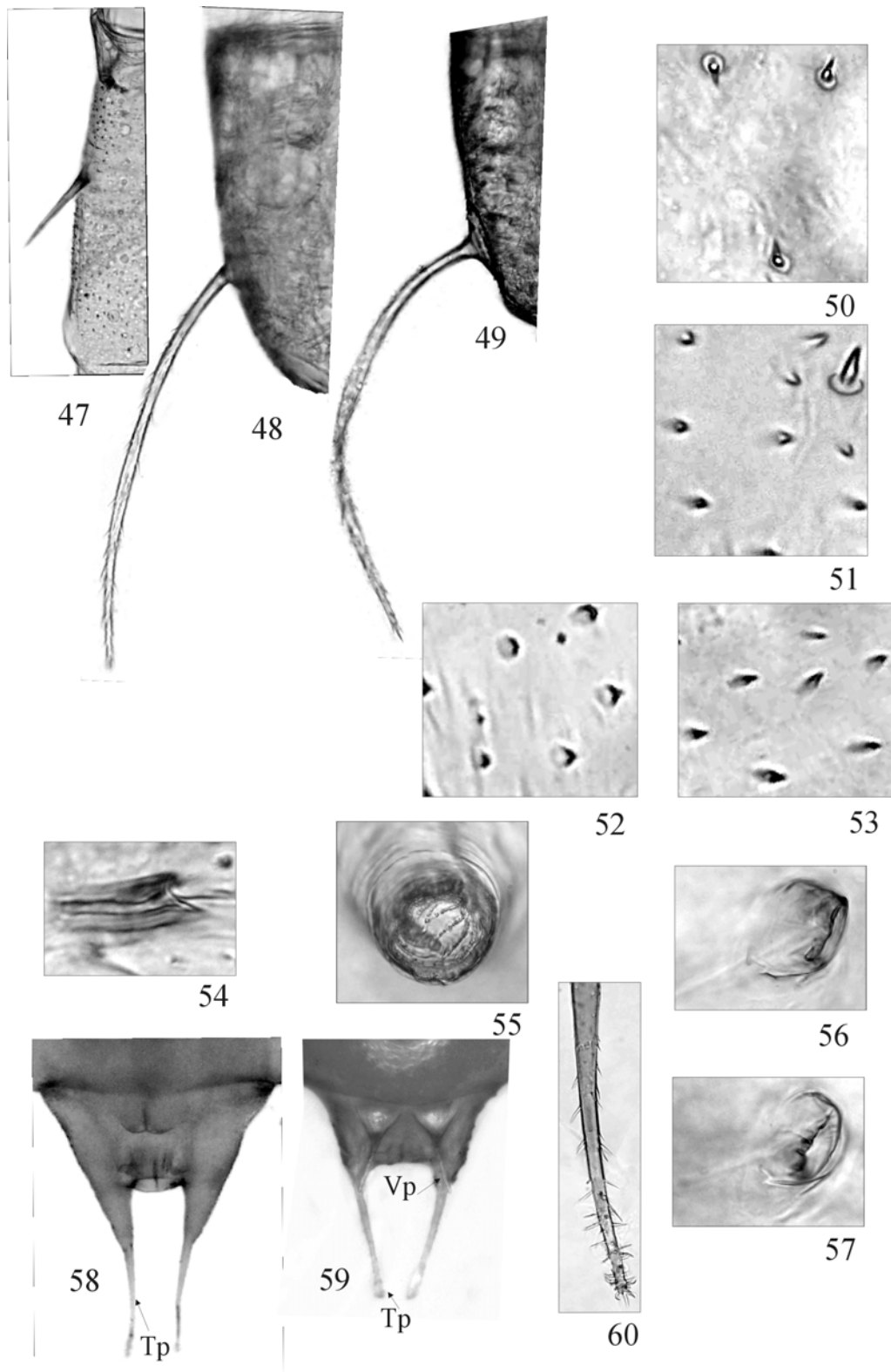
Figs 47-60. – *Rabigus tenuis*, pupa. 47-49 – Lateral margin with setiform projection of abdominal segment III (47), VII (48) and VIII (49); 50–53 – microstructure of the abdomen: central part of abdominal tergite III (50), anterior part of tergite IV (51), tergite V (52), tergite VII (53); 54 – lateral cuticular structure of the first abdominal tergite; 55 – spiracles functional; 56, 57 – spiracles atrophied; 58, 59 – terminal sternite of male (58) and female (59) (Tp – terminal prolongation, Vp – ventral prolongation); 60 – terminal prolongation.
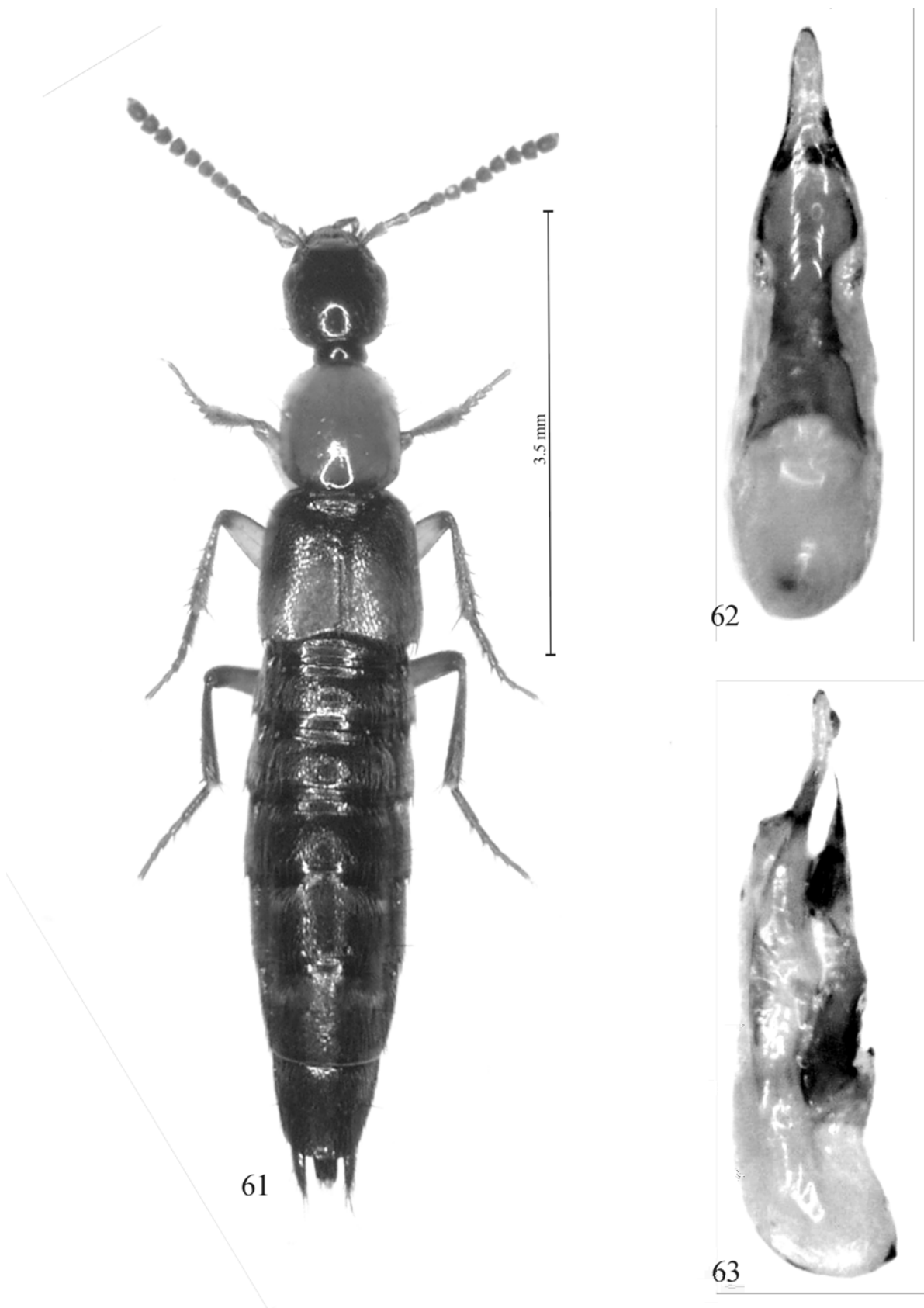
Figs 61-63. – *Rabigus tenuis*, adult. 61 – Habitus; 62, 63 – aedeagus in ventral aspect (62) and lateral aspect (63).

Fig. 64. – The intensity of oviposition of 6 females of *Rabigus tenuis* (at temperature of 24°C±3).

TABLE 1

Occurrence in the rearing of the different developmental stages of *Rabigus tenuis* at the daily temperature of 24°C (±3) (L_{1-2} larval instars, ?=possibility occurrence, ^{NG}=new generation, ^{OG}=old generation).

Egg																		
L₁								?	?									
L₂								?	?									
L₃									?	?								
Prepupa									?	?	?							
Pupa									?	?	?							
^{NG}Adult									?	?	?	?						
^{OG}Adult	?	?																
Decade	1	2	3	1	2	3	1	2	3	1	2	3	1	2	3	1	2	3
Month		IV			V			VI			VII			VIII			IX	

TABLE 2

Duration of immature stages of *Rabigus tenuis* at the daily temperature of 24ºC ±3) (N=number of specimens).

Duration (days)				
Stages	Range of duration	Mean	Mortality (%)	N
Egg	2-12	6	29.5	200
L_1	3-10	5.2	35.5	141
L_2	3-8	5.6	42.9	91
L_3	3-8	4.3	38.5	52
Prepupa	2-5	3.5	18.8	32
Pupa	5-9	6.7	11.5	26
Completed development	**23-41**	**26**	**88.5**	**23**

TABLE 3

The morphological differences between L_1 and L_3 of *Rabigus tenuis* (Fe=profemur, Tb=protibia, Tu=protarsungulus; Nrs=number of setae, Nrl=number of solenidium; (*1, 2,…*)=codes of lacking setae; Micr=microstructure; measurements in mm)

Character	L_1	L_3	Figure
Head			
Width	0.46-0.48	0.65-0.68	-
Length	0.58-0.64	0.83-0.90	-
Colour	yellowish-brown	brown	-
Ratio length to width of head	1.3	1.2	12, 13
Nrs: dorsal side-epicranial part (E)	28 (*15, 26*)	32	12, 13
Length ratio of antennal segments: I:II:III:IV respectively	1:2.2:3:2.1	1.0:1.9:2.1:1.1	16, 18
Ratio width (y) to length (x) of antennal segment I	y/x 1.8 x	y/x 1.1x	16, 18
Ratio length to width of antennal segment II	1.5 x	2.3x	16, 18
Ratio length to width of antennal segment III	1.8 x	2.5x	16, 18
Nrl: antennal segment III	1	2	16, 18
Ratio length to width of cardo	1.1 x	1.3x	24, 25
Ratio length to width of stipes	2.1 x	2.8x	24, 25
Length ratio of cardo and stipes	1:1.9	1:1.5	24, 25
Length ratio of maxillary palp of segments: I:II:III:IV respectively	1.1:1.6:1.5:1	1.5:1.9:1.7:1	24, 25
Nrs: stipes	5	7	23, 24, 25
Length ratio of mala and segment I of maxillary palp	1:1.1	1:1.4	23, 24, 25
Ratio length to width of segment I of maxillary palp	1.2	1.8	24, 25
Ratio length to width of segment II of maxillary palp	2.1	2.4	24, 25
Thorax			
Width of pronotum	0.44-0.45	0.69-0.79	-
Nrs: Fe, Tb, Tu respectively	11 (*3,5,9,12,14,16,17,19-24*), 9 (*4,5,8-11,16-18*), 2 (*3*)	24, 18, 3	30, 31
Abdomen			
Colour of terigite	colourless	grey-white	-
Colour of sternite	colourless	yellowish-white	-
Nrs: terigite I	32 (*11*)	34	32, 33
Nrs: tergites II-VIII	30 (*1, 4, 7, 10, 12*)	40	32, 33
Nrs: sternite I	16 (*3*)	18	35, 36
Nrs: sternites II-VIII	26 (*6, 9*)	30-32	35, 36
Nrs: tergite IX	12 (*5, 8, 9*)	18	37, 39, 40
Nrs: sternite IX	12 (*5*)	14	38, 39, 40
Nrs: urogomphus I	18 (*10, 14, 16, 21-24*)	25	41, 42
Length ratio of urogomphus segment I, II and apical seta	1.8:1:1.6	3.5:1:2.0	41, 42
Micr: abdominal tergites I-IX	-	-	32A,C, 33A,C-F, 37A-E,
Micr: abdominal tergite X	-	-	37F, 37G
Micr: urogomphus	-	-	41A, 41B, 42A, 42B

DISCUSSION

On the basis of their morphology, the eggs of 40 Central European species of Staphylininae Latreille, 1802, have been categorized into nine groups (STANIEC & PIE-TRYKOWSKA-TUDRUJ (2007b). Following this classification, eggs of *R. tenius* were included into the *Philonthus atratus* group, which comprises such species as: *Philonthus atratus* (Gravenhorst, 1802), *P. corvinus* Erichson, 1839, *P. lepidus* (Gravenhorst, 1802), *P. micans* (Gravenhorst, 1802), *P. punctus* (Gravenhorst, 1802), and *P. rubripennis* Stephens, 1832. Morphological characters that distinguish the egg of *R. tenius* from the eggs of species mentioned above cover a) the number of non-

branched longitudinal ridges 35; b) aeropyles between longitudinal ridges in 10 rows each of 6-8 aeropyles; c) moderately widened end of posterior projection (this feature is shared with *P. atratus*, *P. corvinus* and *P. lepidus*); d) ratio of the length of egg to the length of its posterior projection 2.8-5.6:1.0; e) length: 0.90-1.04mm, similar to the size of the egg of *P. rubripennis* 0.98-1.10mm.

The morphological differences between L_1 and L_3 of *R. tenuis* are listed in Table 3.

Out of 63 genera representing the subtribe Philonthina Kirby, 1837 in the world, only the morphology of the larval stages of species belonging to a few genera are known so far (HERMAN, 2001). Morphological characters distinguishing the mature larva of *Rabigus* from the other described larvae of the subtribe Philonthina (POTOTSKAYA, 1967; KASULE, 1970; JAMES et al., 1971; TOPP, 1978; BOLLER, 1983; SCHMIDT, 1994; SCHMIDT, 1996; STANIEC, 2004; CHANI-POSSE, 2006) are as follows: 1) body length: 6.10-7.10mm, head width: 0.65-0.68mm; 2) head about 1.2 times as long as wide, almost parallel-sided; 3) each side of head with four stemmata in the cluster; 4) apotome slightly extending beyond tentorial pits; 5) length ratio of anntenal segments I-IV 1.0:1.9:2.1:1.1 respectively; 6) sensory appendage of anntenal segment III almost half as long as segment IV; 7) anterior margin of nasale with nine teeth, paramedian teeth about 2.1 times as long as median tooth; 8) epipharynx with four bunches of straight, long hairs each and 14 cuticular processes posteriorly (Fig. 20); 9) length ratio of segments I-IV of maxillary palp: 1.5:1.9:1.7:1.0 respectively; 10) length ratio of mala and segment I of maxillary palp: 1:1.4; 11) length ratio of segments I-III of labial palps 2.1:1.4:1.0 respectively; 12) ligula setose, 2.5 times as long as wide at base; almost as wide as segment I of labial palp at the base, almost as long as segment I of labial palp; 13) mandible (Fig. 22) with uneven inner margin, without serrations; 14) tibial comb absent; 15) tarsungulus with three setae; 16) segment IX with pair of two-segmented urogomphi; 17) length ratio of pygopod and urogomphi (excluding apical seta) 1:1.2; 18) length ratio of segments I and II of urogomphus and apical seta 3.5:1:2.0 respectively; 19) most setae on abdominal segments and urogomphi rod-shaped and frayed apically; 20) microstructure of urogomphi as in Figs 42A; B.

Comparison of the morphological characters of the larval genera of *Rabigus* and the other genera of the subtribe Philonthina reveals that the mature larva of *R. tenuis* shares the majority of generic characters with those of the genus *Philonthus* (KRANEBITTER & SCHATZ, 2002; PIETRYKOWSKA-TUDRUJ & STANIEC, 2006; STANIEC & PIETRYKOWSKA-TUDRUJ, 2007a; CHANI-POSSE, 2006). The only character that distinguishes the larva of *R. tenuis* from the known larvae of the genus *Philonthus* is the shape of the anterior margin of nasale: *R. tenuis* third lateral teeth (Lt_3) shorter than the first lateral teeth (Lt_1); *Philonthus aerosus* Kiesenwetter, 1851, *P. punctus* (Gravenhorst, 1802) and *P. rubripennis* (Stephens, 1832) third lateral teeth (Lt_3) longer than the first lateral teeth (Lt_1). However, we can assume that the shape of nasale and the length of tooth is a variable character within the genus. In order to confirm this hypothesis it is necessary

to perform additional morphological studies of other species of *Philonthus* and *Rabigus*. Generally, as far as is known now, larval data do not support a separate generic status of *Rabigus*.

The morphology of the pupa for members of the genus *Rabigus* had never been studied up to now. The state of knowledge of Philonthina pupae is negligible, as is the case with the larvae. The pupae of species belonging to only nine genera have been described so far (SZUJECKI, 1965; JAMES et al., 1971; SCHMIDT, 1994; SCHMIDT, 1996; STANIEC, 2001; 2002; 2003; 2004; STANIEC & KITOWSKI, 2004; STANIEC & PIETRYKOWSKA, 2005; STANIEC & PIETRYKOWSKA-TUDRUJ, 2007a). Of these, the descriptions of pupae of three genera: *Belonuchus*, *Cafius* and *Remus*, are too superficial and inaccurate to be included in the comparative analysis on the generic level. Therefore, we compared these stages of *R. tenuis* with those of species of closely related genera: *Bisnius* Stephens, 1829, *Erichsonius* Fauvel, 1874, *Gabrius* Stephens, 1829, *Hesperus* Fauvel, 1874, *Neobisnius* Ganglbauer, 1895 and *Philonthus*. The pupa of *R. tenuis* can be separated from known pupae of Philonthina by the following features: a) cocoon; b) hind tarsi slightly protruding over posterior margin of segment IV (morphological segment VI) clearly visible abdominal segment; c) six pairs of setiform projections on abdomen (four short and two long); d) 10-12 number of setiform projections on pronotum; e) antennae reaching almost two thirds of length of elytra; e) the structure of the atrophied spiracles; f) body length 3.43-3.82mm; g) pronotum 1.1 times as long as wide.

One of the above-mentioned characters i.e. the length of hind tarsi protruding over posterior margin of VI morphological abdominal segment, was not observed in any hitherto described species. In view of the current state of knowledge of the pupae, we can consider it as a feature of *Rabigus* at the genus level. The presence of a cocoon is a common feature of *Rabigus* and *Gabrius*. However, we should notice its shape in two genera. The cocoon in *R. tenuis* is oval, while in *Gabrius splendidulus* (Gravenhorst, 1802) it is more roundish. However, in order to find whether the length of hind tarsi and the cocoon shape is a stable character within genera, the pupae of other species of *Rabigus*, *Gabrius* as well as other genera should be studied. Generally, the pupa of *Rabigus* is the most similar in morphology to the pupa of *Philonthus* (STANIEC & PIETRYKOWSKA-TUDRUJ, 2007a).

ACKNOWLEDGEMENTS

REFERENCES

BOLLER F (1983). Zur Larvalmorphologie der Gattung *Philonthus* Curtis (Coleoptera, Staphylinidae). Spixiana, 6:113-131.

Burakowski B, Mroczkowski M & Stefańska J (1980). Chrząszcze Coleoptera – Kusakowate Staphylinidae. część 2, Katalog Fauny Polski, XXIII, Warszawa, 7:1-272.

Chani-Posse MR (2006). Larval morphology and chaetotaxy of *Philonthus* Stephens (Coleoptera: Staphylinidae) based on descriptions of eight species from Argentina. Annales Zoologici, 56:7-28.

Derunkov AV & Melke A (2001). Staphylinidae bez Micropeplinae i Pselaphinae. In: Gutowski JM & Jaroszewicz (eds), Katalog Fauny Puszczy Białowieskiej, IBL, Warszawa: 133-147.

Herman LH (2001). Catalog of the Staphylinidae (Insecta: Coleoptera) 1758 to the end of the second Millennium. VI. Staphylininae group (Part 3). Bulletin of the American Museum of Natural History, 265:3021-3839.

Hinton HE (1981). Biology of insects eggs. Vol. 2. Pergamon Press, Oxford New York Toronto Sydney Paris Fankfurt.

James GJ, Moore J & Legner EF (1971). The larval and pupal stages of four species of *Cafius* (Coleoptera: Staphylinidae) with notes on their biology and ecology. Transactions on the San Diego Society of Natural History, 16:279-290.

Kasule FK (1970). The larvae of Paederinae and Staphylinidae (Coleoptera: Staphylinidae) with keys to the known British genera. Transactions of the Royal Entomological Society of London, 122:49-80.

Koch K (1989). Die Käfer Mitteleuropas, Ökologie. Goecke & Evers Verlag, Krefeld.

Kranebitter P & Schatz I (2002). The larval instars of *Philonthus aerosus* Kiesenwetter (subgenus Kenonthus Coiffait) from the central Alps (Tyrol, Austria) with a comparison of the known species of the genus (Coleoptera, Staphylinidae). Entomologische Blätter, 98:61-74.

Lohse GA & Lucht WH (1989). Die Käfer Mitteleuropas. 1. Supplementband mit Katalogteil. Goecke & Evers Verlag, Krefeld.

Lucht WH (1987). Die Käfer Mitteleuropas, Katalog. Goecke & Evers Verlag, Krefeld.

Paulian R (1941). Les premiers états des Staphylinoides (Coleoptera) étude de morphologie comparée. Mémoires du Muséum National d'Histoire Naturelle, 15:1-361.

Pietrykowska-Tudruj E & Staniec B (2006). Description of the egg and larva of *Philonthus punctus* (Gravenhorst, 1802) (Coleoptera, Staphylinidae, Staphylininae). Deutsche Entomologische Zeitschrift, 53:179-192.

Pototskaya VA (1967). Opredelitel' lichinok korotkonadkrylykh zhukov evropeiskoi chasti SSSR. Academiya Nauk SSSR, Izdatel'stvo Nauka, Moskva.

Schmidt DA (1994). Notes on the biology and a description of the egg, third instar larva and pupa of *Neobisnius sobrinus* (Coleoptera: Staphylinidae). Transaction of the Nebraska Academy of Science, 21:55-51.

Schmidt DA (1996). Description of the immature of *Erichsonius alumnus* Frank and *E. pusio* (Horn) (Coleoptera: Staphylinidae). The Coleopterists Bulletin, 50:202-215.

Smetana A (1958). Fauna ČSR. Svazek 12. Drabčíkovití-Staphylinidae. I. Staphylinidae. (Řád: Brouci-Coleoptera). Československé Akademie Věd, Praha.

Smetana A (1959). Bestimmungstabelle der mitteleuropäischen Arten der Gattung *Philonthus* Curt. Sensu lato. Entomologische Blätter für Biologie und Systematik der Käfer, 54:140-175.

Solodovnikov AY (2007). Larval chaetotaxy of Coleoptera (Insecta) as a tool for evolutionary research and systematics: less confusion, more clarity. Journal of Zoological Systematics and Evolutionary Research, 45:120-127.

Solodovnikov AY & Newton A (2005). Phylogenetic placement of Arrowinini trib.n. with the subfamily Staphylininae (Coleoptera; Staphylinidae), with revision of the relict South African genus *Arrowinus* and description of its larva. Systematic Entomology, 30:3-44.

Staniec B (1991). Rzadkie Staphylinidae (Coleoptera) ze wschodniej Polski. Wiadomości entomologiczne, 10:207-213.

Staniec B (2001). A description of the pupa of *Philonthus quisquiliarius* (Gyll.) and *P. nigrita* (Grav.) (Coleoptera: Staphylinidae). Polish Journal of Entomology, 70:39-49.

Staniec B (2002). A description of the pupae of *Philonthus albipes* (Gravenhorst, 1802) and *P. varians* (Paykull, 1789) (Coleoptera: Staphylinidae: Staphylininae). Genus, 13:337-343.

Staniec B (2003). Description of the pupa of *Philonthus corvinus* Erichson, 1839, *P. micans* (Gravenhorst, 1802), and *P. punctus* (Gravenhorst, 182) (Coleoptera: Staphylinidae). Genus, 14:15-26.

Staniec B (2004). The pupae of *Ontholestes murinus* (Linnaeus, 1758), *Philonthus rectangulus* Sharp, 1874 and a supplement to the pupal morphology of *Philonthus succicola* Thomson, 1860 (Coleoptera: Staphylinidae). Genus, 15:37-46.

Staniec B & Kitowski I (2004). A description of the pupae of *Philonthus umbriatilis* (Gravenhorst, 1802), *P. lepidus* (Gravenhorst, 1802) and *Bisnius* (=*Philonthus* sensu lato) *nitidulus* (Gravenhorst, 1802) (Coleoptera: Staphylinidae). Genus, 15:47-58.

Staniec B & Pietrykowska E (2005). The pupae of *Gyrohypnus fracticornis* (Müller, 1776) and *Philonthus tenuicornis* Mulsant & Rey, 1853 (Coleoptera: Staphylinidae). Genus, 16:331-339.

Staniec B & Pietrykowska-Tudruj E (2007a). Developmental stages of *Philonthus rubripennis* Stephens, 1832 (Coleoptera, Staphylinidae, Staphylininae) with comments of its biology. Deutsche Entomologische Zeitschrift, 54:95-113.

Staniec B & Pietrykowska-Tudruj E (2007b). Comparative morphology of the eggs of the sixteen Staphylininae species (Coleoptera; Staphylinidae). Deutsche Entomologische Zeitschrift, 54:235-252.

Szujecki A (1965). Obserwacje nad rozwojem i biologią *Philonthus fuscipennis* Mann. (Coleoptera, Staphylinidae). Fragmenta Faunistica, 12:165-175.

Szujecki A (1980). Klucze do oznaczania owadów Polski, Chrząszcze – Coleoptera, cz. 24c, Kusakowate- Staphylinidae, Kusaki- Staphylininae. Państwowe Wydawnictwo Naukowe, Warszawa.

Topp W (1978). Bestimmungstabelle für die Larven der Staphylinidae. In: Klausnitzer B (ed), Ordung Coleoptera (Larven). Bestimmungsbücher zur Bodenfauna Europas, Berlin: 10:304-334.

Light thresholds for colour vision in workers of the ant *Myrmica sabuleti* (Hymenoptera, Formicidae)

Marie-Claire Cammaerts & David Cammaerts

Faculté des Sciences, CP 160/11, Université libre de Bruxelles, 50, Av. F. Roosevelt, 1050, Bruxelles, Belgium
e-mail: mtricot@ulb.ac.be

ABSTRACT. Previous studies suggested that workers of the ant species *Myrmica sabuleti* have different light thresholds for distinguishing different colours. Here we assess these thresholds and find that the light thresholds required to distinguish colours from grey are lower than those necessary to discriminate between two colours. The two thresholds are somewhat lower for ants trained under low versus high light intensity. In every case, the ants' threshold decreases from red to violet. All these thresholds are lower than those required for perceiving shapes. The visual system of workers of *M. sabuleti* under very low light intensity may thus consist of discriminating only coloured spots from grey and under slightly higher light intensity, differently coloured elements where the eyes are used in superposition mode. Under high light intensity, these ants see (although not sharply) shapes and lines, using their eyes in apposition mode. Moreover, workers of this species demonstrated their best colour discrimination in seeing the colours yellow and blue under high light intensity, and green and violet under low light intensity. Therefore, these ants' visual system may be adapted to the quantitative and qualitative variations in natural light during the day.

KEY WORDS : colour vision, eyes, *Myrmica sabuleti*, perception threshold, vision

INTRODUCTION

Though ants primarily use chemical signals to perform most of their tasks (communicating, following a trail, perceiving marked areas), they also need some visual perception to accomplish several activities (foraging, returning to the nest after having discovered a new food source or new nest site) (OLIVEIRA & HÖLLDOBLER, 1989; CHAMERON et al., 1998; SALO & ROSENGREN, 2001; PASSERA & ARON, 2005). Insect vision has previously been studied in detail, but most authors have worked on insects with large eyes and good vision (Odonata, Lepidoptera, Diptera, Hymenoptera such as wasps, bees etc…) (WEHNER, 1981 and references therein). In ants, this field of study is in its infancy and tends to be physiological in nature, e.g., JANDER (1957), VOWLES (1965) and VOSS (1967). Generally, the ants studied so far have large eyes (e.g. *Formica* sp*., Cataglyphis bicolor, Gyganthyops destructor*) (WEHNER, 1981). The visual system in ants with (comparatively) small eyes has scarcely been studied. Given that ethological studies have already been conducted on *Myrmica sabuleti* Meinert 1861 (CAMMAERTS & CAMMAERTS, 1980), we decided to investigate this species' visual perception (CAMMAERTS, 2004 a; 2005; 2006; 2007 a; b). During the study of colour perception in workers of *M. sabuleti*, it was found that, under high light intensity, these ants were sensitive essentially to yellow and blue, while under low light intensity their highest sensitivities occurred for green and violet. Consequently it was presumed that these workers may have different light thresholds for different colours (i.e. different minimum light intensities necessary to perceive different colours). In the present paper, we investigate this issue, connect the results to previous ones, propose a visual system for workers of *M. sabuleti*, and compare our conclusions to those of other authors. This may be of interest because visual thresholds have not yet been precisely assessed in

insects even if many studies have been conducted on their visual perception (for instance CHITTKA, 1996; GIURFA et al., 1996; 1997; WEHNER, 1981; BRISCOE & CHITTKA, 2001; VOROBYEV et al., 2001; KELBER et al., 2003).

MATERIALS AND METHODS

Collection and maintenance of ants

Colonies of *M. sabuleti* were collected from Höghe Martelingen (Luxembourg; 49° 40' 30" N, 5° 45' 00" E) and from the Aise valley (Belgium; 49° 49' 39" N, 5° 15' 26" E). They were divided into a total of 30 smaller experimental colonies (5 series, labelled A to E), of six colonies (numbered 1 to 6), demographically similar, each containing about 250 workers, a queen and brood. These colonies were maintained in a laboratory, in a window-less room, at constant temperature (20°C±1°C) and humidity. Light was provided by OSRAM concentra lamps (60W) attached to the ceiling. The spectrum of this light was measured using a grating spectrograph (an Acton Spectrapro-500i) with CCD camera (Princetin Instrument TEA/CCD-1100-PF) detection and an optical fibre probe. The slit opening was 100μm and the grating was 600grooves/mm (500nm blaze). The spectrum was obtained by registering successive sections of 80nm, with an overlap of 45nm, the probe being maintained in front of an OSRAM concentra lamp, after these sections were assembled. The entire resulting broadband spectrum (shown in Fig. 2) revealed that the illumination contained all wavelengths of visible light and almost no UV light. The light intensity was assessed using a luxmeter (a Testoterm 0500 luxmeter built by Testoterm GmbH & Co (D-7825, Lenzkirch)). Two light intensities, 10,000 lux and 600 lux, were used in the course of our study. Light intensity was adjusted using a dimmer such that the intensity of illumination and not the shape of the wavelength spec-

trum was changed. These light intensities were previously used to reveal the capability of workers of *M. sabuleti* to discriminate colours from greys and from one another (Cammaerts, 2007 a).

The ants nested in one or two glass tubes half-filled with water, a cotton plug separating the ants from the water (Fig. 1). The glass tubes were deposited into a polyethylene tray (47cm x 22cm x 7cm) whose borders were covered with talcum and the tray served as a foraging area. Sugared water was permanently provided in a small glass tube closed by a cotton plug. Pieces of dead cockroach were provided twice a week on a small piece of glass when no experiments were planned or performed, since this meaty food was used as a reward during the training phases of each experiment (see experimental protocol).

Experimental apparatus

Experimental apparatuses were built of paper (Canson ®) of the following colours: grey, red, yellow, green, blue, and violet, these names being the ones given by Canson, and expressing only how these colours appear to the human eye. The spectra of the broadband emission of the light reflected by (or transmitted through) each coloured paper were measured using the above- described spectrograph (with CCD camera detection and an optical fibre probe) by holding the probe in front of a piece of paper of each colour with a lighted OSRAM concentra lamp being located either above or, more easily behind, the paper. These measurements were difficult because very little light reached the fibre probe. Nevertheless, the light spectra reflected by (or transmitted through) the grey paper had no maximum whereas those by (or through) the other coloured papers yielded maxima around 640nm (red), 550nm (yellow), 525nm (green), 425nm (blue), 445nm and 375nm (violet), the last extending up to about 360nm. To confirm these measurements, pieces (2cm x 2cm) of paper of each colour were boiled for 5 minutes in 10mL of water, tingeing the water in the respective colour. We checked that the colours of the tinged waters were exactly the same as those of the corresponding boiled papers. Then, the spectra of the light absorbed by the different coloured waters were obtained using a CARY 50-varian UV-visible spectrophotometer (Cary, USA; sensitivity range: 200-1,000nm; maximum scan rate of 24,000nm per minute; Xenon lamp) and the Cary Win UV software. Next, based on the spectrum of the delivered light (Fig. 2, upper graph) and of the spectra of the light absorbed by the waters tinged by the papers, the spectra of the light reflected by each of the coloured papers were calculated using the relation $Lr(=t)=Lo/10^{La}$ where $Lr(=t)$ is the reflected (or transmitted) light, Lo is the delivered light and La is the absorbed light. These calculated spectra are shown in Fig. 2 (lower graphs, above the photo of the apparatus) and are in agreement with the spectra obtained using the grating spectrograph. Small differences are likely due to the differences between the xenon lamp in the spectrophotometer and the OSRAM lamp used with the grating spectrograph. The light intensity reflected by grey and each coloured paper was measured using the luxmeter as detailed above and was the same for all the papers under low light intensity, and

nearly identical under high light intensity. Evidently, the light intensity reflected by the used papers varied with the intensity of the delivered light, which was therefore standardised for all the manipulations (600 or 10,000 lux as stipulated in the above paragraph).

Each experimental apparatus consisted of a disk (diameter=8cm) made of two half-disks of two differently coloured papers attached by means of a piece of glued paper (Fig. 2). To determine the ants' thresholds that allow discrimination between grey and colour, one half-disk was made of grey paper and the other of either red, yellow, green, blue, or violet paper. To determine thresholds that allow ants to distinguish between two colours, the two half-disks were made of two differently coloured papers. The combinations used were red and yellow, yellow and green, green and blue, blue and violet, and violet and red (Fig. 2).

Each experiment was performed simultaneously on six colonies; identical but other (new) apparatus were used on the one hand for training the ants and on the other for testing them (see experimental protocol). Thus, a total of 12 experimental apparatuses were built to perform a single experiment.

Experimental protocol
(Appendix, upper part)

The protocol used the differential operant conditioning system to obtain the ants' conditioned response to a colour in the presence of grey or of another colour. This system, like the operant conditioning one (Cammaerts, 2004 c), generally consists of initially performing a control experiment before any training, then placing the animals in a situation where they are rewarded each time they give the correct response. Progressively, the animals associate the correct response to the presence of a reward. The system finishes by a test experiment to check the acquisition of the conditioning by the animals. After successful conditioning, the threshold (in our case the minimum light intensity necessary) to elicit the conditioned response (i.e. for responding to the correct colour) could be assessed by testing the animals under stepwise increases in stimulation. In the present work, the timing of the successive steps of the protocol is identical to that used to reveal the ants' light and dark adaptation (Cammaerts, 2005).

The experiments were conducted either under 10,000 lux or under 600 lux, each time simultaneously on the six colonies of a series maintained for four days under the respective experimental light intensity and having received no meat during these four days. The ants' visual thresholds for distinguishing colours from grey as well as colours from one another were assessed under the two light intensities, yielding a total of four series of experiments (each series involving five experiments: see tables). All the threshold assessments followed the same protocol. First, an experimental apparatus was deposited horizontally, on the tray of each of the six colonies of a series (an identical apparatus was used for each colony) and a control experiment was performed (see below: quantification of the ant response). Immediately thereafter, the apparatus was removed from the tray of each colony, and identical ones (those designed for the training phases) were deposited, also horizontally, on each tray. A

piece of dead cockroach was deposited, on a small piece of glass, on one of the two half-disks of the apparatus; the half-disk of the same colour for each colony; which is hereafter referred to as the "correct half-disk" (the one associated with the reward) (Fig. 1). This protocol enabled the ants to go through differential operant conditioning within six days. During that 6-day training period, the apparatuses were turned and relocated 6 to 12 times in order to avoid some efficient pheromone deposit by foragers as well as spatial learning by the ants (i.e. the learning of a localisation) (CAMMAERTS, 2004 b). Meat was replaced whenever necessary but not periodically to avoid temporal learning (i.e. learning of a given hour or periodicity) (CAMMAERTS, 2004 b). During this training phase, the ants progressively associated the "correct half-disk" to the presence of meat. After this training phase, the experimental apparatuses were removed from the foraging area, and those used during the control (those designed for the tests, free from any pheromonal deposits) were presented (at places differing from those where the apparatuses were located at the end of the training phase). A test was then conducted (see below: quantification of the ants' responses). Thereafter, the ants were conditioned again over three more days in the presence of the apparatus designed for training, the apparatus being once more randomly and not periodically turned and relocated three to six times during the three training days. After this second training phase, a second test was performed using the appropriate apparatus. Next, the ants were conditioned again for one day, and the following day was used to assess the visual threshold necessary for discriminating the "correct half-disk" from the other (grey or coloured) one. Here, the light intensity was lowered to 1 or 0.5 lux (this being nearly darkness) and a first test was performed. Then, the light intensity was progressively increased, step by step (Tables 1 to 4, column 1), and a test was conducted at each step. The experiment ended when at least as many ants responded correctly as had correctly responded during each of the two previously conducted tests (see above, conditioning protocol).

Quantification of the ant response (Appendix, lower part)

During the control, during the two tests (to assess the ants' conditioning) and during each test made with increasing light intensity (to assess the ants' threshold), the ants present on each half-disk presented to the six colonies were counted once for each colony, as quickly as possible (usually in 12 seconds) to avoid light adaptation, this process being then immediately repeated 14 more times, yielding a total of 180 counts (2 x 6 x 15, usually in three minutes). What we counted was the ants' responses, one ant being thus able to give several responses in the course of the counting time. The mean value of the fifteen counts was established separately for each half-disk, for each of the six colonies. Two mean values were thus obtained for each colony (see the table in the appendix). These 12 mean values allowed statistical analysis of ant response as follows: the difference between the mean value corresponding to the "correct half-disk" and that corresponding to the "wrong one" was calculated for each colony (for each test) and for the corresponding control. Then, the six differences obtained for a test were compared to the six corresponding differences obtained for the previously performed control by using the non-parametric Wilcoxon rank test (SIEGEL & CASTELLAN, 1988). The ants' responses were considered to be significant at P<0.05. This level of probability indicated that the ants can see the difference between the "correct and the wrong half-disk", enabling us to detect the lowest light intensity the ants required to see this difference (i.e. the ants' light threshold).

Additionally, the mean of the above-mentioned six mean values was calculated for each half-disk, for the control and for each of the tests. Tables 1 to 4 give these 'global means' as well as the calculated proportion of ants present on the "correct half-disk", for each control and each tests.

Common legend to Tables 1 to 4: Under either 10,000 lux or 600 lux, the ants (of series A to E, each consisting of six colonies) were trained to find food on a coloured half-disk (**in bold in the tables**) *versus* the other, differently coloured half-disk, as detailed in 'Materials and Methods' and summarised in the appendix. During the control (before the training), the test 1 (after 6 training days), the test 2 (after 3 more training days) and each of the tests conducted with increasing light intensity in order to assess thresholds, the ants were confronted with the two differently coloured half-disks free of food and of any ant secretions. Their responses were quantified via 15 counts for each half-disk (see 'Materials and Methods' and the appendix) by: - columns 2 and 3: their mean numbers present on each coloured half-disk; - column 4: the proportion of 'correct' responses; - column 5: the results of non-parametric Wilcoxon tests applied to the counted numbers of ants.
NS: non-significant result at P=0.05; → indicates the ants' threshold, with [when lying between two values.
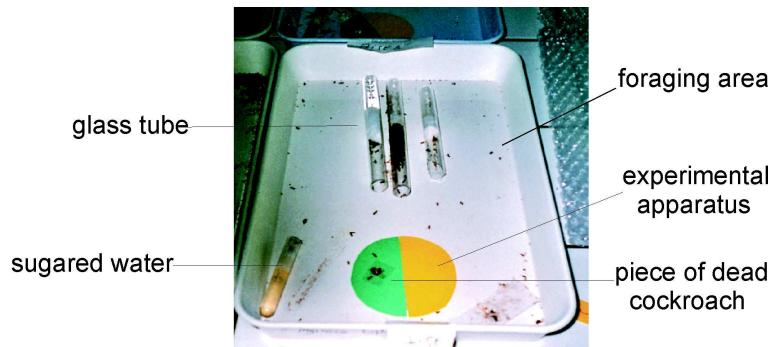
Fig. 1. – Experimental design. An experimental colony during a training phase.
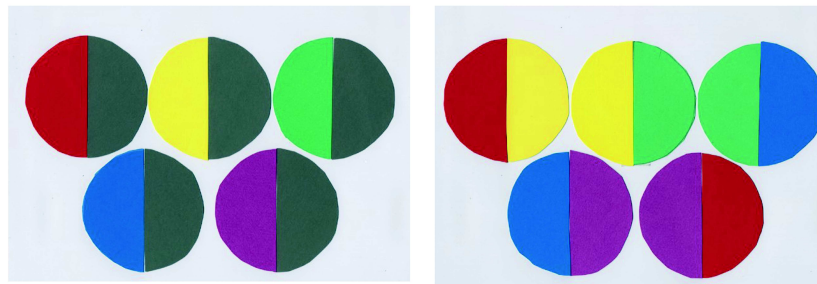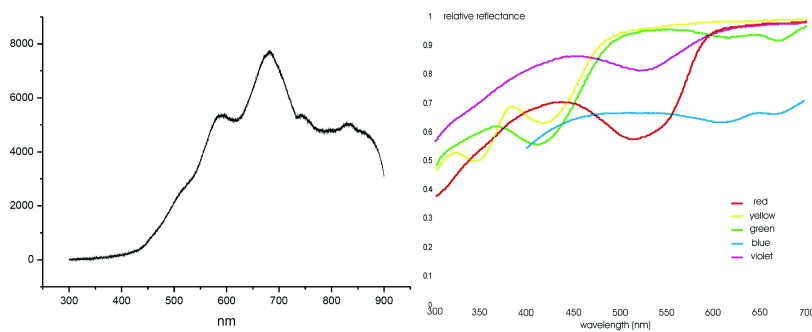
Fig. 2. – Spectra of the delivered light (upper left graph) and of the light reflected by the coloured papers (upper right coloured graphs). Experimental apparatus used to assess the ants' light thresholds for distinguishing colours from grey (lower left disks) and for distinguishing two colours (lower right disks).
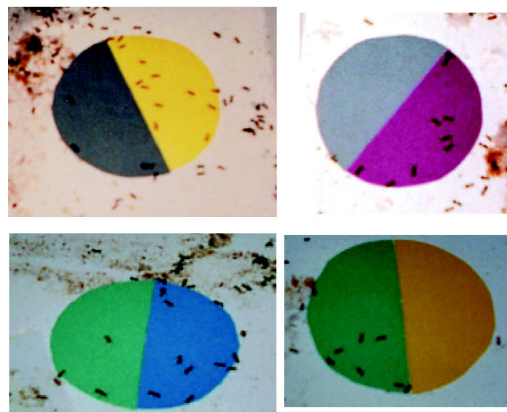
Fig. 3. – Examples of ant responses while assessing the lower light intensities they need to distinguish between colours and grey or between two colours.
Upper left: responses to yellow versus grey, after training under 10,000 lux
Upper right: responses to violet versus grey, after training under 600 lux
Lower left: responses to blue versus green, after training under 10,000 lux
Lower right: responses to green versus yellow, after training under 600 lux

TABLE 1

Ants' light thresholds for distinguishing colours from grey, after training under 10,000 lux

Series steps		Mean numbers on each colour		% correct responses	P
A		grey	scarlet		
Control		3.25	4.05	55	-
Test 1		4.51	8.09	64	0.031
Test 2		2.34	6.16	72	0.016
Lux	1	3.22	3.39	51	NS
	1.5	5.22	4.22	45	NS
	2	5.89	5.00	46	NS
	2.5	5.00	7.06	59	NS
	3	5.00	5.72	53	NS
	3.5	5.39	7.80	59	NS
	4	5.38	8.89	62	NS
	6	6.11	9.11	60	NS
	→8	6.17	9.83	61	0.031
	10	6.00	10.05	63	0.016
B		grey	yellow		
Control		1.96	2.16	52	-
Test 1		0.83	3.01	78	0.016
Test 2		0.44	1.99	82	0.016
Lux	1	3.28	3.34	50	NS
	1.5	2.78	2.78	50	NS
	2	2.33	2.00	46	NS
	2.5	1.67	2.72	62	NS
	3	1.78	2.39	57	NS
	3.5	1.56	2.45	61	NS
	→4	1.33	3.11	70	0.016
	6	1.83	3.50	66	0.016
C		grey	green		
Control		6.17	4.78	44	-
Test 1		1.22	3.32	60	0.031
Test 2		1.81	4.33	68	0.016
Lux	1	1.95	2.28	54	NS
	1.5	2.17	3.06	59	NS
	2	2.11	3.44	62	NS
	2.5	3.00	4.33	59	NS
	3	2.83	4.34	60	0.031
	→3.5	1.95	3.33	63	0.016
D		grey	blue		
Controle		2.34	1.98	46	-
Test 1		0.69	2.30	77	0.016
Test 2		1.26	2.93	70	0.016
Lux	1	3.33	3.89	54	NS
	1.5	1.94	2.56	57	NS
	2	2.39	2.56	52	NS
	→2.5	1.72	3.78	69	0.016
	3	1.89	3.61	66	0.016
	3.5	1.28	2.83	69	0.016
	4	1.72	3.06	64	0.016
	6	1.34	2.78	67	0.016
E		grey	violet		
Control		1.49	1.12	43	-
Test 1		1.33	2.76	67	0.031
Test 2		1.43	2.87	67	0.016
Lux	1	1.45	1.00	41	NS
	1.5	1.28	1.45	53	NS
	→2	0.78	2.28	75	0.016
	2.5	0.56	2.00	78	0.016
	3	0.50	1.78	78	0.016

TABLE 2

Ants' light thresholds for distinguishing colours from grey, after training under 600 lux.

Series Steps		Mean numbers on each colour		% correct responses	P
A		grey	scarlet		
Control		3.72	4.23	57	-
Test 1		2.82	7.24	72	0.016
Test 2		3.79	6.39	63	0.031
Lux	1	3.89	4.56	54	NS
	1.5	4.39	4.78	52	NS
	2	4.28	4.83	53	NS
	2.5	5.78	5.50	49	NS
	3	7.22	7.22	50	NS
	3.5	7.28	8.89	55	NS
	→4	5.95	11.28	65	0.016
	6	5.95	10.06	63	0.031
B		grey	yellow		
Control		3.37	3.25	49	-
Test 1		1.78	2.87	62	0.016
Test 2		2.91	4.86	63	0.016
Lux	1	2.94	2.33	44	NS
	1.5	2.83	2.89	50	NS
	2	2.00	2.94	60	NS
	→2.5	1.00	2.33	70	0.016
	3	1.33	2.83	68	0.016
C		grey	green		
Control		1.96	1.85	49	-
Test 1		1.49	4.34	74	0.016
Test 2		2.05	4.91	71	0.016
Lux	1	2.78	3.06	52	NS
	1.5	3.95	4.56	54	NS
	→2	2.83	4.72	63	0.016
	2.5	2.56	4.95	66	0.016
D		grey	blue		
Control		1.56	1.49	49	-
Test 1		0.97	2.11	69	0.016
Test 2		0.82	1.89	70	0.016
Lux	1	2.39	2.78	54	NS
	→1.5	2.06	3.72	64	0.016
	2	1.61	4.39	73	0.016
E		grey	violet		
Control		1.00	0.78	44	-
Test 1		0.56	2.26	80	0.016
Test 2		0.83	2.11	72	0.016
Lux	0.5	1.33	1.72	56	NS
	→1	0.67	1.22	65	0.031
	1.5	0.61	1.67	73	0.016

TABLE 3

Ants' light thresholds for distinguishing between two colours, after training under 10,000 lux.

Series Steps		Mean numbers on each colour		% correct responses	P
A		scarlet	**yellow**		
Control		4.11	3.35	45	-
Test 1		3.53	6.68	65	0.016
Test 2		2.64	5.64	68	0.016
Lux	1	3.17	3.00	49	NS
	1.5	3.61	3.78	51	NS
	2	2.50	2.67	52	NS
	2.5	3.17	3.00	49	NS
	3	3.67	3.28	47	NS
	3.5	3.78	3.39	47	NS
	4	3.33	3.61	52	NS
	6	2.78	4.17	60	NS
→8		2.61	8.72	77	0.016
	10	3.00	5.72	66	0.016
	12	3.50	5.33	60	0.016
B		yellow	**green**		
Control		2.26	1.58	41	-
Test 1		1.28	2.36	65	0.016
Test 2		1.82	3.13	63	0.016
Lux	1	2.22	2.95	57	NS
	1.5	3.45	3.56	51	NS
	2	2.89	3.56	55	NS
	2.5	3.39	4.33	56	NS
	3	3.22	3.06	49	NS
	3.5	3.56	3.44	49	NS
	4	2.67	3.17	54	NS
→6		1.78	3.56	67	0.016
	8	1.17	3.67	76	0.016
C		green	**blue**		
Control		3.35	3.66	52	-
Test 1		0.94	2.44	72	0.016
Test 2		0.89	2.92	77	0.016
Lux	1	3.00	2.28	43	NS
	1.5	3.00	2.78	48	NS
	2	2.61	2.78	52	NS
	2.5	2.39	1.94	45	NS
	3	2.83	2.50	47	NS
	3.5	2.78	2.78	50	NS
[	4	2.72	3.56	57	NS
→[	6	1.89	4.42	70	0.016
	8	1.44	3.94	67	0.016
D		blue	**violet**		
Control		1.40	1.22	47	-
Test 1		0.53	1.41	72	0.016
Test 2		1.04	1.98	72	0.016
Lux	1	2.06	2.00	49	NS
	1.5	2.00	1.72	46	NS
	2	1.95	1.67	46	NS
	2.5	1.83	1.56	46	NS
	3	1.67	1.56	48	NS
→3.5		1.00	2.06	67	0.031
	4	1.33	4.11	76	0.016
	6	0.50	1.89	79	0.016
	8	0.45	2.22	83	0.016
E		violet	**scarlet**		
Control		1.11	1.23	53	-
Test 1		0.47	1.86	80	0.016
Test 2		0.89	2.72	75	0.016
Lux 1		2.22	2.45	52	NS
	1.5	1.17	1.17	50	NS
	2	1.45	1.45	50	NS
→2.5		0.83	2.28	73	0.016
	3	0.67	1.95	74	0.016
	3.5	0.72	2.17	75	0.016
	4	0.72	2.00	74	0.016

TABLE 4

Ants' light thresholds for distinguishing between two colours, after training under 600 lux.

Series steps		Mean numbers on each colour		% correct responses	P
A		scarlet	**yellow**		
Control		6.20	5.53	47	-
Test 1		4.25	6.27	60	0.031
Test 2		2.25	3.99	64	0.016
Lux	1	2.83	3.11	52	NS
	1.5	4.45	5.45	55	NS
	2	3.50	3.28	48	NS
	2.5	3.22	4.11	56	NS
	3	3.17	4.33	57	NS
	3.5	3.06	4.95	62	NS
	4	2.94	4.39	60	NS
→/ 6		3.11	5.22	63	0.016
B		yellow	**green**		
Control		2.51	2.54	50	-
Test 1		3.65	6.38	64	0.031
Test 2		2.07	5.44	72	0.016
Lux	1	4.06	4.99	55	NS
	1.5	2.34	2.39	50	NS
	2	2.50	2.67	52	NS
	2.5	2.00	2.72	58	NS
	3	2.61	3.72	59	NS
→3.5		1.00	2.89	74	0.016
	4	1.28	3.39	73	0.016
	6	1.84	4.06	69	0.016
C		green	**blue**		
Control		4.25	3.60	46	-
Test 1		2.13	5.08	70	0.016
Test 2		2.33	4.90	68	0.016
Lux	1	1.22	2.05	63	NS
	1.5	2.28	2.89	56	NS
	2	1.72	2.95	63	NS
→2.5		1.17	3.50	75	0.016
	3	1.72	3.33	66	0.031
	3.5	1.78	3.83	68	0.016
D		blue	**violet**		
Control		2.38	2.13	47	-
Test 1		0.62	1.85	75	0.016
Test 2		0.89	2.29	72	0.016
Lux	0.5	1.89	1.89	50	NS
	1	1.22	1.28	51	NS
	1.5	1.61	1.83	57	NS
→2		0.78	2.22	74	0.016
	2.5	0.67	2.11	76	0.016
E		violet	**scarlet**		
Control		1.36	1.52	53	-
Test 1		0.61	1.39	70	0.016
Test 2		0.78	2.22	74	0.016
Lux	0.5	0.84	0.95	53	NS
	1	0.56	0.72	56	NS
→1.5		0.67	1.17	64	0.031
	2	0.61	1.95	76	0.016
	2.5	0.61	1.89	76	0.016
	3	0.39	1.61	81	0.016

RESULTS

Thresholds for distinguishing colours
from grey

After training under high light intensity, the ants could distinguish each presented colour from grey (Table 1). The lowest light intensities (=thresholds) required to perform this distinction were very low in general: about 8 lux for red, 4 lux for yellow (Fig. 3, upper left photo), 3.5 lux for green, 2.5 lux for blue and 2 lux for violet (Table 1). The threshold for discriminating a colour from grey thus decreased from red to violet.

After training under low light intensity, the proportion of ants having distinguished a colour from grey were generally lower than those having done so after training under high light intensity (Table 2). On the other hand, the lower light intensities required to see colours other than grey were generally smaller than those previously assessed (see above) but the same decrease from red to violet was observed. Indeed, the values were about 4 lux for red, 2.5 lux for yellow, 2 lux for green, 1.5 lux for blue and 1 lux for violet (Fig. 3, upper right photo) (Table 2).

Thresholds for distinguishing two colours
from one another

After having been trained under high light intensity, workers of *M. sabuleti* were able to discriminate all the presented colours from one another with nearly the same efficiency (Table 3). The lower light intensities (=thresholds) required to correctly respond to two presented colours were somewhat higher than those needed to see a colour other than grey; again, these light thresholds decreased from red to violet. More precisely, the thresholds for colour discrimination were about 8 lux for yellow versus red, 6 lux for green versus yellow, 5 lux for blue versus green (Fig. 3, lower left photo), 3.5 lux for violet versus blue and 2.5 lux for red versus violet (Table 3).

After training under low light intensity, the ants also distinguished each colour from another one, but the mean proportions of ants doing so were lower than those observed after having trained the ants under high light intensity (Table 4). The lower light intensities required to respond correctly to the two presented colours were all smaller than those required for correct responses after training under high light intensity; again, the values decreased from red to violet. In fact, the corresponding thresholds were about 5 lux for yellow versus red, 3.5 lux for green versus yellow (Fig. 3, lower right photo), 2.5 lux for blue versus green, 2 lux for violet versus green and 1.5 lux for red versus violet (Table 4).

DISCUSSION

The present work attempts to measure the lowest light intensities (the light thresholds) that workers of *M. sabuleti* require to be able to see colours other than grey and to be able to discriminate between two colours. These thresholds are very low, and those allowing discrimination between colours and grey are lower than those required to distinguish between two colours. After train-ing under high light intensity, the ants' thresholds are higher than those acquired after training under low light intensity. The lower thresholds observed after mainte-nance and training under low light intensity are in agree-ment with the light and dark adaptation previously revealed for the species (CAMMAERTS, 2005). In every case (colour versus grey or colour versus another colour; training under high or under low light intensity), the ants' thresholds decreased from red to violet.

Even if our experimental protocol and method of quan-tification may have their limitations, the conclusions remain valid since potential limitations are identical for all the experiments (use of same papers, lamps, instru-ments etc…) and the conclusions are qualitative and com-parative in nature. Although one might criticise our experiments because of a potential bias due to ant phe-romones, we believe this to be unlikely as the experimen-tal apparatuses were often relocated in the ants' foraging areas. Consequently, olfactory cues were likely not used by foragers when making their choices between two col-ours.

In a keystone paper on ant vision (especially colour vision), KRETZ (1979) showed that, for a given light intensity, the visual response varies with the wavelength used, i.e. increases from longer wavelengths (red) to shorter ones (violet). To obtain a similar response for red and violet, the author would need to decrease the light intensity (from red to violet); accordingly, the ant's visual thresholds would be higher for red and lower for violet, as is in agreement with our results.

On the other hand, it was previously shown (CAMMAE-RTS, 2007 a) that the ability of workers of *M. sabuleti* to discriminate a colour from grey or one colour from another one was highest for blue and yellow under 10,000 lux and for violet and green under 600 lux. This observa-tion is confirmed by the proportions of ants correctly responding during the two tests made before assessing the ants' thresholds obtained in the present work, and after having trained these ants under either 10,000 lux (Table 1) or 600 lux (Table 2). In these two mentioned tests as well as in the previous work on the subject (CAMMAERTS, 2007 a), the assessment concerned the ants' ability to dis-criminate between two broadband spectra. This is similar to the determination by VON HELVERSEN (1972, second part of his work) of the bee's abilities to discriminate between wavelengths. By detecting light thresholds for colour perception in ants, we estimate the spectral sensi-tivity of ants, similar to the measurements made by VON HELVERSEN (1972, first part of his work, Figs 6; 9; 11). Our results and those of VON HELVERSEN are in agree-ment: ants and bees present the best abilities for two wavelengths of the visible light and their sensitivity to wavelength increases from red to violet: i.e. with the light frequency.

Our results can also be compared to those of HORI et al. (2006) and of NEUMEYER (1981). HORI et al. (2006) trained bees with monochromatic lights associated with a reward of sucrose solution delivered to the antennae and proboscis for eliciting the proboscis extension reflex. The authors found that bees conditioned with a 540nm light stimulus also responded to a 618nm but not to a 439nm light stimulus, reacting, however, when this last stimulus

was switched off. According to the authors, this shows that the tested insects were not conditioned to increases in light intensity or temperature but effectively to colours (a fact we judge also true for our experiments) and that their results are in agreement with those of NEUMEYER (1981). This last author investigated successive colour contrast as well as colour constancy in bees by training freely flying insects to land on one of nine differently-coloured test fields. The author tested bees under various yellow and blue illuminations. In doing so, NEUMEYER (1981) revealed the bee's colour constancy and pointed out the chromatic adaptation of these insects, the most probable mechanism allowing colour constancy. In the present work, we show light adaptation for colour vision in workers of *M. sabuleti* and we obtained qualitatively identical colour discrimination under two light intensities, in favour of a colour constancy in this species.

CAMMAERTS (2005) measured light thresholds needed by workers of *M. sabuleti* to see an object. These "form thresholds" depend on the light intensity under which the ants are maintained. If maintained under 10,000 lux, the ants present a light threshold of 165 lux (an experimentally-assessed value); if maintained under 600 lux, they acquire a light threshold of 22.44 lux (a calculated value using the set up by CAMMAERTS (2005) function: thr=11.6xe$^{0.027i)}$. The present study goes beyond the perception of form and tests the ants' perception of colours other than grey as well as their distinction between two colours. The "form thresholds" (CAMMAERTS, 2005) are higher than the "grey/colour" and the "two different colours" thresholds. This suggests that, for precisely seeing form, the ants may use their eyes in apposition mode (WEHNER & GEHRING, 1999 p. 424), requiring higher light intensity. In contrast, superposition mode (WEHNER & GEHRING, 1999 p. 424) may be used to discriminate colours from grey or different colours, consequently requiring lower light intensity. In other words, superposition mode allows grey/colour distinction under very low light intensities, and colour/colour distinction under slightly higher light intensities. Under high light intensities, apposition mode allows ants to see lines and shapes (never very sharply because they fail in discriminating some lines and shapes from one another, CAMMAERTS, 2006). This succession of capabilities depending on light intensity differs from that of mammals, which perceive shapes and lines under low light intensities and distinguished colours only under rather high light intensities (WEHNER & GEHRING, 1999 p. 420). Under high light intensity, the ants' best abilities occur for yellow and blue; under low intensity, their best abilities are for green and violet (CAMMAERTS, 2007 a). Their colour perception ability shifts thus towards shorter wavelengths in response to decreasing light intensity. This allows for their colour vision to be adapted to shifting natural light conditions during the day. In other words, colour vision in ants may be qualitatively identical and quantitatively similar throughout the day.

Another, even lower light threshold might exist for ants: one in which they might see that something differs from darkness. Ants may be confronted with such a very low light threshold inside their nest, enabling them to orient themselves either towards the outside or the inside of the nest.

After having been maintained under low light intensity, the ants acquire a lower light threshold (CAMMAERTS, 2005; present paper). They thus became more sensitive to light after maintenance under low light intensity and even more so in darkness. Accordingly, the ants likely perceive being shifted from a bright environment to being placed under a red filter as being in near-darkness. On the other hand, a shift from darkness to red light would not be perceived as complete darkness. This resolves the polemic between authors about ants' sensitivity to red light and explains the results of DEPICKERE et al. (2004).

Light and dark adaptation (as conducted in the laboratory on *M. sabuleti:* CAMMAERTS, 2005 and present work) has been studied under natural conditions on *Formica polyctena* by MENZEL & KNAUT (1973). Those authors revealed two adaptations. A first adaptation occurs at sunrise while light intensity is still low and involves a major modification of pigment arrangement. A second light adaptation occurs thereafter, when light intensity increases. This cytological observation leads to the speculation that, during sunrise, the ants' eyes initially function in superposition mode and undergo some adaptation; they then change and function as apposition ones, once again undergoing some light adaptation. This interpretation agrees with our work (CAMMAERTS, 2005 and present study).

MENZEL & KNAUT (1973) studied the chromatic adaptation for several wavelengths in response to increasing light intensity, cytologically, in *F. polyctena*. This adaptation occurs in different cells and differs according to wavelength. This would explain one of our present results: thresholds for colour perception of workers of *M. sabuleti* depend on the colour and therefore on wavelength.

In one of his numerous works on bee visual perception, MENZEL (1981) demonstrated two thresholds in the detection of spectral stimuli: a lower one for the absolute detection of the stimulus and a higher one for the perception of colour hue. These observations echo those reported here for *M. sabuleti.* MENZEL (1981) termed the range lying between the two thresholds (the achromatic lower one and the chromatic higher one) the achromatic interval. The author concluded that, at light intensities near visual threshold, bees use neurally-derived achromatic signals: under such low light intensities, the output of all receptors from a single ommatidium is pooled in a neural strategy that produces achromatic signals. This deduction is also supported by the present results: workers of *M. sabuleti* use their eyes as superposition ones under light intensities nearly equalling the visual threshold values.

The capability of workers of *M. sabuleti* to distinguish colours versus grey on one hand, and different colours on the other, can be compared to the bee's ability to detect and discriminate coloured patterns (HEMPEL DE IBARRA et al., 2001; 2002). The summation of photoreceptor cell signals in bees under light intensity approaching thresholds values is corroborated by the study of VOROBYEV et al. (2001). At such low light intensities, the authors found that some experimentally-measured thresholds were lower than the theoretically-calculated ones. This is because, under very low light intensities, several photore-

ceptors 'work together' (i.e. their neural signals are pooled), yielding good visual perception, as also illustrated by the work of WARRANT et al. (1996).

Nonetheless, ants are not bees, and even if similarities with the bee visual system exist, ants present specific visual characteristics. As formulated in the review by MENZEL & BACKHAUS (1991), insects have specific adaptations in their colour vision systems, and research should concentrate on these species-specific adaptations. The present study, together with previous ones (CAMMAERTS, 2005; 2007 a), provides detailed information on the subject, supporting and expanding upon earlier knowledge.

ACKNOWLEDGEMENTS

REFERENCES

BRISCOE AD & CHITTKA L (2001). The evolution of colour vision in insects. Annual Revue of Entomology, 46:471-510.

CAMMAERTS M-C (2004 a). Some characteristics of the visual perception of the ant *Myrmica sabuleti.* Physiological Entomology, 29:472-482.

CAMMAERTS M-C (2004 b). Classical conditioning, temporal learning and spatial learning in the ant *Myrmica sabuleti.* Biologia, 59:243-256.

CAMMAERTS M-C (2004 c). Operant conditioning in the ant *Myrmica sabuleti.* Behavioural Processes, 67:417-425.

CAMMAERTS M-C (2005). Sensitivity and adaptation of *Myrmica sabuleti* workers (*Hymenoptera: Formicidae*) to light. Myrmecologische Nachrichten, 7:77-86.

CAMMAERTS M-C (2006). Discrimination visuelle de formes, de contours, de nombres d'éléments et de l'orientation d'un élément par la fourmi *Myrmica sabuleti.* Belgian Journal of Entomology, 8:43-54.

CAMMAERTS M-C (2007 a). Colour vision in the ant *Myrmica sabuleti* Meinert, 1861 (Hymenoptera: Formicidae). Myrmecologische Nachrichten, 10:41-50.

CAMMAERTS M-C (2007 b). Perspective vision in workers of *Myrmica sabuleti* Meinert, 1861 (Hymenoptera, Formicidae). Myrmecologische Nachrichten, 10:21-26.

CAMMAERTS M-C & CAMMAERTS R (1980). Food recruitment strategies of the ants *Myrmica sabuleti* and *Myrmica ruginodis.* Behavioural Processes, 5:251-270.

CHAMERON S, SCHATZ B, PASTERGUE-RUIZ I, BEUGNON G & COLLETT TS (1998). The learning of a sequence of visual patterns by the ant *Cataglyphis cursor.* Proceedings of the Royal Society of London, B, 265:2309-2313.

CHITTKA L (1996). Optimal sets of colour receptors and opponent processes for coding of natural objects in insect vision. Journal of Theoretical Biology, 181:179-196.

DEPICKERE S, FRESNEAU D & DENEUBOURG J-L (2004). The influence of red light on the aggregation of two castes of the ant, *Lasius niger.* Journal of Insect Physiology, 50:629-635.

GIURFA M, VOROBYEV M, KEVAN P & MENZEL R (1996). Detection of coloured stimuli by honeybees; the role of chromatic and achromatic contrasts. Journal of Comparative Physiology A, 178:699-709.

GIURFA M, VOROBYEV M, BRANDT R, POSNER B & MENZEL R (1977). Discrimination of coloured stimuli by honeybees: alternative use of achromatic and chromatic signals. Journal of Comparative Physiology A, 180:235-243.

HEMPEL DE IBARRA N, GIURFA M & VOROBYEV M (2001). Detection of coloured patterns by honeybees through chromatic and achromatic cues. Journal of Comparative Physiology A, 187:215-224.

HEMPEL DE IBARRA N, GIURFA M & VOROBYEV M (2002). Discrimination of coloured patterns by honeybees through chromatic and achromatic cues. Journal of Comparative Physiology A, 188:503-512.

HORI S, TAKEUCHI H, ARIKAWA K, KINOSHITA M, ICHIKAWA N, SASAKI M & KUBO T (2006). Associative visual learning, color discrimination, and chromatic adaptation in the harnessed honeybee *Apis mellifera* L. Journal of Comparative Physiology A, 192:691-700.

JANDER R (1957). Die optische Richtungsorientierung der Roten Waldameise (*Formica rufa* L.). Zeitschrift für Vergleichende Physiologie, 40:162-238.

KELBER A, VOROBYEV M & OSORIO D (2003). Animal colour vision – behaviourl tests and physiological concepts. Biological Reviews, 78:81-118.

KRETZ R (1979). A behavioural analysis of colour vision in the ant *Cataglyphis bicolor (Formicidae, Hymenoptera).* Journal of Comparative Physiology A, 131:217-233.

MENZEL R (1981). Achromatic vision in the honeybee at low light intensities. Journal of Comparative Physiology A, 141:389-393.

MENZEL R & BACKHAUS W (1991). Colour vision in insects. In: GOURAS P (ed), The perception of Colour. Macmillan, London, 6, pp. 262-293.

MENZEL R & KNAUT R (1973). Pigment movement during light and chromatic adaptation in the retina cells of *Formica polyctena (Hymenoptera, Formicidae).* Journal of Comparative Physiology A, 86:125-138.

NEUMEYER C (1981). Chromatic adaptation in the Honeybee: Successive color contrast and color constancy. Journal of Comparative Physiology A, 144:543-553.

OLIVEIRA PS & HÖLLDOBLER B (1989). Orientation and communication in the Neotropical ant *Odontomachus bauri* Emery (*Hymenoptera: Formicidae, Ponerinae*). Ethology, 83:154-166.

PASSERA L & ARON S (2005). Les Fourmis: comportement, organisation sociale et évolution. Les Presses scientifiques du CNRC, Ottawa, Canada. pp 480.

SALO O & ROSENGREN R (2001). Memory of location and site recognition in the ant *Formica uralensis (Hymenoptera: Formicidae).* Ethology, 107:737-752.

SIEGEL S & CASTELLAN NJ (1988). Non parametric Statistics for the Behavioural Sciences. Mc Graw-Hill International Editions, Singapore, pp. 396.

VON HELVERSEN O (1972). Zur spektralen Unterschiedsempfindlichkeit der Honigbiene. Journal of Comparative Physiology A, 80:439-472.

VOROBYEV M, BRANDT R, PEITSCH D, LAUGHLIN SB & MENZEL R (2001). Colour thresholds and receptor noise: behaviour and physiology compared. Vision Research, 41:639-653.

VOSS C (1967). Uber das Formensehen der roten Walddameise (*Formica rufa-G*ruppe). Zeitschrift für Vergleichende Physiologie, 55:225-254.

Vowles DM (1965). Maze learning and visual discrimination in the wood ant (*Formica rufa*). British Journal of Psychology, 56:15-31.

Warrant EJ, Porombka T & Kirchner W (1996). Neural image enhancement allows honeybees to see at night. Proceedings of the Royal Society of London B, 261:1521-1526.

Wehner R (1981). Spatial Vision in Arthropods. In: Autrum H (ed), Comparative Physiology and Evolution of Vision in Invertebrates. C: Invertebrates Visual Centres and Behavior II. Springer-Verlag, Berlin, Heidelberg, New-York, pp. 287-616.

Wehner R & Gehring W (1999). Biologie et physiologie animale. – Thieme Verlag. Traduit par Meyer C – De Boeck Université, pp. 418-429.

Appendix: experimental protocol and quantification of ant responses

Protocol of an experiment

Performed on six colonies successively:

a 4-day period of starvation and light intensity adaptation

a control (with the apparatus designed for tests)

a 6-day period of training (with the apparatus designed for training)

a first test (with the apparatus designed for tests)

a 3-day period of training (with the apparatus designed for training)

a second test (with the apparatus designed for tests)

a 1-day period of training (with the apparatus designed for training)

the assessment of the ants' threshold for the "correct" colour versus either grey or another colour by conducting successive tests (with the apparatus designed for tests) with stepwise increases in light intensities.

Quantification of ant responses

An example: threshold for **green (gr)** (the "correct" colour) *versus* yellow (ye) after adaptation and training under 600 lux.

Columns 2 to 7: mean numbers of ants present on each half-disk

Column 8: mean (=global mean) of the previous means

Column 9: proportion of "correct" responses

Column 10: results of non-parametric Wilcoxon tests applied to the mean numbers (specifically to the differences between the "correct" and the "wrong" mean numbers). N, T, P according to the nomenclature of Siegel & Castellan (1988).

Colonies	1		2		3		4		5		6		Mean		%	N	T	P
Colours	Ye	gr	Ye	gr	Ye	gr	Ye	gr	Ye	gr	Ye	gr	Ye	gr				
Control	1.80	1.47	0.67	0.67	2.47	2.07	6.80	6.80	1.13	1.13	2.20	3.07	2.51	2.54	50			
Test 1	4.60	7.13	0.00	2.00	2.67	5.47	11.6	16.5	0.33	2.00	2.67	5.13	3.65	6.38	64	6	21	0.016
Test 2	1.40	4.67	0.33	2.67	2.00	4.93	6.40	13.1	1.00	3.33	1.26	3.93	2.07	5.44	72	6	21	0.016
Threshold assessment																		
Lux 1	2.67	5.33	2.67	5.33	6.67	8.33	5.67	4.33	3.00	2.33	3.67	4.33	4.06	4.99	55	6	15	NS
1.5	1.67	1.33	2.00	2.33	2.67	2.33	3.67	2.67	0.67	2.00	3.33	3.67	2.34	2.39	50	5	8	NS
2	2.33	6.00	1.00	1.67	5.00	3.00	3.67	2.67	1.00	1.00	2.00	1.67	2.50	2.67	52	5	- 9	NS
2.5	3.00	4.33	1.33	2.67	1.00	2.33	4.00	4.33	1.00	1.00	1.67	1.67	2.00	2.72	58	5	13	0.094
3	2.67	5.00	1.67	2.00	4.33	3.67	2.33	4.67	1.00	1.33	3.67	5.67	2.61	3.72	59	6	20	0.031
3.5	1.33	3.66	0.33	1.33	1.67	5.00	1.67	5.00	1.00	1.00	0.00	1.33	1.00	2.89	74	5	15	0.031
4	0.00	2.67	0.00	1.00	2.67	5.00	2.00	4.33	2.33	5.00	0.67	2.33	1.28	3.39	73	6	21	0.016
6	1.00	4.33	0.00	1.00	2.00	4.67	1.67	4.33	2.67	4.67	3.67	5.33	1.84	4.06	69	6	21	0.016

The ants' threshold lies between 3 and 3.5 lux.

The cnidae of the acrospheres of the corallimorpharian *Corynactis carnea* (Studer, 1878) (Cnidaria, Corallimorpharia, Corallimorphidae): composition, abundance and biometry

Fabián H. Acuña[1] & Agustín Garese

Departamento de Ciencias Marinas. Facultad de Ciencias Exactas y Naturales. Universidad Nacional de Mar del Plata. Funes 3250. 7600 Mar del Plata. Argentina.
[1] **Researcher of CONICET.**

Corresponding author : *facuna@mdp.edu.ar*

ABSTRACT. *Corynactis carnea* is a common corallimorpharian in the southwestern Atlantic Ocean, particularly in the Argentine Sea, and possesses spherical structures called acrospheres at the tips of its tentacles, characterized by particular cnidae. Twelve specimens were collected to identify and measure the types of cnidae present in the acrospheres, to estimate their abundance and to study the biometry of the different types. The cnidae of the acrospheres are spirocysts, holotrichs, two types of microbasic b-mastigophores and two types of microbasic p-mastigophores. Spirocysts were the most abundant type, followed by microbasic p-mastigophores and microbasic b-mastigophores; holotrichs were the least abundant. The size of only the spirocysts fitted well to a normal distribution; the other types fitted to a gamma distribution. A high variability in length was observed for each type of cnida. R statistical software was employed for statistical treatments. The cnidae of the acrospheres of *C. carnea* are compared with those of other species of the genus.

KEY WORDS : cnidocysts, biometry, acrospheres, Corallimorpharia, Argentina.

INTRODUCTION

The Corallimorpharia form a relatively small, taxonomically-neglected group of skeletonless Anthozoa comprising no more than 40-50 species (DEN HARTOG et al., 1993). They are most closely related to the scleractinian corals and may even be considered as such. The taxonomy of the group is not well established and there is no concensus about the number of genera and families. In the most literal view, there are four families, one of which, Corallimorphidae, has three genera: *Corallimorphus* (Moseley, 1877), *Corynactis* (Allmann, 1846), and *Pseudocorynactis* (den Hartog, 1980). These are represented in both shallow coastal waters and the deep sea, and all three genera occur in the eastern Atlantic.

Corynactis carnea (Studer, 1878) is common in the southwestern Atlantic Ocean, mainly in the Argentine Sea, and its distribution was mentioned by many authors (CARLGREN, 1927; RIEMANN-ZÜRNECK, 1986; DEN HARTOG et al., 1993; GENZANO et al., 1996; ZAMPONI et al., 1998). This sea anemone forms pseudocolonies due to its asexual reproduction (DEN HARTOG, 1980; DEN HARTOG et. al., 1993) and is characterized by a high colour variation. Spherical structures called acrospheres are found at the tips of its tentacles, and are diagnostic of the family Corallimorphidae (RIEMANN-ZÜRNECK & IKEN, 2003). Such structures have adhesive batteries extremely effective in the capture of zooplankton, mainly crustaceans (ROBSON, 1988). The acrospheres have cnidae (all types of cnidocysts present in a particular structure or species) composed of at least four different types of cnidocysts, while in tentacles only the spirocysts are present. The cnidocysts (nematocysts, spirocysts and ptychocysts) are subcellular structures characteristic of the phylum Cnidaria. They vary in terms of their morphology and their functions, which include defence, aggression, feeding and larval settlement (FRANCIS, 2004). Cnidocysts also are important in the taxonomy of the group, and their description is necessary in any systematic work. The cnidae of *C. carnea* were incompletely documented by CARLGREN (1927), who did not distinguish the different types of cnida or describe the biometry of the capsules. ACUÑA et al. (2003; 2004 and 2007) provided important information on the size distribution of different types of cnidocysts, and also on modern statistical tools (generalized linear models) that allow statistical comparisons of nonnormal size distributions, using more powerful proofs than traditional non-parametric tests. The goals of this paper are to study the composition, abundance and biometry of the cnidae of the acrospheres of the sea anemone *C. carnea* from the Argentine Sea.

MATERIALS AND METHODS

Specimens of *C. carnea* were collected during a survey performed by the "Oca Balda" (10/9/88) (expedition 04-88). The individuals came from 38º11'S - 57º03'W, at a depth of 59m, temperature 10.3ºC, salinity 33.7‰. Samples were fixed in 5% formaldehyde and subsequently in ethanol. In the laboratory, squashes of acrospheres from 12 individuals were made to identify and measure the length of cnidocysts, using a Zeiss Axiolab microscope with oil immersion at 1000x magnification. The cnidocysts were classified according to ENGLAND (1991). A microscope with a digital camera attached also was used for photography of the cnidae.

For estimation of cnidocyst abundance, four randomly-selected zones in each of the 12 squashes (one per individual) were chosen, and all identified capsules were counted. For statistical analyses, 30 capsules of each type from the acrospheres were measured. A total of 2160 measurements (30 capsules x 6 types of cnida x 12 individuals) were taken. Statistically-descriptive parameters, such as the types of size distribution and the cnidocyst sizes, were compared among individuals. Normality of size distribution was tested for each cnidocyst by means of a Shapiro-Wilks test ($\alpha=0.05$). If normality was confirmed, an ANOVA was carried out in order to compare the cnidocyst sizes among specimens. In cases with non-normal distribution, a model with different distribution errors and other functional relationship between lengths and individuals for each cnidocyst type was evaluated. In this way, a Generalized Linear Model (GLM) with gamma errors was fitted, using the R program (EVERITT, 2005). The model form was:

$$g \text{ (length)}=\beta_0+\beta_1 \text{ individual}+\varepsilon$$

Then, in order to evaluate possible differences in the sizes of each cnida among individuals, a t-test was performed for the coefficients of the model (β_1).

RESULTS

Cnidae composition

The cnidae of the acrospheres of *C. carnea* are composed of the following types: spirocysts with an elongated capsule and no spines distinguishable, spirally-coiled thread (Fig. 1a); holotrichs with a quite wide capsule and a thread with spines along whole length (Fig. 1b); microbasic b-mastigophore 1 with an elongated capsule and a thread with two distinct parts, a terminal tubule and a basal shaft with a length about 1/3 the length of the capsule, and a parallel-sided shape of the undischarged thread (Fig. 1c); microbasic b-mastigophore 2 with the same features as the previous type, except that the shaft has a length equivalent to 1/8 the length of the capsule (Fig. 1d); microbasic p-mastigophore 1 with an oval capsule and a thread with a terminal tubule and a basal shaft with a V-shape of the undischarged thread, which has a length equal to 1/2 the length of the capsule (Fig. 1e); and finally, microbasic p-mastigophore 2 with the same features as p-1, with the exception that the capsule has a more elongated shape and the length of the shaft is less than 1/4 the length of the capsule (Fig. 1f).
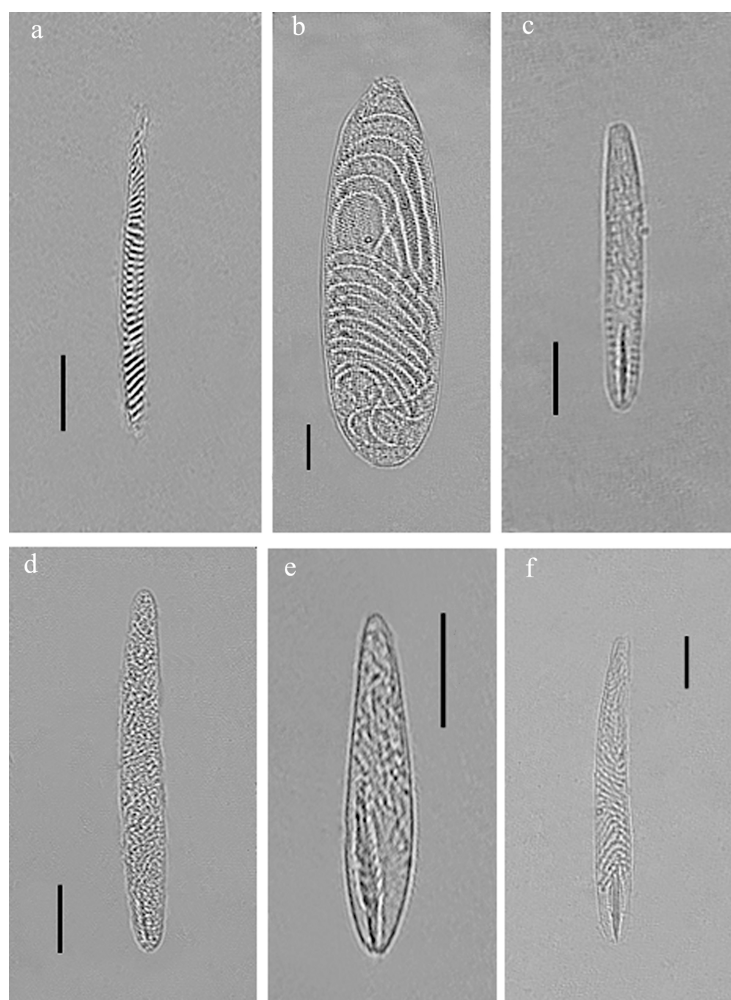
Fig. 1. – Cnidae of the acrospheres of *C. carnea.* (a) spirocyst, (b) holotrich, (c) microbasic b-mastigophore 1, (d) microbasic b-mastigophore 2, (e) microbasic p-mastigophore 1, (f) microbasic p-mastigophore 2. Bar: 10μm.
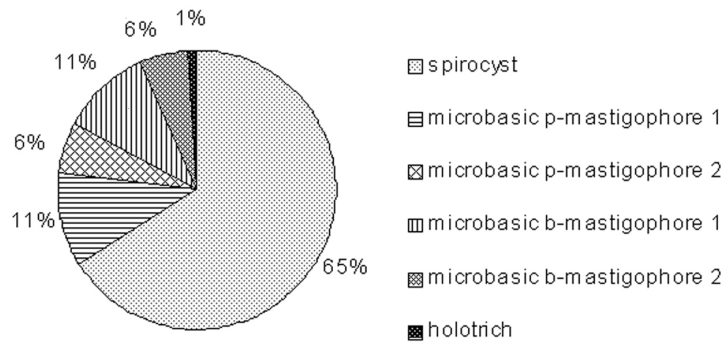
Fig. 2. – Abundances of the different cnidocyst types.

Size ranges of spirocysts were 22-80 x 2-4μm in length and width respectively, the holotrichs between 54-98 x 13-31μm, the microbasic b-mastigophores 1 between 31-70 x 4-6μm, the microbasic b-mastigophores 2 between 30-86 x 5-8μm, the microbasic p-mastigophores 1 between 20-55 x 5-10μm and the microbasic b-mastigophores 2 between 43-88 x 4-8μm.

Abundance of different cnidocysts

The pooled data of abundances for all types of cnidocysts in the 12 individuals are shown in Fig. 2. Clearly, the spirocysts are the most abundant cnida, followed by the microbasic p-mastigophores 1 and 2, and microbasic b-mastigophores 1 and 2, while the least abundant were the holotrichs, which were found in only five of the specimens.

Biometry

Statistically-descriptive parameters

The statistically-descriptive parameters for each cnida from the 12 analyzed individuals are shown in Tables 1-4. It can be observed that the holotrichs are the largest type (Table 2), while the microbasic p-mastigophores 1 are the smallest (Table 4).

TABLE 1

Descriptive statistical parameters of spirocysts

Indiv. Nº	mean	std. dev.	CV	min.	max.
1	47.76	7.63	0.16	35	63
2	49.16	12.52	0.25	29	74
3	48.23	9.24	0.19	22	64
4	51.06	11.13	0.22	30	67
5	47.43	10.56	0.22	33	73
6	51.30	10.91	0.21	29	68
7	46.56	10.01	0.21	28	67
8	58.16	12.30	0.21	30	80
9	53.46	13.33	0.25	30	80
10	51.03	11.01	0.22	27	80
11	52.76	9.13	0.17	37	74
12	55.16	9.82	0.18	31	70

Mean, standard deviation (std. dev.), minimum (min.) and maximum (max.) in μm. CV (coefficient of variation).

TABLE 2

Descriptive statistical parameters of holotrich

Indiv. Nº	mean	std. dev.	CV	min.	max.
1	74.50	7.55	0.10	55	89
2	75.50	7.62	0.10	61	87
3	75.76	6.21	0.08	65	88
4	76.26	7.74	0.10	57	91
5	84.63	6.85	0.08	72	98
6	72.60	8.98	0.12	54	89
7	82.26	6.37	0.08	65	95
8	79.40	7.00	0.09	66	90
9	86.80	7.64	0.09	67	98
10	76.60	5.51	0.07	61	85
11	79.03	5.62	0.07	68	92
12	78.76	7.93	0.10	62	94

Mean, standard deviation (std. dev.), minimum (min.) and maximum (max.) in μm. CV (coefficient of variation).

TABLE 3

Descriptive statistical parameters of microbasic b-mastigophores

Type	Indiv. Nº	mean	std. dev.	CV	min.	max.
1	1	42.83	3.98	0.09	38	54
	2	41.30	3.36	0.08	33	47
	3	40.00	4.41	0.11	32	49
	4	39.96	3.89	0.10	32	46
	5	42.00	4.82	0.11	35	59
	6	40.26	4.26	0.11	31	46
	7	45.90	6.74	0.15	38	70
	8	43.33	4.17	0.10	36	50
	9	40.96	3.09	0.08	35	46
	10	40.83	3.54	0.09	32	46
	11	39.10	3.77	0.10	31	45
	12	41.00	2.57	0.06	35	46
2	1	48.00	5.27	0.11	42	61
	2	51.33	8.14	0.16	40	65
	3	51.93	12.84	0.25	37	86
	4	43.30	5.05	0.12	31	53
	5	43.70	6.69	0.15	30	53
	6	44.40	6.30	0.14	35	64
	7	59.76	10.08	0.17	40	76
	8	53.10	5.56	0.10	44	66
	9	61.80	12.01	0.19	43	83
	10	51.73	7.95	0.15	41	74
	11	45.73	4.94	0.11	40	59
	12	51.50	8.73	0.17	31	72

Mean, standard deviation (std. dev.), minimum (min.) and maximum (max.) in μm. CV (coefficient of variation).

TABLE 4

Descriptive statistical parameters of microbasic p-mastigophores

Type	Indiv. Nº	mean	std. dev.	CV	min.	max.
1	1	33.23	1.83	0.06	30	38
	2	31.36	4.68	0.15	21	41
	3	36.36	5.35	0.15	27	46
	4	31.43	4.93	0.16	20	43
	5	40.60	7.81	0.19	27	55
	6	30.83	3.29	0.11	23	36
	7	34.43	5.68	0.16	25	45
	8	35.40	6.28	0.18	26	48
	9	31.86	2.73	0.09	26	38
	10	31.83	3.47	0.11	26	39
	11	31.80	4.52	0.14	23	41
	12	29.56	3.69	0.12	21	35
2	1	69.30	7.42	0.11	56	88
	2	59.73	6.57	0.11	43	70
	3	67.26	7.85	0.12	55	82
	4	69.76	7.10	0.10	53	79
	5	61.76	6.12	0.10	50	73
	6	59.23	6.71	0.11	45	70
	7	75.56	5.98	0.08	57	84
	8	69.13	5.39	0.08	58	78
	9	72.50	6.58	0.09	60	85
	10	59.86	5.17	0.09	51	70
	11	60.56	6.18	0.10	48	70
	12	65.36	6.29	0.10	52	75

Mean, standard deviation (std. dev.), minimum (min.) and maximum (max.) in μm. CV (coefficient of variation).

Normality test

According to the analyses of residuals, normality of size distribution was accepted for the spirocysts (p=0.653). However, for the holotrichs (p=0.003), microbasic b-mastigophores 1 (p<0.001), microbasic b-mastigophores 2 (p=0.001), microbasic p-mastigophores 1 (p=0.024) and microbasic p-mastigophores 2 (p=0.017), a normal distribution of the capsule sizes was rejected. Fig. 3 shows the Q-Q plots of residuals vs. normal expected values of each cnida.

ANOVA

An ANOVA test revealed that the sizes of spirocysts varied significantly among the 12 individuals (F=3.11, p<0.0005). These differences are illustrated with boxplots (Fig. 4).
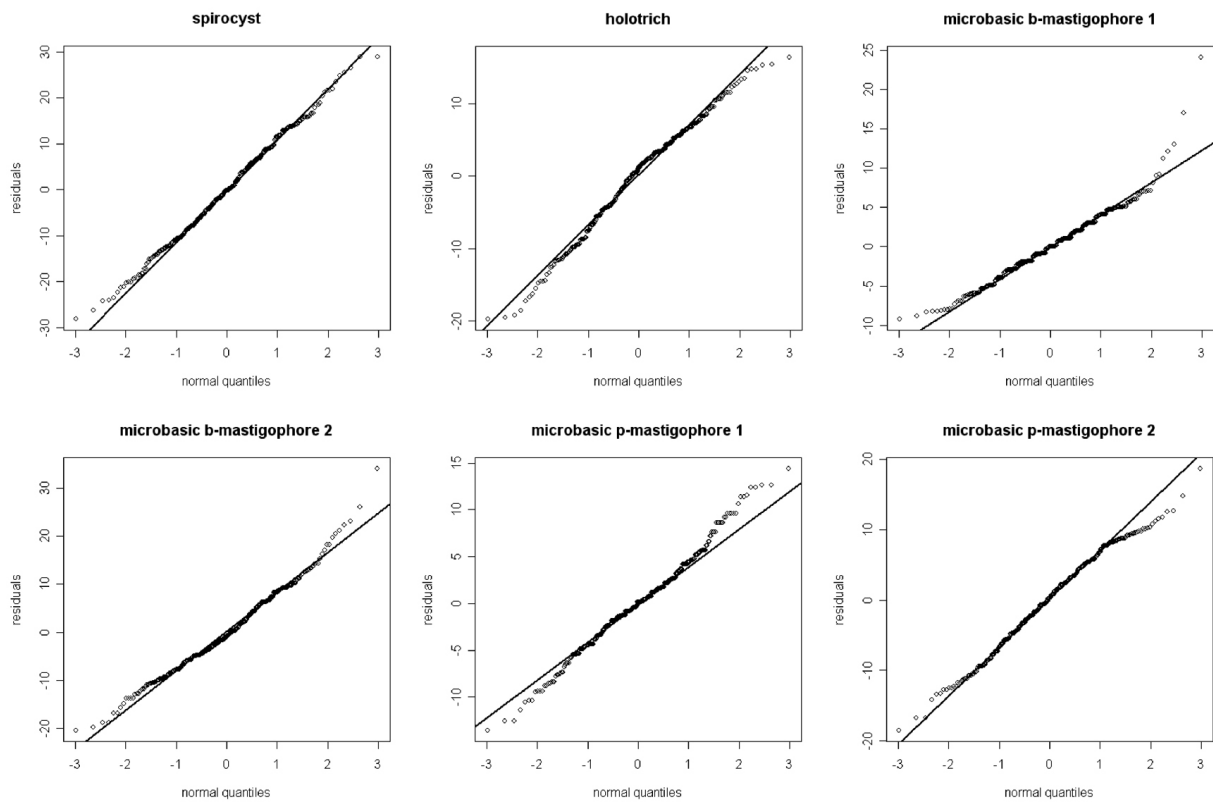
Fig. 3. – Q-Q plots of residuals vs. normal distribution.
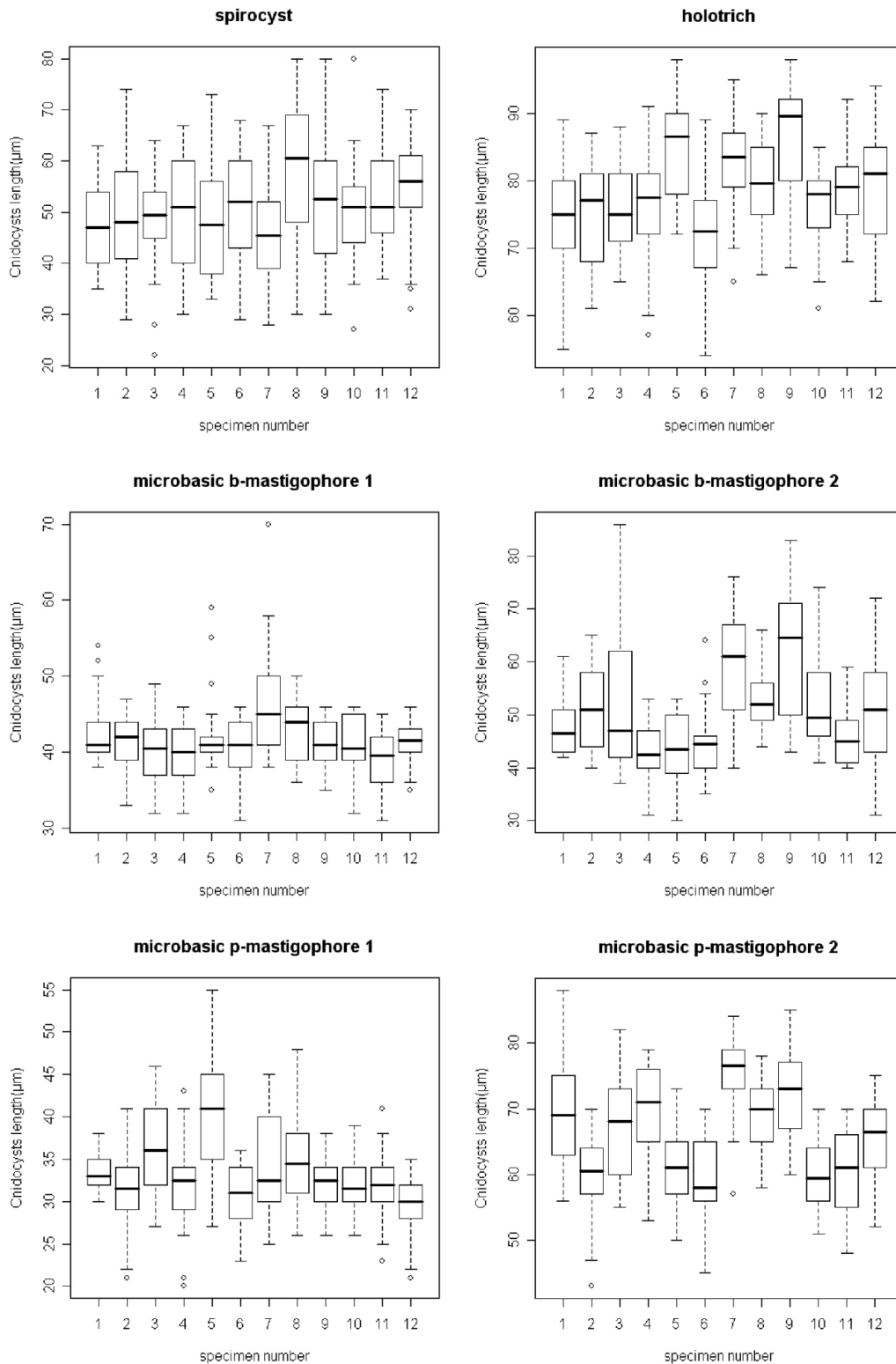
Fig. 4. – Box-plots of cnidocysts lengths. Outliers: o

Generalized Linear Models (GLM)

Sizes of holotrichs, microbasic b- mastigophores 1 and 2, and microbasic p- mastigophores 1 and 2 fitted very well to a GLM with gamma errors (Fig. 5). This was con-firmed by the homogeneous coefficients of variation (Tables 2-4), despite the variation of the mean (Acuña et al., 2007). The sizes of the above cnidocysts also varied significantly between individuals (Table 5 and Fig. 4).
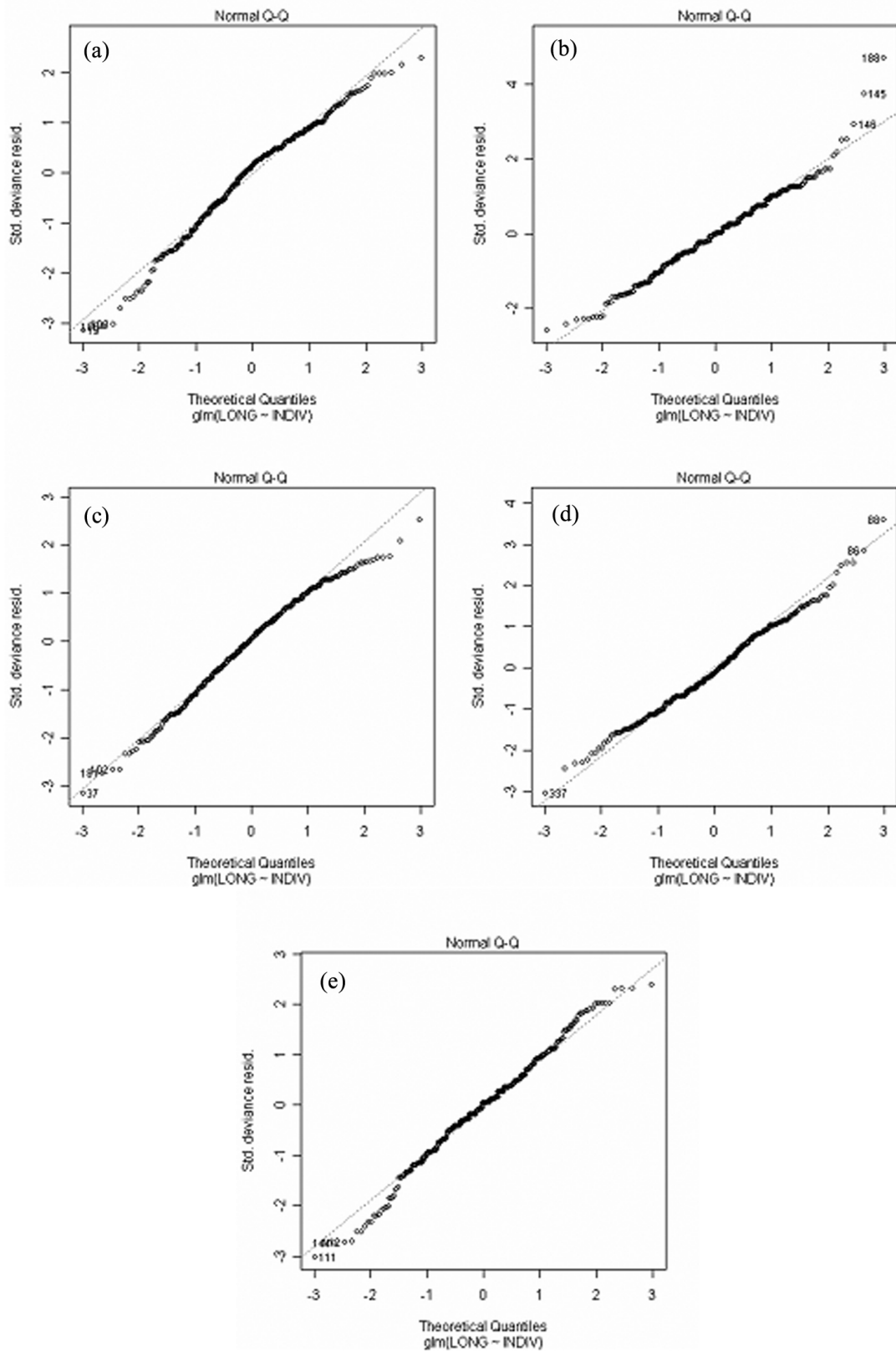
Fig. 5. – Q-Q plots of residuals vs. theorical quantiles of GLM. (a) holotrich, (b) microbasic b-mastigophore 1, (c) microbasic b-mastigophore 2, (d) microbasic p-mastigophore 1, (e) microbasic p-mastigophore 2.

TABLE 5

P values of t test for the coefficients of the model (β1). The individual N° 1 is not shown because it was utilized to carry out the comparisons

	holotrich	microbasic b-mastigophore 1	microbasic b-mastigophore 2	microbasic p-mastigophore 1	microbasic p-mastigophore 2
2	0.575	0.157	0.100	0.110	< 0.0001***
3	0.478	0.008 **	0.054	0.013 *	0.246
4	0.324	0.007 **	0.012 *	0.124	0.793
5	< 0.0001 ***	0.445	0.022 *	< 0.0001 ***	< 0.0001 ***
6	0.277	0.017 *	0.056	0.040 *	< 0.0001 ***
7	< 0.0001 ***	0.007 **	< 0.0001 ***	0.326	0.0008 ***
8	0.008 **	0.652	0.014 *	0.081	0.925
9	< 0.0001 ***	0.084	< 0.0001 ***	0.245	0.079
10	0.242	0.064	0.066	0.234	< 0.0001 ***
11	0.013 *	< 0.0001 ***	0.235	0.222	< 0.0001 ***
12	0.020 *	0.090	0.084	0.001 **	0.023 *

significant at levels '***' 0.001 '**' 0.01 '*' 0.05 respectively.

DISCUSSION

Fourteen species within the genus *Corynactis* are considered valid according to FAUTIN (2006). The morphological differentiation of these species is very complicated, due to the difficulty of distinguishing the morphological characters usually used in sea anemone taxonomy (CARLGREN, 1927). Besides, the descriptions of several species are incomplete, mainly in terms of the composition of their cnidae. In the case of *C. carnea,* CARLGREN (1927) only mentioned some types without providing data related to their biometry. In this paper, we examined in detail the cnidae of the acrospheres of many individuals of this corallimorpharian species, and we clearly differentiated the following cnidocysts: spirocysts, microbasic b-mastigophores 1 and 2, microbasic p-mastigophores 1 and 2, and holotrichs. Within the 14 valid species mentioned by Fautin in her database, there are detailed descriptions of the cnidae of only three species: *C. viridis* (Allman, 1846) (DEN HARTOG et al., 1993), *C. californica* (Calgren, 1936) (HAND, 1955) and *C. denhartogi* (Ocaña, 2003). The cnidae of *C. carnea* are very similar to those of *C. viridis* from the Northern Hemisphere. Although DEN HARTOG et al. (1993) used a different nomenclature, this similarity in cnidae also occurs when applying the nomenclature used in this paper (ENGLAND, 1991). In the corallimorpharian *C. californica,* the cnidae composition within the acrospheres also is very similar, but only a single type of microbasic b-mastigophore is recognized. HAND (1955) does not differentiate the cnidae of the acrospheres and tentacles. In the same way, OCAÑA (2003) detailed the cnidae of the acrospheres and tentacles of *C. denhartogi* combined, recognising spirocysts, two holotrichs, two microbasic b-mastigophores and two microbasic p-mastigophores. It is interesting to mention that in other corallimorpharians such as *Rhodactis rhodostoma* (Ehrenberg, 1934), the marginal tentacles contain similar types of nematocysts (types 1 and 2 holotrichs, microbasic p-mastigophore, types 1 and 2 microbasic b-mastigophore) but not spirocysts (LANGMEAD & CHADWICK-FURMAN, 1999).

The abundances of the cnidocysts of *C. carnea* and *C. viridis* follow a similar pattern: the spirocysts are clearly the most abundant, while the other types occur at a low frequency. However, a difference was observed concerning the holotrichs, which in *C. carnea* is the least abundant type, but in *C. viridis* is the second most abundant type. It is interesting to note that in scleractinian corals [closely related to the order Corallimorpharia and sharing the same categories of cnidocysts (DEN HARTOG, 1980; DEN HARTOG et al., 1993; PIRES, 1997)], there are modified tentacles (sweeper tentacles), whose tips are referred to as acrospheres and that contain a different proportion among the different cnidocyst types in comparison with *C. carnea.* For example, the tips of the tentacles of *Montastrea cavernosa* (Linnaeus, 1766) have 63% holotrichs (DEN HARTOG, 1977), while in *Galaxea fascicularis* (Linnaeus, 1758) the microbasic b-mastigophores make up 50% and the spirocysts 40% of the cnidae (HIDAKA & MIYAZAKI, 1984; HIDAKA & YAMAZATO, 1984).

Some authors have found a normal distribution of the capsule lengths of cnidocysts (WILLIAMS, 2000; ARDELEAN & FAUTIN, 2004; FRANCIS, 2004), but others have not, at least for acontiarian sea anemones, the actiniarian *Oulactis muscosa* (Drayton in Dana, 1846) and zoanthids (ACUÑA et al., 2003; 2007 and references therein). THOMASON & BROWN (1986) showed clearly that generalizations cannot be made concerning the statistical distribution of the cnidae in scleractinian corals. In *C. carnea,* normality of size distributions was rejected for five of the six types of cnidocysts. However, a normal model fitted very well to the spirocysts, this being coincident with the results obtained by FRANCIS (2004) for the sea anemone *Anthopleura elegantissima* (Brandt, 1835). According to our results and those of other authors, we conclude that a normal distribution is uncommon, and the statistical distribution of cnidae size must be tested before any biometric analysis.

Sizes of the cnidocysts of *C. carnea* varied between individuals. Studies carried out in the acontiarian sea anemones *Haliplanella lineata* (Verrill, 1869), *Tricnidactis errans* (Pires, 1988), *Anthothoe chilensis* (Lesson, 1830) and the actiniarians *O. muscosa* and *A. elegantissima* (ACUÑA et al., 2003; 2007; FRANCIS, 2004), also showed intraspecific variation in capsule sizes. This variability reduces the taxonomic value of cnidocysts, and

could be explained by the supply and demand of cnidocysts for the sea anemones (ROBSON, 1988).

According with the results obtained here, the cnidae of the acrospheres of *C. carnea* are similar to those of other species of the genus. This species is part of the *C. viridis*-complex, along with *C. viridis*, *C. annulata (*Verrill, 1866); *C. chilensis* (Carlgren, 1941) and *C. delawarei* (Widersten, 1976), because of their distribution (Atlantic Ocean and Pacific of South America) and morphological similarity (DEN HARTOG et al., 1993). Because of this similarity and high intraspecific variability (colour and cnidocyst sizes), it is clearly necessary to revise the genus *Corynactis* and this species complex, perhaps using molecular characters that are useful especially when the morphological ones are obscure or difficult to distinguish.

ACKNOWLEDGMENTS

REFERENCES

ACUÑA FH, EXCOFFON AC, ZAMPONI MO & RICCI L (2003). Importance of nematocysts in taxonomy of acontiarian sea anemones (Cnidaria, Actiniaria): a statistical comparative study. Zoologischer Anzeiger, 242(1):75-81.

ACUÑA FH, RICCI L, EXCOFFON AC & ZAMPONI MO (2004). A novel statistical analysis of cnidocysts in acontiarian sea anemones (Cnidaria, Actiniaria) using generalized linear models with gamma errors. Zoologischer Anzeiger, 243(1-2):47-52.

ACUÑA FH, EXCOFFON AC & RICCI L (2007). Composition, biometry and statistical relationships between the cnidom and body size in the sea anemone *Oulactis muscosa* (Cnidaria: Actiniaria). Journal of the Marine Biological Association of the United Kingdom, 87:415-419.

ARDELEAN A & FAUTIN DG (2004). Variability in nematocysts from a single individual of the sea anemone *Actinodendron arboreum* (Cnidaria: Anthozoa: Actiniaria). Hydrobiologia, 530/531:189-197.

CARLGREN O (1927). Actiniaria and Zoantharia. Further Zoological Results of the Swedish Antarctic Expedition 1901-1903, 2(3):01-102.

ENGLAND KW (1991). Nematocysts of sea anemones (Actiniaria, Ceriantharia and Corallimorpharia: Cnidaria): nomenclature. Hydrobiologia, 216/7:697-691.

EVERITT BS (2005). An R and S-Plus Companion to Multivariate Analysis. Springer, (Internet address: http://www.r-project.org/).

FAUTIN DG (2006). Hexacorallians of the World: sea anemones, corals, and their allies. (Internet address: http://hercules.kgs.uk.edu/hexacoral/anemone2/index.cfm).

FRANCIS L (2004). Microscaling: Why Larger Anemones Have Longer Cnidae. Biological Bulletin, 207:116-129.

GENZANO GN, ACUÑA FH, EXCOFFON AC & PÉREZ CD (1996). Cnidarios bentónicos de la Provincia de Buenos Aires. Lista sistemática, distribución y estrategias de colonización. Actas de las VI Jornadas de Ciencias Naturales de La Pampa, pp. 113-121.

HAND C (1955). The sea anemones of central California Part I. The corallimorpharian and athenarian anemones. Wasmann Journal of Biology, 12(3):345-375.

HARTOG JC DEN (1977). The marginal tentacles of *Rhodactis sanctithomae* (Corallimorpharia) and the sweeper tentacles of *Montastrea cavernosa* (Scleractinia); their cnidom and possible function. Proceedings, Third International Coral Reef Symposium, 1:463-469.

HARTOG JC DEN (1980). Caribbean shallow water Corallimorpharia. Zoologische Verhandelingen, 176:1-83.

HARTOG JC DEN, OCAÑA O & BRITO A (1993). Corallimorpharia collected during the CANCAP expeditions (1976-1986) in the south-eastern part of the North Atlantic. Zoologische Verhandelingen, 282:1-76.

HIDAKA M & MIYAZAKI I (1984). Nematocyst discharge and surface structure of the ordinary and sweeper tentacles of a scleractinian coral, *Galaxea fascicularis*. Galaxea, 3:119-130.

HIDAKA M & YAMAZATO K (1984). Intraspecific interactions in a scleractinian coral *Galaxea fascicularis*: induced formation of sweeper tentacles. Coral Reefs, 3:77-85.

LANGMEAD O & CHADWICK-FURMAN NE (1999). Marginal tentacles of the corallimorpharian *Rhodactis rhodostoma.* 1. Rol in competition for space. Marine Biology, 134:479-489.

OCAÑA O (2003). *Corynactis denhartogi* (Anthozoa: Corallimorpharia) a new species of soft hexacoral from New Zealand waters. Zoologische Verhandelingen, 345:257-268.

PIRES DO (1988). *Tricnidactis errans* n. gen., n. sp. (Cnidaria, Actiniaria, Haliplanellidae), from Guanabara Bay, Rio de Janeiro, Brazil. Revista Brasileira do Biologia, 48:507-516.

PIRES DO (1997). Cnidae of Scleractinia. Proceedings of the Biological Society of Washington, 110:167-185.

RIEMANN-ZÜRNECK K (1986). Zür Biogeographie des Südwestatlantik mit besonderer Beraksichtigung der seeanemonen (Coelenterata: Actiniaria). Helgoländer Meeresuntersuchungen, 40:91-149.

RIEMANN-ZÜRNECK K & IKEN K (2003). *Corallimorphus profundus* in shallow Antarctic habitats: Bionomics, histology, and systematics (Cnidaria: Hexacorallia). Zoologische Verhandelingen, 345:367-386.

ROBSON EA (1988). Problems of supply and demand for cnidae in Anthozoa. In: HESSINGER DA & LENHOFF HM (eds), The biology of the nematocysts, Academic Press, San Diego: 179-207.

THOMASON JC & BROWN BE (1986). The cnidom: an index of aggressive proficiency in scleractinian corals. Coral Reefs, 5:93-101.

WILLIAMS RB (2000). Measurements of cnidae from sea anemones (Cnidaria: Actiniaria), III: ranges and other measures of statistical dispersion, their interrelation and taxonomic relevance. Scientia Marina, 64:49-68.

ZAMPONI MO, GENZANO GN, ACUÑA FH & EXCOFFON AC (1998). Studies of benthic cnidarian populations along a transect off Mar del Plata (Buenos Aires, Argentina). Russian Journal of Marine Biology, 24(1):7-13.

Wound keratins involved in mucous granule extrusion during differentiation of amphibian keratinocytes

Lorenzo Alibardi & Mattia Toni

Department of Biology, University of Bologna, Italy

Corresponding author : L. Alibardi, Dipartimento di Biologia evoluzionistica sperimentale, via Selmi 3, University of Bologna, 40126, Bologna, Italy ; Tel +39 051 2094257 ; Fax +39 051 2094286 ; E-mail: lorenzo.alibardi@unibo.it

ABSTRACT. The synthesis of specific keratins in differentiating amphibian epidermis has been studied by autoradiography after tritiated histidine injection, immunocytochemistry and immunoblotting. Most labeling is present in upper spinosus and corneous layers suggesting higher protein synthesis in these differentiating keratinocytes. In the epidermis of the toad *Bufo viridis* and of the newt *Triturus vulgaris* most of the synthesized epidermal proteins are keratins of acidic-neutral type, including K6, K16, and K17-like keratins of 45-60kDa. Proteins of lower molecular weight and with basic pI are present in very low amounts or are absent. Ultrastructural immunolabeling for K6 and K16 keratins shows that they are associated with dense material among keratin filaments and with dense mucous granules, but not with tonofilament bundles of differentiating keratinocytes. After the release of mucous granules in upper keratinocytes of the intermediate layer and in pre-corneous keratinocytes, the immunolabeling for the above keratins is localized along the plasma membrane of maturing keratinocytes. This distribution is similar to that of actin, and suggests that actin together with K6, K16, and K17-like keratins may be involved in the process of extrusion of mucous-containing glycoproteins from differentiating amphibian keratinocytes.

KEY WORDS : Amphibian epidermis ; Mucous granules ; Ultrastructure ; Immunocytochemistry ; Wound keratins.

INTRODUCTION

The adult amphibian epidermis comprises a basal layer, 3-5 intermediate cell layers, and a stratum corneum that generally consists of a single layer of dead keratinocytes (FOX, 1994 ; WARBURG et al., 1994 ; ALIBARDI, 2001). The limited cornification of superficial cells in amphibian epidermis allows for cutaneous respiration before the corneous layer is replaced (BUDZ, 1977). These studies have shown two types of submicroscopic granules, one type of 0.4-0.9μm diameter and another type of 0.1-0.2μm diameter, in differentiating keratinocytes (BANI, 1966 ; CERESA-CASTELLANI, 1969 ; LODI & BANI, 1971 ; LAVKER, 1972 ; 1974).

The smaller granules probably contain mainly mucous or glycoproteins while some of the larger ones contain glycoproteins and perhaps other proteins involved in the process of keratinization and coating of the cell membrane of superficial keratinocytes (BUENO et al., 1981 ; NAVAS et al., 1987). The latter ultrastructural studies coupled to lectin histochemistry have indicated that at least some small mucous granules may represent the equivalent of the "membrane coating granules" or multilamellar bodies present in mammalian keratinocytes (MENON & NORLEN, 2002).

Mucous and sparse lipid-like bodies are either extruded extracellularly (small granules) or dispersed intracellularly (some of the large granules). Lipids contribute to limiting water-loss from the epidermis, especially in more terrestrial amphibians such as hylids and bufonids (LAVKER, 1972 ; 1974 ; LILLYWHITE & MADERSON, 1982 ; TOLEDO & JARED, 1993). Glycoproteins coat the plasma membrane of maturing keratinocytes of the pre-corneous or replacement layer and of the corneous layer, like lipids coat the cornified cell envelope of mammalian corneo-cytes. High amounts of glycoproteins are produced in the epidermis and they are secreted extracellularly. The extrusion of mucous granules probably requires the production of specific cytoskeletal proteins.

The large granules may also release, apart from glycoproteins, some matrix proteins that contribute to the process of maturation of the corneous layer (LAVKER, 1972 ; 1974 ; FOX, 1994 ; ALIBARDI, 2001). The molecular nature of inter-keratin or matrix material in amphibian keratinocytes, however, remains unsolved. Matrix proteins in mammalian epidermis, including the histidine-rich filaggrins, are essential for the formation of the corneous material present within mature keratinocytes and along cornified cell membranes (RESING & DALE, 1991 ; KALININ et al., 2002).

Previous studies have shown that tritiated histidine is incorporated in amphibian epidermis, from newt, frog and toad (ALIBARDI, 2002 ; 2003 ; ALIBARDI et al., 2003). These studies have indicated that keratins (alpha- or intermediate filament keratins) and a small amount of proteins incorporating histidine are synthesized in the upper cells of the intermediate layer and of the replacement layers in amphibian epidermis. Other studies have shown that a slightly basic keratin of 63kDa is a major protein of adult epidermis in *Xenopus laevis* (NISHIKAWA et al., 1992). Immunocytochemical studies have, however, shown that in adult epidermis more acidic than basic keratins are present (ALIBARDI, 2001 ; 2002) but the specific types are not known.

Among acidic keratins, mammalian K16 and K17 are known to be upregulated during epidermal wounding and regeneration (MCGOWAN & COULOMBE, 1998a;b). This is also likely for reptilian epidermis covering the amputated tail or limbs (ALIBARDI & TONI, 2005). As amphibian epidermis is capable of extensive regeneration to cover

amputated limbs or broad areas of injured skin, it would be interesting to evaluate the presence of K16 and K17 acidic keratins, and of K6, a basic keratin also upregulated in regenerating epidermis.

In the present study, the specific nature of some of the keratins produced during epidermal differentiation has been analyzed using autoradiography, immunocytochemistry, and immunoblotting for wound keratins (K6, K16, and K17) and for actin, a ubiquitous cytoskeletal protein associated with cell motility and cytoskeletal re-arrangement.

MATERIALS AND METHODS

Animals and experiments

Adult specimens of toad (*Bufo viridis*; n=9) were injected with 3-4μCi/g body weight of tritiated histidine (L-2,5-3H-Histidine, specific activity 53.0Ci/mmol, Ge Healthcare, UK) diluted in saline. Adult specimens of newt (*Triturus vulgaris*; n=17) received 6-8μCi/g body weight of tritiated histidine as previously reported (ALIBARDI, 2003). This allowed evaluation of protein synthesis in the main epidermal layers.

Five newts received 2-3μCi/g body weight of tritiated thymidine (3H-TdR, Amesham, specific activity 70-90Ci/mM). This treatment allowed evaluation of the sites of cell proliferation and time of migration through the epidermal layers.

After sacrifice of the animals by decapitation, the skin from ventral trunk, tail and digits areas in both species was collected at 4 and 8 hours post-injection, and prepared for autoradiography. From the specimens that received tritiated thymidine, samples were collected at 4-5 hours (n=5), 4 days (n=2), and 6-7 days (n=3) post injection.

Fixation, immunocytochemistry and autoradiography

Skin fragments of 2 by 4mm were fixed for 3-5 hours in 4% paraformaldehyde in 0.1M phosphate buffer at pH 7.4, dehydrated, and embedded in Durcupan or Bioacryl resins (SCALA et al., 1992) as previously detailed (ALIBARDI, 2001; 2002). Other tissues were fixed in 2.5% glutaraldehyde in 0.1M phosphate buffer for 5 hours, post-fixed in 2% osmium tetroxide, dehydrated and embedded in Durcupan resin. The latter tissues were studied under the electron microscope for routine ultrastructural analysis of the epidermis.

Tissues were sectioned with an ultramicrotome in order to obtain sections of 2-5μm in thickness. Sections from Araldite- or Bioacryl-embedded tissues were stained with 0.5% toluidine blue and studied under the light microscope. Sections from Bioacryl-embedded tissues were collected over chromoalume-albumin coated slides for the following application of immunocytochemical reactions.

Immunocytochemistry was performed using the anti-cytokeratin antibodies to K6, K16 and K17 (generous gift from Dr. P. Coulombe, Johns Hopkins University, USA). These are rabbit polyclonal antibodies that recognize specific epitopes of mouse keratins 6 and 16 (data in TAKAHASHI et al., 1994; McGowan & Coulombe, 1998a;b). The anti-total actin here employed is a general antibody against actin produced in rabbit.

Semithin sections were pre-incubated for 30 minutes at room temperature with 2% BSA in 0.05M Tris/HCl buffer at pH 7.6 containing 5% normal goat serum. The sections were later incubated overnight at 0-4°C in the primary antibody diluted in the Tris buffer (1:200 for the K6, K16, or K17 antibodies and actin antibody). In controls, the primary antibody was omitted. Sections were rinsed in buffer and incubated with secondary HRP-conjugated antibody (SIGMA, anti-rabbit for K6, K16, K17-incubated tissues) at 1:50 dilution. Detection was performed using a DAB-hydrogen peroxide reaction.

Other sections of 40-90nm thickness were collected with the ultramicrotome on nickel grids, and incubated in the primary antibody medium with Tris buffer and 1% Cold Water Fish Gelatin as reported above (no primary antibodies were used in controls). The dilution for K6, K16 and anti-actin was 1:200. After being rinsed in the buffer, sections were incubated for 1 hour at room temperature in the secondary antibody (anti-mouse IgG anti-rabbit, conjugated with 10nn gold particles to be visualized under the electron beam) diluted 1:40 in the Tris buffer. After rinsing, sections on grids were stained for 5 min in 2% uranyl acetate, and then observed under a Philips CM-100 electron microscope.

For light and ultrastructural autoradiography (see details in ALIBARDI, 2003), sections of 2-5μm thickness were attached to glass slides and then coated with Nuclear emulsion for light microscopic autoradiography (Ilford K5), developed and fixed 1-2 months after exposure. Thin sections (40-90nm thick) were coated with Nuclear emulsion for electron microscopic autoradiography (Ilford L4), developed and fixed after 3-4 months of exposure. Thin sections were lightly stained with uranyl acetate and lead citrate, and observed under a CM 100 Philips electron microscope operating at 60-80kV.

Electrophoresis, autoradiography and immunoblotting

The remaining skin from the whole body of injected animals was frozen in liquid nitrogen and stored at -80°C before protein analysis (SYBERT et al., 1985). Tissues were incubated in 5mM EDTA in phosphate buffered saline (PBS) for 5min at 50°C and 4min in cold PBS, then the epidermis was separated from the dermis by dissection under the stereomicroscope. The epidermis was homogenized in 8M urea/50mM Tris-HCl (pH 7.6)/0.1M 2-mercaptoethanol/1mM dithiothreithol/1mM phenylmethylsulphonyl fluoride. The particulate matter was removed by centrifugation at 10,000g for 10min. Protein concentration was assayed by the Lowry method before electrophoresis.

For monodimensional electrophoretic analysis, proteins were denatured by boiling the extracted solution in the Sample Buffer for 5min. Then, 50-100μg of protein was loaded in each lane and separated in 10% or 12% SDS-polyacrylamide gels (SDS-PAGE) according to LAEMMLI (1970). For two-dimensional electrophoretic analysis, the Ettan IPGphor III IEF System (Ge Health-

care, U.K.) was used for the isoelectrofocusing (IEF). An 80μg protein sample (containing 2% CHAPS (Sigma, USA) and 1% carrier ampholyte mixture, pH 3,5-10 (Ge Healthcare, U.K.)) was loaded onto a 7cm (pH 3-10) strip (Ge Healthcare, U.K.). Application of the strips and the running procedure were carried out as described by the manufacturer. The following protocol was used. Rehydratation was performed for 12h at room temperature and was followed by the IEF, step by step, from 0.5h 500V, 0.5h 1000V, 0.5h 5000 gradually, and for 1h at 5000V. Strips were kept at 50V until loaded on the second dimension. Before starting the second dimension, the strips were equilibrated for 10min in 6M urea, 30% glycerol, 50mM Tris, pH 6.8, and 2% DTT. Afterward, strips were briefly rinsed with double distilled water and equilibrated in 6M urea, 30% glycerol, 50mM Tris, pH 6.8, and 2.5% iodoacetamide for an additional 10min. The second dimension was carried out in 12% SDS-polyacrylammide gels by using the MiniProtean III electrophoretic apparatus (Bio-Rad). After electrophoresis gels were immunoblotted on nitrocellulose paper or exposed for autoradiography.

For autoradiography experiments, gels were fixed in 2-propanol:distilled water:acetic acid (25:65:10) solution for 30 minutes. The gels were incubated in Coomassie blue, a staining solution designed for the detection of proteins separated in polyacrylamide gels. Afterwards, the gels were incubated in Amplify solution (Ge Healthcare, UK) for 15min and dried with a gel dryer (BioRad, USA) for about two hours at 80°C. Finally, gels were exposed to X-ray film (X-Omat LS, Kodak, USA) at –80°C for 3-4 weeks, in autoradiographic boxes equipped with intensifying screens, and films were developed to obtain final fluorographs.

For western blotting, the proteins separated in SDS-PAGE were transferred to nitrocellulose paper. Ponceau red, a reversible staining solution designed for rapid (5 minutes) staining of protein bands on nitrocellulose membranes, was used after western blot to verify the protein transfer. The membranes were then incubated with primary antibodies directed against keratins K6 (diluted 1:1000), K16 (diluted 1:2000) and K17 (diluted 1:5000). Detection was performed using the enhanced chemiluminescence procedure developed by Amersham (ECL, Amersham, UK). In electrophoresis experiments, Wide Range (MW 6500-20 500) molecular weight markers (Sigma, USA) were used.

RESULTS

Autoradiography and immunocytochemistry

Thymidine-labeled nuclei in the epidermis of *T. vulgaris* were mainly present in sparse cells of the basal and sometimes also in the first suprabasal layers at 4 hours post-injection (Fig. 1A). Numerous silver grains were present over the nuclei of these cells (data not shown). At four days post-injection, sparse cells with labeled nuclei, with variable numbers of silver grains per cell, were still present in the basal layer and in suprabasal layers but not in the corneous layer (Fig. 1B). At six days post-injection, cells in suprabasal layers and some in the corneous layer were seen (Fig. 1C). In both species, the corneous layer appeared as a thin superficial coat of the epidermal surface (Figs 1C-D). This was confirmed by the electron microscopic analysis on the epidermis of *T. vulgaris*, which showed a very thin corneous layer above a stratified epithelium (Fig. 1E). Detailed observation of the pre-corneous (replacement) layer in the epidermis of both the newt *T. vulgaris* and toad *B. bufo* disclosed large amounts of mucous-like granules, many of which appeared to be releasing material into the extracellular space facing the corneous layer (Fig. 1F). The latter was denser than the inner epidermal layers and contained a thick meshwork of keratin filaments and a dense cornified cell membrane.

Autoradiographic analysis of the epidermis 4 and 8 hours after histidine injection in *T. vulgaris* and in *B. viridis* showed that silver grains were mainly localized over the cytoplasm of pre-corneous layers (Figs 2A-C). Grains were more frequently observed in the cytoplasm of these cells, often associated with denser areas among keratin filaments (Fig. 2D). Silver grains were also present in dense areas among packed keratin filaments in cells forming the corneous layer and in dense material associated with the plasma membrane (Fig. 2D).

The immunolabeling for cytokeratins K6 and K16 was weak in the epidermis of *T. vulgaris* using light microscopic immunocytochemistry, but immunoreactive sites were only detected in upper pre-corneous and corneous layers (Fig. 3A). Under the electron microscope, K6 and K16 antibodies applied to the epidermis of *T. vulgaris* showed a similar pattern of labeling. They showed a scarce or diffuse immunolabeling over tonofilaments of cells of the upper intermediate and pre-corneous keratinocytes. Most of the labeling was instead associated with mucous and dense granules, or with a dense material not limited by a membrane, that was present in localized areas of the cytoplasm of differentiating and pre-corneous keratinocytes (Figs 3B-C). Gold labeling was also more intense along the plasma membrane and the periphery of desmosomes in pre-corneous and corneous cells (Figs 3C-D), where dense material resembling that of mucous granules was present (Fig. 3E). No significant labeling was seen over tonofilament bundles of desmosomes or among the packed keratin filaments of the corneous layer.
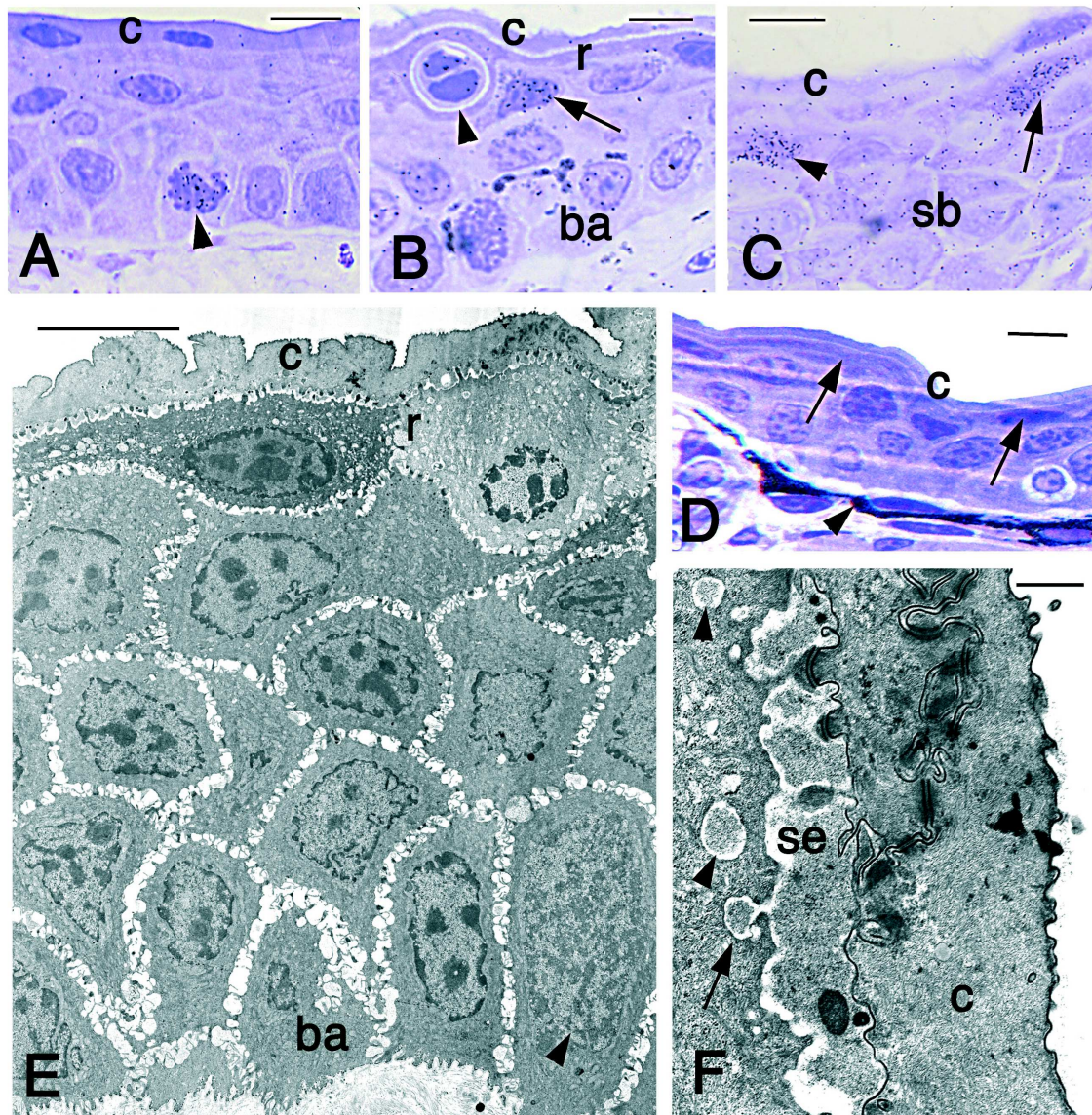
Fig. 1. – Light autoradiography for thymidine in the tail epidermis of *T. vulgaris* (**A-C**), for the digit epidermis of *B. viridis* (**D**) and ultrastructure of the tail epidermis of *T. vulgaris* (**E-F**). **A**, mitosis in still-labeled basal cell (arrowhead) at 4 days post-injection. Bar 10μm. **B**, labeled cell (arrow) in upper spinosus layer 4 days post-injection. The arrowhead points to a likely phagocyte. Bar 10μm. **C**, labeled cells in upper (arrow) and pre-corneous layer (arrowhead) 4 days post-injection. Bar 10μm. **D**, epidermis of the toad *B. viridis* with indicated the corneous layer (arrows). The arrowhead points to melanophores. Bar 10μm. **E**, general view of newt tail epidermis with polygonal basal cells (the arrowhead points to a mitotic cell) and forming precorneous (replacement) layer. Bar 10μm. **F**, detail on pale mucous granules (arrowheads) in pre-corneous layer. The arrow indicates a granule discharging into the extracellular space where mucous-like material is present. Bar 0.5μm. **Legends**: ba, basal layer; c, corneous layer; r, replacement (pre-corneous) layer; sb, supra-basal layers; se, secreted material
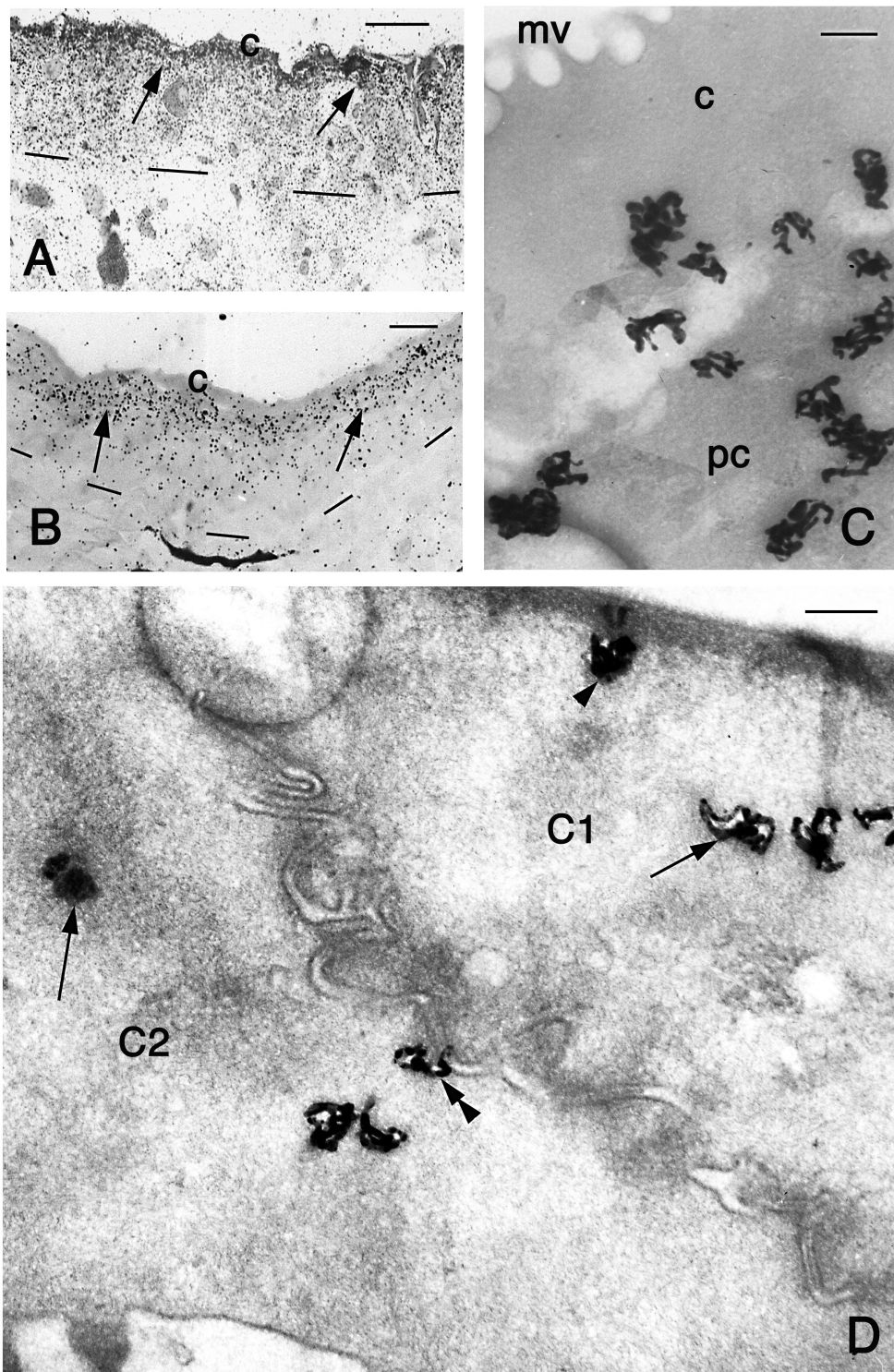
Fig. 2. – Light (**A-B**) and electron-microscopic (**C-D**) autoradiography of the epidermis 4 hours post-injection of tritiated histidine. **A**, most silver grains are localized toward the corneous layer (arrows) of the tail epidermis of *T. vulgaris*. Bar 10μm. **B**, silver grains mainly present over the pre-corneous layer of the ventral epidermis of the toad *B. viridis* (arrows). Bar 10μm. **C**, detail of trace (silver) grains over most of the pre-corneous layer of newt digit epidermis. Bar 200nm. **D**, detail of trace grains associated with denser areas (arrows), the surface (arrowhead), or near desmosomal junction (double arrowhead) in two differentiating corneous cells (C1 and C2) of digit epidermis in toad *B. viridis*. Bar 200nm. Dashes underlie the basal layer of the epidermis. **Legends**: c, corneous layer; pc, pre-corneous layer.
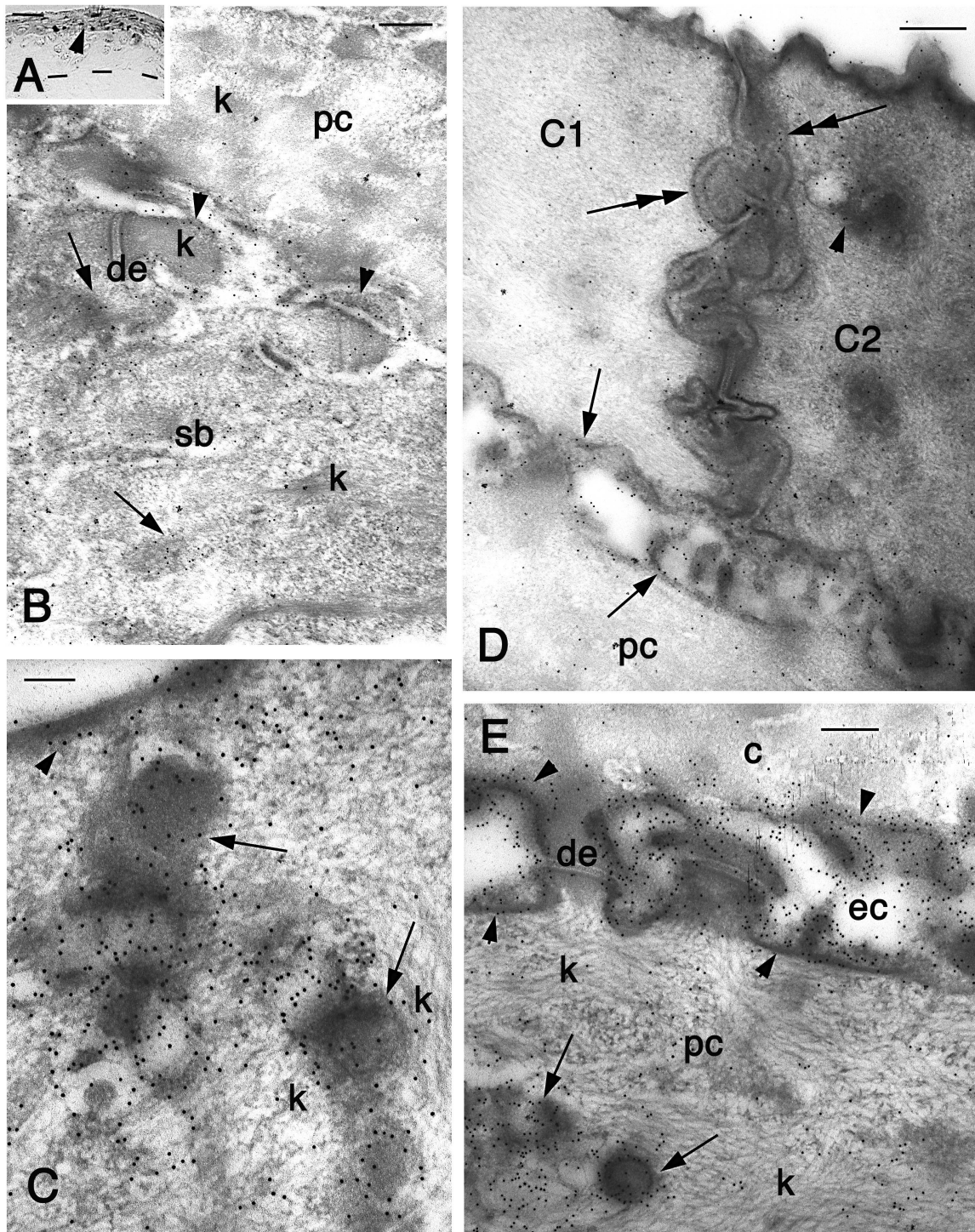
Fig. 3. – Immunolabeling with K16 of the epidermis of *T. vulgaris*. **A**, light microscopy shows a weak but positive reaction in upper layers of the digit epidermis (arrowhead). Dashes underlie the basal layer of the epidermis. Bar 20µm. **B**, diffuse gold labeling of upper spinosus cell of digit epidermis. More concentrated labeling is seen on denser areas (arrows) and along the plasma membrane (arrowheads). Keratin bundles are not or little labeled. Bar 250nm. **C**, detail of dense areas associated with granules (arrows) or with the plasma membrane (arrowhead) in pre-corneous cell of tail epidermis. Keratin filaments are not labeled. Bar 100nm. **D**, labeling along the cell surface of pre-corneous and corneous cells (arrows) of tail epidermis, along the junctions between two corneocytes (C1 and C2, double arrows), and in a dense material within the corneous material (arrowhead). Bar 200nm. **E**, detail on the intense labeling (arrowheads) present on the surface of a pre-corneous and a corneous cell of digit epidermis. The arrows indicate labeling on dense granules but not over keratin filaments. **Legends**: de, desmosome; ec, extracellular space; k, keratin bundles; pc, precorneous cell; sb, suprabasal cell.
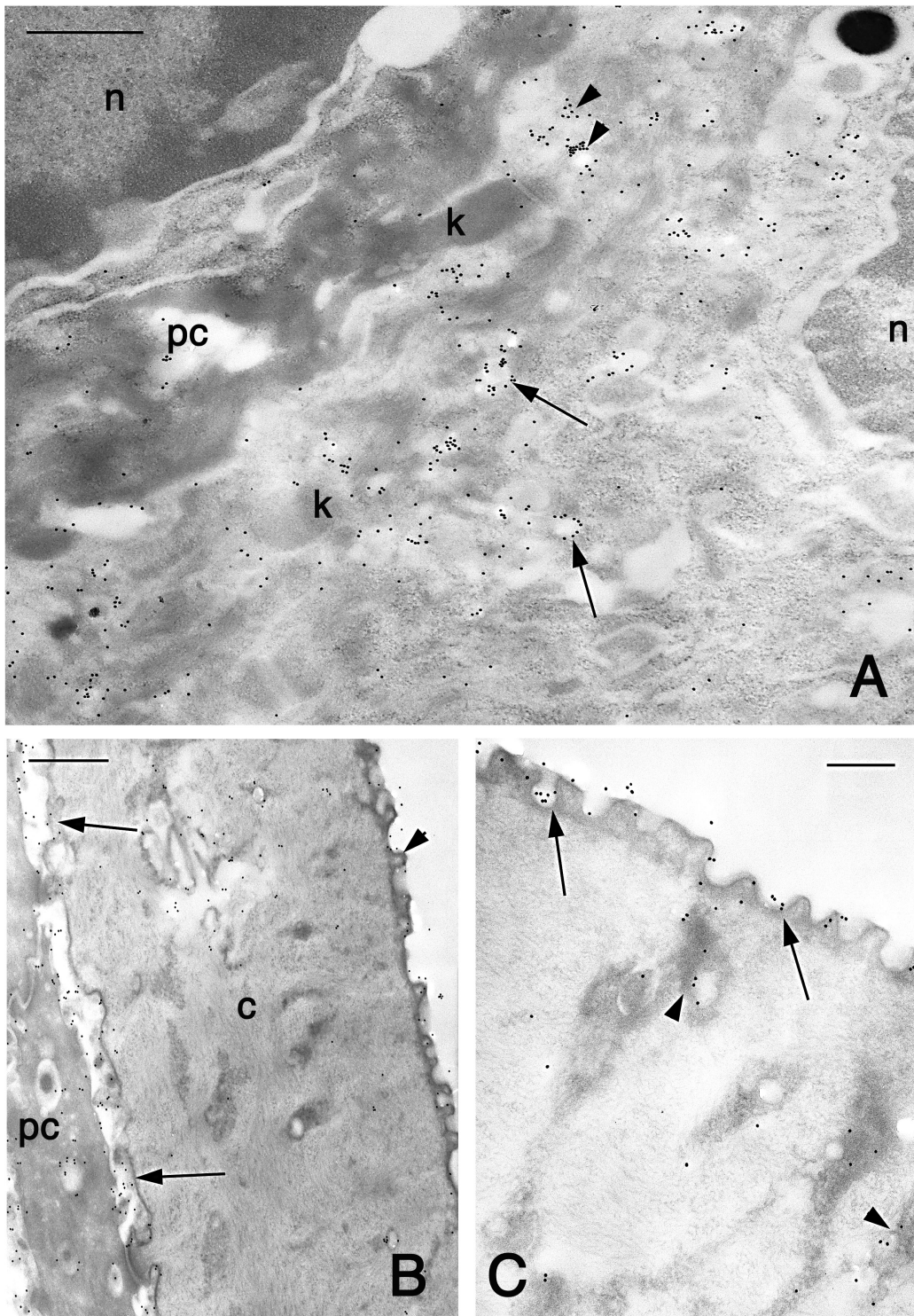
Fig. 4. – Ultrastructural immunolocalization of actin in the digit epidermis of the newt *T. vulgaris*. **A**, upper spinosus cell showing gold labeling mainly associated with pale mucous granules (arrows), some in phase of discharging their amorphous content into the extracellular space (arrowheads). Bar 0.5μm. **B**, immunolabeling mainly associated with the inner surface (arrows) and the outer surface with microvilli (arrowhead) of the corneous layer. Bar 250nm. **C**, detail of the labeling (arrows) on the microvillar surface of the stratum corneum. Other labeling is present over denser areas among the pale keratinized material (arrowheads). Bar 150nm. **Legends**: c, stratum corneum; k, keratin bundles; n, nucleus; pc, stratum precorneum.

The ultrastructural immunolabeling with the actin antibody in the epidermis of *T. vulgaris* showed most of the labeling in upper intermediate and pre-corneous cells, especially associated with pale vesicles or, less commonly, with denser areas, but no gold particles were associated with keratin bundles (Fig. 4A). Some of these vesicles appeared in a stage of discharging their material into the extracellular space. In pre-corneous cells, most gold particles were associated with the peripheral cytoplasm of the plasma membrane but not with desmosomes (Fig. 4B). In the corneous layer, gold particles were seen in more electron-dense areas along the inner and outer rim of cytoplasm, and the plasma membrane (Fig. 4C).

Electrophoresis, autoradiography and immunoblotting

The protein pattern of epidermal proteins (stained with Coomassie blue) showed that essentially most of the proteins were represented by alpha-keratins in both newt (*T. vulgaris*, Fig. 5A) and toad (*B. viridis*, Fig. 5B).

In the newt *T. vulgaris* one-dimensional electrophoresis showed most bands concentrated at 45-64kDa, and less intense bands at 33-35, and 18kDa (Fig. 5A1). In two-dimensional electrophoresis gels (Fig. 5A2), some protein

spots were seen at 48-50kDa with pI at 5.2-5.5, 6.2 and 7.0. Other spots at 55-57kDa showed pI at 5.2, 5.6-6.2, and 6.8. Finally, spots of 65kDa showed pI at 5.3-5.7, 5.9-6.2, 6.8-7, and 7.2. The band at 18kDa that was present in one-dimensional electrophoresis was not clearly seen in two-dimensional-gels. The one-dimensional autoradiographic examination showed main labeled bands at 42-45 and 55-60kDa, and a much weaker one around 30kDa (Fig. 5A3). The 2D-autoradiographic examination showed reactive spots around 45kDa with pI at 5, 6 and 6.8, and another, diffuse spot at 62-65kDa with pI at 5.0-5.5 (Fig. 5A4). Very small to undetectable spots were seen around 30kDa.

Similarly, in the toad *B. viridis*, most of the proteins were not well resolved in mono- and two-dimensional gels, and were concentrated in the alpha-keratin range, at 44-60kDa (Figs 5B1-2). Main spots were seen at 44kDa with pI at 5.0-5.5, at 50-52kDa with pI at 4.8-5.2 and 5.5, at 55kDa with pI around 6, at 60-64kDa with pI at 5-6.2, and 7.0-7.7. The autoradiographic analysis in one-dimensional gels showed main bands at 30 and 50-52kDa (Fig. 5B3). In two-dimensional gels only, we observed positive spots at 45-47kDa with pI at 5.0-5.6 and 6, and at 55-57kDa with pI at 6.2-6.5 and 7.0-7.2 (Fig. 5B4). A very weak and diffuse spot around 20kDa with pI 8 was seen.
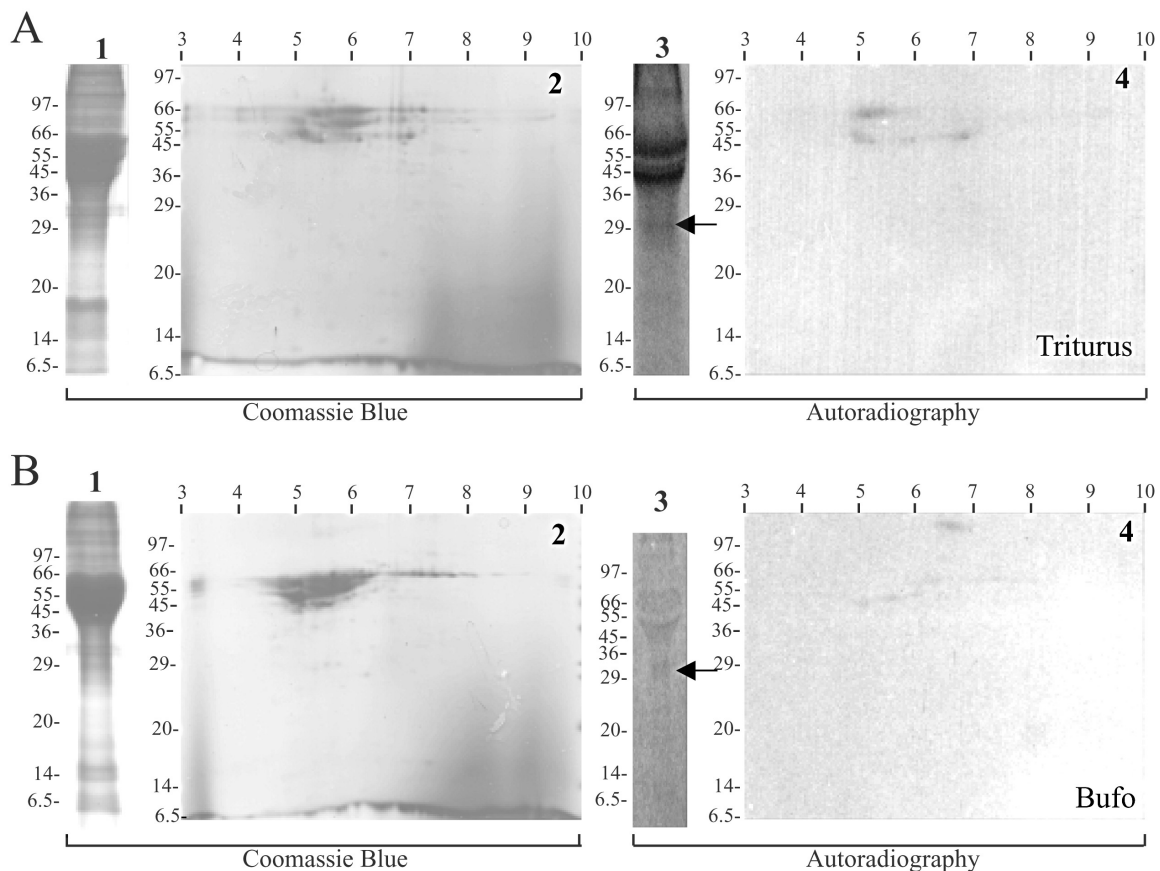
Fig. 5. – One-dimensional (A1, 3 and B1, 3) and two-dimensional (A2, 4 and B2, 4) electrophoretic patterns of epidermal proteins. Coomassie pattern (A1-2) and relative autoradiography (A3-4) in *T. vulgaris*. Coomassie blue (B1-2) and relative autoradiography (B3-4) in *B. viridis* (see text for details). The arrows indicate a weakly labeled band at 30kDa. Numbers in abscissa indicate pH, those in ordinate indicate molecular weight.
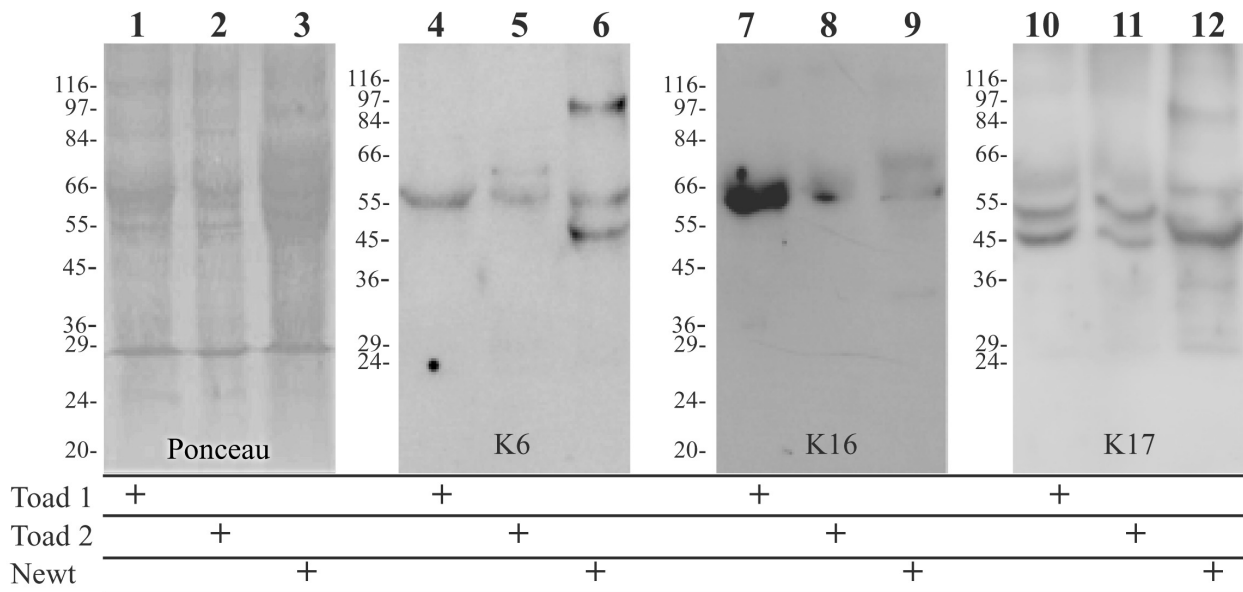
Fig. 6. – One-dimensional protein patterns stained by using Ponceau red (1-3) or K6 (4-6), K16 (7-9), and K17 (10-12) antibodies on *B. viridis* and *T. vulgaris* epidermal proteins (see text for further details).

The presence of protein bands that cross-react with K6, K16, and K17 antibodies was revealed by one-dimensional immunoblotting of epidermal proteins (Fig. 6). In samples from the epidermis of *B. viridis* (Fig. 6, lanes 1 & 2) K6 bands were seen at 55kDa (Fig. 6, lanes 4 & 5). K6 reactive bands appeared at 45, 55, and above 80kDa in the newt (Fig. 6, lane 6).

With the K16 antibody, positive bands were seen at 60-65kDa for the toad *B. viridis* (Fig. 6, lines 7 & 8), and weak bands were seen at 65-70kDa for the newt *T. vulgaris* (Fig. 6, lane 9). Finally, the K17 antibody showed bands at 45, 53 and a weaker band at 60kDa for the toad (Fig. 6, lanes 10 & 11), and at 45, 57 and a weak band above 80kDa for the newt (Fig. 6, lane 12).

DISCUSSION

Previous and the present studies show that in amphibian epidermis proliferation occurs in the basal and also suprabasal layers (LUCKENBILL, 1965; FOX, 1994; ALIBARDI, 2002). Therefore early differentiating cells of the intermediate layers can represent a population of expanding (transiently expanding) keratinocytes in amphibians. In normal conditions, with an active shedding (BUDZ, 1977), the time of migration of undifferentiated cells from the basal to the corneous layer occurs between 8 and 14 days. Main proteins synthesized from migrating keratinocytes are keratins and mucous with its specific glycoproteins.

Previous research on *Xenopus laevis*, a model amphibian, has indicated that cells of the upper stratum spinosus and pre-corneous layer synthesize numerous and specific proteins in preparation for cornification, including a type II, basic keratin of 63kDa (ELLISON et al., 1985; NISHIKAWA et al., 1992). That particular keratin appears as one of the main components of the pre-corneous and corneous layers of the post-metamorphosis epidermis of *X. laevis*. Other studies showed that the main keratins found in adult amphibian epidermis comprise acidic, type I keratins, of 45-55kDa and pI 5-5.5 (HOFFMANN et al., 1985). At least three spots of type II keratins of 64-66kDa were also found in high amounts in the adult epidermis of *X. laevis*. The latter possess a slightly basic pI at 7-7.4, and were characterized in their nucleotide and amino acid sequence showing extensive glycine-rich regions in the variable regions (HOFFMANN et al., 1985).

Proteins with similar values of MW and pI have been reported in the present study on the newt *T. vulgaris* and the toad *B. bufo*. The present study indicates that the main keratins produced in the epidermis of these amphibian species (as labeled with tritiated histidine) are acidic or neutral (pI at 5-7), especially in the newt, which is a more aquatic species than the toad. In the latter some more basic keratins of 62-66kDa and pI at 7.0-7.7 are present in the epidermis, but in much smaller amounts than the acidic keratins.

The silver labeling after histidine injection has indicated an association mainly with dense areas among keratin filaments in differentiating keratinocytes and in those of the stratum corneum (ALIBARDI, 2003; ALIBARDI et al., 2003). The study has also indicated that some of the synthesized proteins (mucins, glycoproteins, or inter-keratin proteins) are associated with dense material present on the surface of pre-corneous and corneous cells, and along the cell junctions. These sites are the same as where most of the immunoreactivity for keratins K6, K16 and for actin is found, suggesting that high amounts of these proteins are also actively synthesized during keratinocyte differentiation in amphibian epidermis. We could not observe any specific pattern in the localization of the above keratins. Therefore these keratins appear associated with a general process of extrusion of glycoproteins, but not with the specific secretion of different glycoconiu-

gates responsible for their different localization in amphibian epidermis (ZACCONE et al., 1987). The increased immunolabeling for actin in upper and pre-corneous keratinocytes resembles a similar pattern observed in superficial keratinocytes in fish where the microfilament (actin) cytoskeleton sustains the formation of the dynamic superficial microridges (WHITEAR, 1977).

The immunoultrastructural study has shown that K6- and K16-like proteins are associated with dense granules or matrix material produced amongst the usual network of keratin filaments. K6-K16-like proteins do not make long bundles as do the other cytokeratins. The latter are responsible for the formation of the typical bundles of keratin filaments (tonofilaments) in basal, intermediate and pre-corneous cells, but the specific keratins composing the long bundles are not known in the two species analyzed in the present study.

The immunoreactive bands for K6, K16 and K17 fall within the range of more abundant types of keratins reported for the epidermis of *X. laevis*, such as the 49, 53, 56 and 63-64kDa (HOFFMANN & FRANZ, 1984; ELLISON et al., 1985; HOFFMANN et al., 1985; NISHIKAWA et al., 1992). An explanation for this result is that the specific epitopes present in mammalian K6, K16, and K17, against which the antibodies were produced (in TAKAHASHI et al., 1994; McGOWAN & COULOMBE, 1998a;b), can be present in non-orthologous keratins of amphibians. However, the lack of any labeling in long bundles of filaments also suggests that the observed immunolabeling is specifically directed to keratins that are absent from tonofilaments but are localized in a more diffuse network connected to the dense material or mucous granules present in differentiating amphibian keratinocytes.

In mammalian keratinocytes, numerous alpha-keratins of type I (basic, K1-K8) and type II (acidic, K9-K19) are present (MOLL et al., 1982; O'GUIN et al., 1987; COULOMBE & OMARY, 2002). One type I and one type II keratin form a base pair that gives origin to single alpha-keratin filaments, and then to keratin bundles called tonofilaments. Among keratins, K6, K16 and K17 form a special group whose members do not form typical tonofilaments but remain separated or incorporated into small bundles, typical for wound keratinocytes (McGOWAN & COULOMBE, 1998a;b; FREEDBERG et al., 2001). This is also the case for reptilian wound keratinocytes that cover the amputated limb or tail stumps (ALIBARDI & TONI, 2005). These keratins probably have elastic properties, and are upregulated during wound healing of mammalian wounds where they mainly replace keratins of tonofilaments. The association with actin may therefore determine the formation of an elastic cytoskeletal network within amphibian keratinocytes.

In *T. vulgaris* keratinocytes, K6/K16-immunoreactive-like keratins surround secretory granules, especially those containing mucous, that are later secreted extracellularly among upper spinosus keratinocytes, and that participate in the formation of the coat membranes of pre-corneous and corneous cells. Therefore some of the keratins produced in newt epidermis are used for the extrusion of mucous and glycoproteins to coat the cell surface of pre-corneous or corneous cells. Among these glycoproteins that contain N-acetyl-glucosammine and galactose, a protein at 52 and others at 110-150kDa have been found in the adult epidermis (VILLALBA et al., 1992).

The presence of wound-like keratins (K6, K16 and K17) or of keratins containing characteristics epitopes for these keratins in normal epidermis of the newt *T. vulgaris* suggests that these or cross-reactive keratins are constitutive cytoskeletal proteins in amphibian keratinocytes. Therefore the production of these proteins does not require a long lag phase after wounding of the epidermis in amphibians, and their synthesis is probably quickly upregulated during epidermal regeneration. The activated keratinocytes are capable of covering the entire amputated surface of a limb in 16-18 hours, a process that is very rapid and efficient in amphibians with respect to other vertebrates. It is well known that amphibian skin produces a specific epidermis, the apical wound epithelium, necessary for the regeneration of the limb, which contains specific keratins (GERAUDIE & FERRETTI, 1998).

The mucous production, the ability to divide in suprabasal layers, and the synthesis of wound-type keratins that do not form long bundles, are characteristics of embryonic or poorly specialized keratinocytes. Besides, K6, K16 and most of all K17 keratins have elastic properties, and their association with actin may indicate that in the normal epidermis these proteins participate in the cytoskeletal mechanism of movement of organelles toward the plasma membrane for extrusion of their secretion. It is known that mucous contains anti-microbial substances, which help the innate protective immunity of the skin (FOX, 1994). Destruction of the dynamic keratin network from parasitism may therefore impair the resistance of the epidermis to infections. In fact, it appears that after infection of the epidermis by chytridiomycetes, keratinocytes lose their typical, diffuse keratin network, and prematurely form the dense corneous material of mature cells of the stratum corneum (BERGER et al., 1998; 2005). This premature cornification may limit the amount of mucous eliminated in the replacement and corneous layers, but further study is required on this point.

Within the limitation of our techniques, the present study suggests that non-keratin proteins or those in the range of 20-30kDa with basic pI are low to absent in amphibian epidermis. Only in *B. viridis*, the more terrestrial species, is a possible diffuse spot of protein present at 20kDa with pI around 8. This very low amount suggests that possibly, basic proteins in this range are very scarce in normal epidermis. It may be that specialized keratins and higher amounts of "keratin associated proteins" (KAPs) are present in tissues with a higher degree of cornification than the epidermis, such as the claws of the frog *Xenopus laevis* (MADDIN et al., 2007) or the beak of frog tadpoles (LUCKENBILL, 1965). The presence of KAPs in amphibian epidermis remains to be studied using more sensitive methods, but it is likely that amphibian KAPs may be present in regions where an intense cornification takes place, such as claws and the larval beak (FOX, 1994; WARBURG et al., 1994).

CONCLUSIONS

In conclusion, the present study indicates that mainly acidic-neutral keratins of 55 and 65kDa are synthesized in adult epidermis, among which are elastic types of keratins (K6,16,17-like wound keratins). The latter may work together with actin to permit the movement of mucous granules toward the cell surface and their secretion to coat the plasma membrane of maturing keratinocytes.

ACKNOWLEDGMENTS

REFERENCES

ALIBARDI L (2001). Keratinization in the epidermis of amphibians and the lungfish: comparison with amniote keratinization. Tissue & Cell, 33:439-449.

ALIBARDI L (2002). Immunocytochemical localization of keratins, associated proteins and uptake of histidine in the epidermis of fish and amphibians. Acta Histochemica, 104:297-310.

ALIBARDI L (2003). Ultrastructural localization of histidine-labelled interkeratin matrix during keratinization of amphibian epidermis. Acta Histochemica, 105:273-283.

ALIBARDI L & TONI M (2005). Wound keratins in the regenerating epidermis of lizard suggest that the wound reaction is similar in the tail and limb. Journal of Experimental Zoology, 303A:845-860.

ALIBARDI L, SPISNI E & TONI M (2003). Presence of putative histidine-rich proteins in the amphibian epidermis. Journal of Experimental Zoology, 297A:105-117.

BANI G (1966). Osservazioni sull'ultrastruttura della cute di Bufo bufo (L.) e modificazioni a livello dell'epidermide in relazione a differenti condizioni ambientali. Monitore Zoologico Italiano, 74:93-124.

BERGER L, SPEARE R, DASZAK P, GREEN D, CUNNINGHAM AA, GOGGIN CL, SLOCOMBE R, RAGAN MA, HYATT AD, MCDONALD KR, HINES HB, LIPS KR, MARANTELLI G & PARKES H (1998). Chytridiomycosis causes amphibian mortality associated with population declines in the rain forest of Australia and Central America. PNAS, 95:9031-9036.

BERGER L, HYATTN AD, SPEARE R & LONGCORE JE (2005). Life cycle stages of the amphibian chytrid Batrachochytrium dendrobatidis. Disease of Aquatic Organisms, 68:51-63.

BUDZ PE (1977). Aspects of moulting in anurans and its control. In: SPEARMAN RIC (ed), Comparative Biology of skin. Symp. Zool. Soc. London. Academic Press Inc: 317-334.

BUENO C, NAVAS P, AIJON J & LOPEZ-CAMPOS JL (1981). Glycoconjugates in the epidermis of Pleurodeles waltlii. Journal of Ultrastructural Research, 77:354-359.

CERESA-CASTELLANI L (1969). Osservazioni ultrastrutturali e istochimiche sulla pelle del Triturus cristatus Laur. Rendiconti Accademia Nazionale Lincei, 46:279-285.

COULOMBE PA & OMARY MB (2002). Hard and soft principles defining the structure, function and regulation of keratin intermediate filaments. Current Opinion in Cell Biology, 14:110-122.

ELLISON TR, MATHISEN PM & MILLER L (1985). Developmental changes in keratin patterns during epidermal maturation. Developmental Biology, 112:329-337.

FOX H (1994). The structure of the integument. In: HEATWOLE H (ed), Amphibian Biology, vol. 1 The integument. Surrey Beatty & Sons. Chipping, Northon NSW: 1-32.

FREEDBERG IM, TOMIC-CANIC M, KOMINE M & BLUMEMBERG M (2001). Keratins and keratinocyte activation cycle. Journal of Investigative Dermatology, 116:633-640.

GERAUDIE J & FERRETTI P (1998). Gene expression during amphibian limb regeneration. International Review of Cytology, 180:1-50.

HOFFMANN W & FRANZ JK (1984). Amino acid sequence of the carboxy-terminal part of an acidic type I cytokeratin of molecular weight 51 000 from Xenopus laevis epidermis as predicted from the cDNA sequence. EMBO Journal, 3(6):1301-6.

HOFFMANN W, FRANZ JK & FRANKE WW (1985). Amino acid sequence microheterogeneities of basic (Type II) cytokeratins of Xenopus laevis epidermis and evolutionary conservativity of helical and non-helical domains. Journal of Molecular Biology, 184:713-724.

KALININ AE, KAJAVA AV & STEINERT PM (2002). Epithelial barrier function: assembly and structural features of the cornified cell envelope. BioEssays, 24:789-800.

LAEMMLI UK (1970). Cleavage of structural proteins during the assemblage of the head of the bacteriophage T4. Nature, 227:680-685.

LAVKER RM (1972). Fine structure of newt epidermis. Tissue &. Cell, 4:663-675.

LAVKER RM (1974). Horny cell formation in the epidermis of Rana pipiens. Journal of Morphology, 142:365-378.

LILLYWHITE HB & MADERSON PFA (1982). The structure and permeability of integument. American Zoologist, 28:945-962.

LODI G & BANI G (1971). Microscopic, submicroscopic and histoenzymologic features of the epidermis of the normal and hypophysectomized crested newt. Bollettino di Zoologia, 38:111-125.

LUCKENBILL LM (1965). Morphogenesis of the horny jaws of Rana pipiens larvae. Developmental Biology, 11:26-49.

MADDIN H, MUSAT-MARCU S & REISZ RR (2007). Histological microsctructure of the claw of the african clawed frog, Xenopus laevis (Anura: Pipidae): implications for the evolution of claws in tetrapods. Journal of Experimental Zoology, 308B:1-10.

MCGOWAN KM & COULOMBE PA (1998a). Onset of keratin 17 expression coincides with definition of major epithelial lineages during skin development. Journal of Cell Biology, 143:469-486.

MCGOWAN KM & COULOMBE PA (1998b). The wound repair-associated keratins 6, 16, and 17. In: HERMAN & HARRIS (eds), Subcellular biochemistry, vol 31: Intermediate filaments. Plenum Press, New York: 173-204.

MENON GK & NORLEN L (2002). Stratum corneum ceramides and their role in skin barrier function. In: LEYDEN JJ & RAWLINGS AV (eds), Skin moisturization. Marcel Dekker Inc, New York-Basel: 31-60.

MOLL R, FRANKE WW, SCHILLER DL, GEIGER B & KREPLER R (1982). The catalogue of human cytokeratins: patterns of expression in normal epithelia, tumours and cultured cells. Cell, 31:11-24.

NAVAS P, VILLALBA JM, BURON MI & GARCIA-HERDUGO G (1987). Lectins as markers for plasma membrane differentiation of amphibian keratinocyets. Biology of the Cell, 60:225-234.

NISHIKAWA A, SHIMIZU-NISHIKAWA K & MILLER L (1992). Spatial, temporal, and hormonal regulation of epidermal keratin expression during development of the frog Xenopus laevis. Developmental Biology, 151:145-153.

O'GUIN MW, GALVIN S, SCHERMER A & SUN TT (1987). Pattern of keratin expression define distinct pathways of epithelial

development and differentiation. In: SAWYER RH (ed), Topics in Developmental Biology. 22. Acc. Press Inc, Orlando, FL, 97-125.

RESING KA & DALE BA (1991). Proteins of keratohyalin. In: GOLDSMITH LA (ed), Physiology, Biochemistry and molecular biology of the skin. 2nd edn, Oxford, University Press, New York: 148-167.

SCALA C, CENACCHI G, FERRARI C, PASQUINELLI G, PREDA P & MANARA G (1992). A new acrylic resin formulation: a useful tool for histological, ultrastructural, and immunocytochemical investigation. Journal of Histochemistry and Cytochemistry, 40:1799-1804.

SYBERT VP, DALE BA & HOLBROOK KA (1985). Icthyosis vulgaris: identification of a defect in synthesis of filaggrin correlated with an absence of keratohyaline granules. Journal of Investigative Dermatology, 84:191-194.

TAKAHASHI K, FOLMER J & COULOMBE PA (1994). Increased expression of keratin 16 causes anomalies in cytoarchitecture and keratinization in transgenic mouse skin. Journal of Cell Biology, 127(2):505-20.

TOLEDO RC & JARED C (1993). Cutaneous adaptations to water balance in amphibians. Comparative Biochemistry and Physiology, 105A:593-608.

VILLALBA JM, BURON MI, ROLDAN JM & NAVAS P (1992). Plasma membrane glycoproteins during anuran amphibian epidermal development. Protoplasma, 172:136-144.

WARBURG MR, LEWINSON D & ROSEMBERG M (1994). Ontogenesis of amphibian epidermis. In: HEATWOLE H, SURREY BEATTY & SONS (eds), Amphibian Biology, vol. 1. The integument. Chipping, Northon NSW: 33-63.

WHITEAR M (1977). A functional comparison between the epidermis of fish and of amphibians. In: SPEARMAN RIC (ed), Comparative biology of the skin, Academic Press, London: 291-313.

ZACCONE G, FASULO S, LO CASCIO P, LICATA A, AINIS L & AFFRONTE R (1987). Lectin-binding pattern on the surface epidermis of *Ambystoma tigrinum* larvae. Histochemistry, 87:431-438.

The Holocene occurrence of the European catfish (*Silurus glanis*) in Belgium: the archaeozoological evidence

Wim Van Neer[1] & Anton Ervynck[2]

[1] **Royal Belgian Institute of Natural Sciences, Vautierstraat 29, B-1000 Brussels, Belgium and Katholieke Universiteit Leuven, Laboratory of Animal Biodiversity and Systematics, Ch. Deberiotstraat 32, B-3000 Leuven, Belgium**
[2] **Flemish Heritage Institute, Phoenix-building, Koning Albert II-laan 19 box 5, B-1210 Brussels, Belgium**

Corresponding author : e-mail: wvanneer@naturalsciences.be

ABSTRACT. An overview is given of the skeletal remains of the European catfish *Silurus glanis* found thus far in Belgian archaeological sites. These finds demonstrate that the species is autochthonous and allow documenting its occurrence and disappearance during the Holocene in the Scheldt and Meuse basins. Possible causes for the local extinction of this catfish are discussed.

KEY WORDS : archaeozoology, extinction, overfishing, Meuse, Scheldt

INTRODUCTION

Well-dated skeletal remains of fish species found during archaeological excavations can help to reconstruct the composition of ancient fish faunas and thus allow establishing the distribution of certain species before the start of human disturbance, such as overfishing or habitat degradation. In this paper, the contribution of archaeozoological finds to the evaluation of the status of the European catfish *Silurus glanis* Linnaeus, 1758 in Belgian waters is documented. Because of its large size and the robustness of its skeleton, *Silurus glanis* is a relatively good prospect for representation in the archaeological and palaeontological record. Its remains have a fair chance of being preserved and can rather easily be retrieved during excavation, whereas smaller fish species have a tendency to be overlooked when no sediment sieving is practiced. The European fossil record of this catfish is poor with few pre-Holocene finds, which are usually only identified at genus level. Miocene records of *Silurus* exist for Ukraine (BELYAEVA, 1948) and Turkey (PIVETEAU, 1978) and Pliocene finds have been reported from Russia, near the Sea of Azov (BAIGUSHEVA, 1971) and from southern France (DEPÉRET, 1885). Middle Pleistocene records of *Silurus* exist for three different sites in Turkmenistan (DUBROVO & NIGAROV, 1990). Holocene finds of *Silurus glanis*, from archaeological sites, are more numerous and have been used in neighbouring countries to reconstruct the zoogeography of the species during the last 10,000 years. This is the case for the Netherlands (BRINKHUIZEN, 1979; HEINRICH, 1994; 2007), northern Germany and southern Scandinavia (HEINRICH, 1994; 2007). However, the available evidence for Belgium has thus far never been compiled. In what follows, all known finds of *Silurus glanis* from Belgian prehistoric and historic archaeological sites is presented and discussed from a palaeozoogeographical point of view.

In the older Belgian fishery literature (e.g., DE SELYS-LONGCHAMPS, 1842; LAMEERE, 1895 or MAES, 1898), the European catfish is not mentioned at all, whereas on one occasion (RAVERET-WATTEL, 1900) it is even stated explicitly that the species is unknown in Belgium. In more recent fishery surveys, the status of the species is considered to be doubtful or is not clearly evaluated (BRUYLANTS et al., 1989; VANDELANNOOTTE et al., 1998). Confusion also arises from more popular accounts. The 'silures' mentioned from the Demer river, a tributary of the Scheldt, in the Belgian fishery bulletin Pêche et Pisciculture (ANONYMOUS, 1926) was considered to be evidence for the occurrence of the species in that river (DE CHARLEROY & BEYENS, 1998). However, this record no doubt refers to the brown bullhead *Ameiurus nebulosus* (Lesueur, 1819) (VRIELYNCK et al., 2003), a north-American silurid that became acclimated to Belgian rivers and pools since 1901 (ROUSSEAU, 1915). The postglacial distribution of *Silurus glanis* includes Central and Eastern Europe, northern Anatolia and goes as far east as the Aral Sea and the Ural mountains (DE NIE, 1996). Towards the west, the natural distribution stops at the Elbe, but there are populations in the northern part of The Netherlands and in southern Sweden that are believed to represent relic populations (HEINRICH, 2007).

Recently, a number of specimens of the European catfish have been recorded from Belgian waters. A first *Silurus glanis* was captured in 1984 in the Meuse basin near Lanaye, but nowadays it is abundant in the entire river and it lives also in the Sambre river and some canals (PHILIPPART, 2007). The species has recently also been reported from the Scheldt and some of its tributaries (the Rupel, the Grote Nete and the Kleine Nete) (BREINE et al., 2007). All these recent records, however, should be considered to represent exotic specimens (cf. VRIELYNCK et al., 2003). Similarly, Dutch records since 1972 in the area of the IJsselmeer and in the Rhine and Waal basins are regarded as escaped or stocked specimens derived from breeding experiments with animals imported from the Donau (NIJSSEN & DE GROOT, 1987). The catfish's occurrence in the Dutch part of the Meuse basin since 1985 is explained in a similar way, and chronologically coincides well with the aforementioned observations made in the Belgian part of the Meuse. Records of *Silurus glanis* west of the Elbe, in the Weser and Ems basins, are also

believed to represent escaped or stocked fish (HEINRICH, 1994; 2007).

MATERIALS AND METHODS

The skeletal remains mentioned in the following survey were found during archaeological excavations and were dated through the characteristics of the context in which they were found, i.e. stratigraphical position and association with datable archaeological finds (lithics, ceramics, or coins, depending on the period). It was also always checked to ensure the finds did not represent residual or intrusive material (i.e. older or younger than the context in which they were found). Unless specified otherwise, the bones have been identified or re-analyzed by the first author. Identification was carried out by comparison with modern reference skeletons housed at the Royal Belgian Institute of National Sciences (RBINS,

Brussels). On well-preserved remains a reconstruction of body size was carried out through comparison with skeletal elements of modern fish of known length. The size reconstructions are given in centimetres standard length (SL: the distance from the snout of the animal to the base of its tail).

RESULTS

The various catfish finds known to date in Belgium are presented in a more or less chronological order, for sites located along the Meuse and the Scheldt basins separately. Because of the geographic proximity to the Belgian territory, finds from Maastricht are also included. The localities mentioned in the text are indicated on Fig. 1. A chronological, cultural and biostratigraphical framework for the archaeozoological evidence is summarised in Fig. 2.
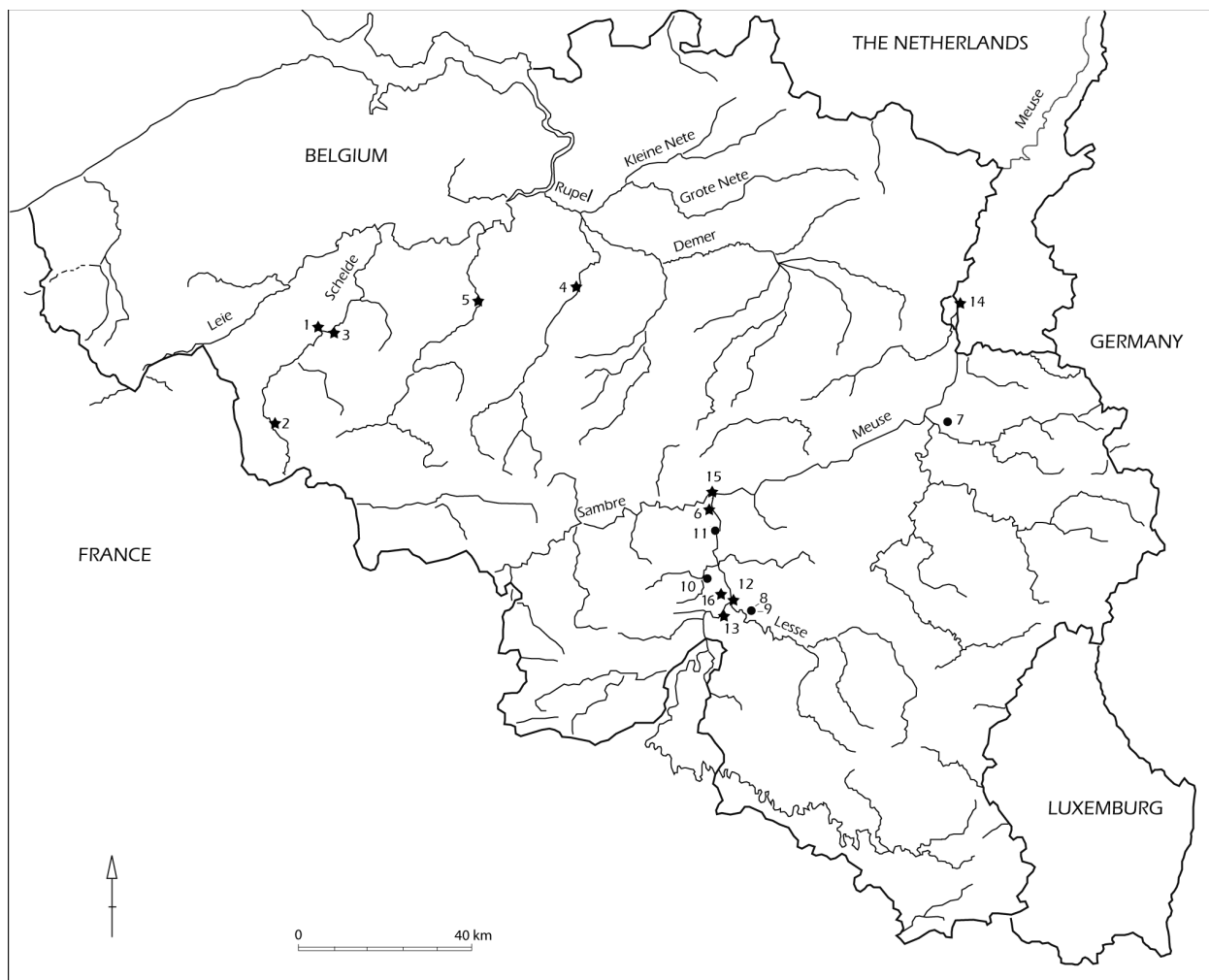
Fig. 1. – Map with the location of Belgian archaeological sites mentioned in the text. Those that yielded *Silurus glanis* are indicated with an asterisk. 1: Oudenaarde-Donk; 2: Tournai; 3: Ename; 4: Grimbergen; 5: Aalst; 6: Néviau; 7: Walou; 8: Trou de Chaleux; 9: Trou du Frontal; 10: Trou du Sureau; 11: Bois Laiterie; 12: Trou de Pont-à-Lesse; 13: Abri du Pape; 14: Maastricht; 15: Namur; 16: Montaigle.
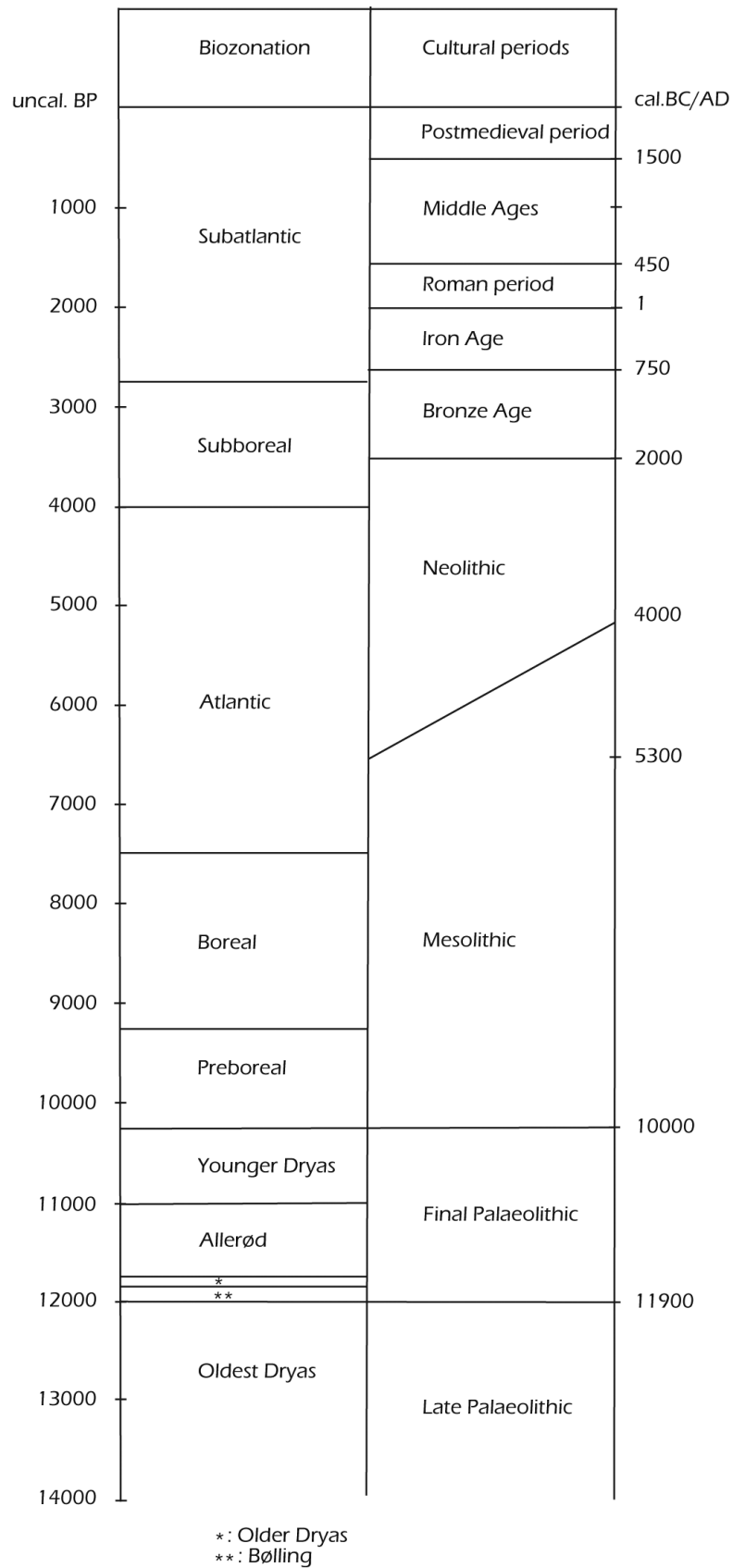
Fig. 2. – Schematic overview of the biozonation (after VERBRUGGEN et al., 1996) and succession of cultural periods (after SLECHTEN, 2004) for Belgium during the Holocene (Preboreal to Subatlantic) and Late Glacial Period.

Scheldt basin

Oudenaarde-Donk: 7 vertebrae and 6 pectoral spines of individuals between 150 and 200cm SL were found during rescue excavations of a waterlogged site near the Scheldt. Identifications were carried out by the first author in 1985 and were briefly mentioned in VAN DER PLAETSEN et al. (1986) and PARENT et al. (1987). The site yielded evidence for occupation by mesolithic hunter-gatherers and subsequently by neolithic people belonging to the Michelsberg culture. The catfish remains were found in unspecified Michelberg contexts that were radio-carbon dated between 5240 ± 70 BP (IRPA-743) and 4990 ± 70 BP (IRPA-667). These dates were calibrated to calendar ages using the Calib. Rev 5.0.1 program STUIVER & REIMER (1986-2005), in conjunction with STUIVER & REIMER (1993). The 2-σ ranges are 4261-3943cal BC for the oldest date and to 3945-3656cal BC for the youngest.

Tournai-Cloître: one pectoral spine of an individual measuring about 140cm SL was found in a destruction layer dated to the 9th (?)-10th centuries AD (BRULET et al. 2004: 158). Excavations carried out thus far in the town of Tournai dealt with sites ranging in time between the 2nd and the 13th century AD. Faunal remains, including fish, occur in many sites, but only one *Silurus glanis* bone was found thus far.

Ename-castrum: a context dating around 1000 AD yielded a single bone of catfish, i.e. a cleithrum of an individual that measured 140-150cm SL. There is no later evidence for the species in the extensive faunal collections that were excavated from other loci at Ename yielding bone dating between the 12th and the 17th century AD (ERVYNCK & VAN NEER, 1992; COOREMANS et al., 1993; ERVYNCK et al., 1994).

Grimbergen-Senecaberg: in a layer dated to the 12th century AD ten large fish bones were found that have been identified by D. Nolf as *Silurus glanis* (GAUTIER & RUBBERECHTS, 1978). The material was not available for re-analysis and an identification of the skeletal elements or a size reconstruction could therefore not be carried out.

Aalst-Oude Vismarkt: a preopercular of a fish measuring 130-140cm SL was found in a context dating to the first quarter of the 14th century AD. For the sake of completeness, it should be mentioned that the pottery, on which the dating was based, also includes a small quantity (3 sherds on a total of about 1000) of residual material dating to the end of the 12th-first half of the 13th century AD (DE GROOTE, 2007, pers. comm.).

Meuse basin

Néviau: a precaudal vertebra has been reported from this rock shelter on the left bank of the Meuse, 5km south of Namur (GILTAY, 1931). The photographs of the specimen in the publication allow us to confirm the identification and show that also the estimated total length of 1.50 meters is correct. The bone reportedly derives from a context that also comprised remains of *Equus* sp., *Cervus elaphus* and lithic material typical for an Upper Magdalenian (Late and Final Palaeolithic) occupation.

Trou de Pont-à-Lesse: the faunal remains from this site, excavated in 1866 by E. Dupont, are stored at the RBINS. The fish bones were recently analyzed for the first time, by the first author. Trou de Pont-à-Lesse yielded 8 skeletal remains of *Silurus glanis*, derived from layers dating to the Neolithic (DUPONT, 1905). The material includes a vomer, an ectopterygoid, a pectoral spine (Fig. 3), and a branchial fragment, all from fish measuring 150-170cm SL. Four additional bones that were poorly preserved, did not allow a size reconstruction: a vertebral centrum, a dentary, a soft fin ray and an unspecified skull roof fragment. No other fish bones are available from this site, probably because no sieving was practiced during excavation.

Abri du Pape: this cave site, located along the Meuse river at about 5km south of Dinant, yielded 10 vertebrae and a fragment of the Weberian apparatus, found in strata 20 and 21, layers with cultural material dating to the Early Mesolithic (VAN NEER, 1999). Three elements were of relatively small individuals (60-70cm SL) and one bone belonged to a fish of 100-120cm SL. Stratum 21 was radiocarbon dated to 8817 ± 85 (GX-19366) (STRAUSS, 1999) which corresponds to a calibrated age of 8225-7653 BC (2-σ range). Another AMS date shows that stratum 20 is about a millennium younger: 7843 ± 85 (GX-19365) or 7030-6928 (12.6%), 6924-6875 (6.6%) or 6864-6503 (80.8%) cal BC.

Maastricht, sites Pandhof, Mabro and Derlon: these three urban contexts yielded five *Silurus glanis* finds of which four are dated between the end of the 4th c. and the 5th c. AD (PIGIÈRE, 2008). The material from the site Pandhof includes a pectoral spine (undated) and a parasphenoid (400-450 AD), both from a fish measuring 90-

Fig. 3. – Left pectoral spine of *Silurus glanis* found in a Neolithic level of Trou de Pont-à-Lesse. The scale bar is 1cm.

100cm SL, as well as a precaudal vertebra, dated to 375-400 AD, of a catfish of 110-120cm SL. The site of Mabro yielded a precaudal vertebra of a fish measuring 130-140cm SL dating to 375-425 AD, and at the Derlon site a fragment of a caudal vertebra (425-475 AD) was found that did not allow size reconstruction.

Namur-Hospice Saint-Gilles: faunal remains from this site cover the Early Roman to post-medieval period, but only in a few Late Roman contexts (late 3rd to early 5th centuries AD) were bones of *Silurus glanis* found (DE CUPERE & VAN NEER, 1993). These include two dentaries of fish that measured 120-130cm SL and two pectoral spines of specimens that were 100-110 and 110-120cm SL long.

Montaigle: below the ruins of this late 13th-16th century castle site, a Late Roman level (AD 270 to 5th c.) was found corresponding to the occupation of a small military garrison (MIGNOT, 1994). The site is located at the confluence of the Molignée and Flavion rivers, about 25km south of Namur. The Roman context yielded a pectoral spine of a catfish that measured about 120cm SL.

Namur-Grognon: a series of cess-pits, dating between the 12th and 17th century AD, with abundant faunal remains, were excavated at this site (VAN NEER & LEN-TACKER, 1996). In a late 15th–early 16th century AD filling, a vertebral centrum was found of a catfish measuring about 120cm SL.

Two additional catfish finds from cave sites in the Meuse basin have been reported in the literature (CASIER, 1957), i.e. from Ramioul rock shelter (Province of Liège) and from Roger cave at Samson (Province of Namur). The Ramioul spine, which is depicted, was claimed to belong to a siluroid, but because of differences with a modern specimen, CASIER (1957: 346) believed that the find could represent a second, still unknown, species of catfish. In reality, this bone is a right half of the dorsal spine of a large cyprinid (see Fig. 4). The feathered appearance of the posterior part of the bone is typical of barbel, *Barbus barbus* (Linnaeus, 1758). The specimen from Roger cave has not been depicted but is said to differ from the Ramioul spine in the curvature of the processes. Taking into account the first erroneous identification, this find may also represent barbel.
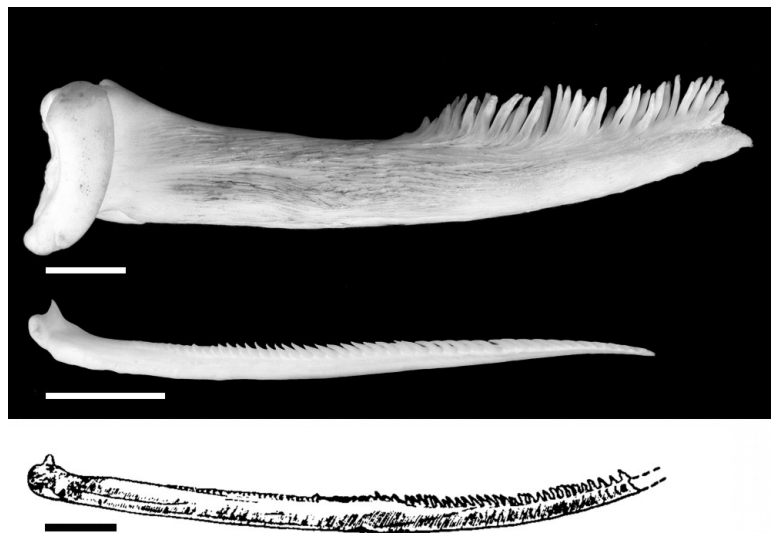
Fig. 4. – Spine depicted by CASIER (1957) compared to a modern *Silurus glanis* pectoral spine (top) and a *Barbus barbus* dorsal spine (middle). Scale bars are 1cm.

DISCUSSION

For the area considered, only 12 localities with specimens of *Silurus glanis* are known thus far, possibly indicating that the species was never very abundant in the Scheldt and Meuse basins. It is unlikely that this low incidence can only be linked to sampling methods used during excavation since the large bones of this species must be easily recovered, even when no sieving is practised. In Central and Eastern Europe, where *Silurus glanis* still occurs naturally today, the species may have been more abundant in the past than in our region. Archaeological sites in those parts of Europe indeed yield numerous hand-collected remains of catfish (SZÉKELYHIDY et al.,

1994). The paucity of finds in Belgium may reflect the fact that the region was a marginal part of the former distribution. Relic populations of the species may have had low population densities and may therefore have been very vulnerable (cf. BOESEMAN, 1975: 55).

The bone of *Silurus glanis* from Néviau (GILTAY, 1931) is the only Late Pleistocene record of this species reported for the Meuse. The species was not found along this river basin in a number of other Palaeolithic cave sites of which the ichthyofauna was recently investigated. This is the case for Walou cave (VAN NEER &. WOUTERS, 2007), where Middle and Upper Palaeolithic material was found, and for four Upper Palaeolithic cave sites, i.e. Trou de Chaleux, Trou du Frontal, Trou du Sureau (VAN NEER et al., 2007) and Upper Magdalenian Bois Laiterie (VAN

NEER, 1997). The specimen from Néviau was attributed to the Upper Magdalenian on the basis of associated lithic material. However, as will be argued below, in that region temperatures during most of the final phases of the Pleistocene must have been too low to allow survival of *Silurus glanis*, although significant climatic oscillations occurring at the end of the Magdalenian produced temperate periods during the so-called Bølling and Allerød interstadials (ENLOE, 2001). The fact that the layer in which the catfish bone was found also yielded remains of horse and red deer, points towards these interstadials. Especially the presence of red deer seems to confirm that climatic conditions must have been relatively mild during the period of deposition of the faunal material. However, given the fact that the recovery methods may not have been ideal in the early 20th century excavations, a younger date can perhaps not be totally excluded. It thus remains advisable to treat this record with great caution, especially since the Néviau find would not only be the only Late Pleistocene record thus far in Belgium, but also in the whole of north-western Europe (SCHLUMBERGER et al., 2001). It would certainly be worth investigating the homogeneity of the artefacts and the faunal material from Néviau, but the RBINS does not house any material from

the site and it is unclear if it is available for study elsewhere.

Old finds of *Silurus glanis* that are more secure from a stratigraphical point of view, are those from Abri du Pape, in the Meuse basin, dating to the Early Mesolithic. This cultural period corresponds to the late Preboreal and Boreal biostratigraphical phases (Fig. 2), when the climate had already become much milder than during the late Pleistocene (Fig. 5). The only other prehistoric site in the Meuse basin that yielded evidence for the species is Trou de Pont-à-Lesse, which is only very roughly dated to the Neolithic. The oldest finds from the Scheldt basin are also Neolithic, and here radiocarbon dates of charcoal from the archaeological layers indicate an age between 4260-3650cal BC. A direct dating of the *Silurus* bones would, at this stage, not be informative since the radiocarbon reservoir effect of the Scheldt and Meuse basin has not yet been established. This means that the bias on radiocarbon dates from biological material out of these aquatic habitats, resulting from the intake of carbon within a different biochemical cycle compared to terrestrial organisms, cannot be corrected, simply because the former basic abundance of radiocarbon is not known for these river basins.
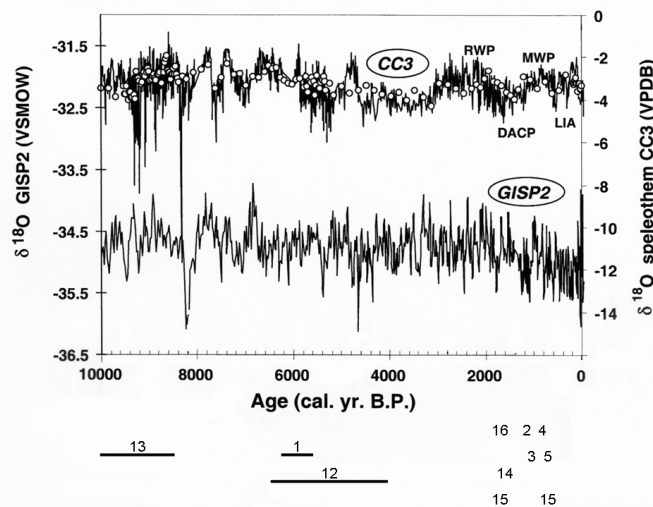
Fig. 5. – Fluctuations in the oxygen (^{18}O/^{16}O) isotope ratio during the Holocene reflecting climatic variations, based on a Greenland ice core drilling (GISP2) and a speleothem from south-western Ireland (CC3) (after MCDERMOTT et al., 2001). The peaks represent warmer periods, the troughs colder. Indicated are the Roman Warm Period (RWP), the Dark Ages Cold Period (DACP), the Medieval Warm Period (MWP), the Little Ice Age (LIA) and the chronological time span of the sites with catfish remains (number codes, see Fig. 1). The site of Néviau has been omitted from this graph because of its weak chronological context.

Following the prehistoric occurrence of *Silurus glanis*, there is a large hiatus until the first new appearance in the Scheldt basin in the High Medieval period (9th-10th c. AD), and in the Meuse basin in the Late Roman period (3rd-5th c. AD). However, this low prevalence could be an artefact of the archaeozoological record, which is very incomplete, in fact almost non-existent, for the Bronze Age and Iron Age in Belgium (ERVYNCK, 1994), and for the Roman and Early Medieval period in the Scheldt area.

The youngest evidence for *Silurus glanis* derives from the Late Medieval period in both basins. For the Meuse, the youngest find dates to the 15th century AD, but in the Scheldt basin the species is only attested with certainty until the 12th century. Possibly the record can be extended to the first quarter of the 14th century if the bone found at Aalst (Oude Vismarkt) proves to be contemporaneous with the majority of the pottery from the context in which it was found.

There are no finds of *Silurus* from the French or Dutch part of the Scheldt basin, but for the Dutch Meuse basin several records exist besides the finds from Maastricht already mentioned. The additional Dutch finds are all located in the estuarine region of the Meuse (for the older sites also partly the common delta area of the Meuse, Rhine and Scheldt) and consist of bones dating between the Neolithic and the Iron Age. Neolithic finds are known from the sites of Hekelingen (Prummel, 1987), Vrijenburg-Barendrecht (Zeiler & Brinkhuizen, 2005) and Albrandswaard-Portland (Brinkhuizen, 2006). Younger sites are the Middle Bronze Age locality Mijnheerenland-Hofweg (van Heeringen & Lauwerier, 1996) and the Early Iron Age site Westmaas-Maaszicht (van Heeringen et al., 1998). These Dutch finds are hence chronologically intermediate between the aforementioned Belgian records for the Meuse, which include both older (Mesolithic Abri du Pape, and possibly also Upper Magdalenian Néviau) and younger finds (Roman and Late Medieval Namur).

The archaeozoological data for the Meuse and Scheldt basin clearly demonstrate that *Silurus glanis* must be considered an autochthonous species. It lived in Belgium from at least Early Mesolithic times, since about 8200-7650cal BC, until the Late Medieval period. Post-medieval, archaeozoological records do not exist and the species is not mentioned in historic sources (chronicles, fishing regulations, feudal legislation, etc.). As already mentioned in the introduction, *Silurus glanis* is also not reported in early scientific (19th c.) fishery literature. Specimens captured in Belgian waters over the last decennia are considered to have escaped from experimental tanks or ponds. All this evidence implies that the species must have become extinct in the Scheldt and Meuse basins several centuries ago.

When trying to find possible explanations for the local disappearance of *Silurus glanis*, it is useful to consider its ecology. European catfish prefer deeper parts of large rivers and lakes, but at the onset of the spawning season they gain shallow, inshore areas. Depending on the region, the reproduction takes place between the end of April and the end of July and it seems that the start of the spawning season is related to the water temperature, which should be at least 18-20°C (Mohr, 1957) or even 20-22°C (Shikhshabekov, 1978). This dependence on a warm breeding season explains why the lower temperatures during the postmedieval Little Ice Age may have had an adverse effect on the survival of the species. Of course, the available climatic reconstructions must be regarded with caution since they are based on very different types of information. Especially the late medieval and the postmedieval data differ in quality. Nevertheless, for the Low Countries, it has been postulated (Buisman, 1998; 2000) that the Little Ice Age lasted from around AD 1430 until the middle of the 19th century. The average temperatures were about 1 to 2 degrees lower than today. Historical research based on chronicles, financial accounts and tree ring studies shows that summers certainly became cooler from about AD 1530 and that the last quarter of the 16th century was the coldest period of the last 1000 years. Such temperature shifts can perhaps have been enough to cause the final demise of the European catfish in our rivers.

Anthropogenic influences provide another explanation for the decline of *Siluris glanis*, as an alternative or in combination with climatic changes. Human interference such as the construction of sluices and other water works may have changed the hydrology of river basins and could have rendered access to suitable spawning grounds difficult. The European catfish may also have been sensitive to overfishing since it is a rather slow growing species with a relatively late maturation (Berg, 1964). In late medieval times, with growing urbanization and population numbers in general, there was indeed a high demand for fish, which caused heavy pressure on the freshwater ichthyofauna, and this resulted in an increased import of marine fish and the development of carpiculture (Ervynck et al., 2004). The facts that the catfish in contrast to, for instance, sturgeon is not mentioned in late medieval texts and that the archaeozoological finds are so rare, suggest that population densities were very low. The Scheldt and Meuse catfish may have been marginal populations that were therefore very vulnerable to anthropogenic and climatic pressure.

CONCLUSIONS

The Belgian archaeozoological record shows that the European catfish *Silurus glanis* once belonged to the autochthonous fauna of the Scheldt and Meuse basins. The species apparently colonised the region in the beginning of the Holocene when climatic conditions became milder, a phenomenon that can also be followed through the archaeofaunas of the Netherlands, northern Germany, Denmark and southern Sweden (Heinrich, 1994; 2007; Lepiksaar, 2001). In late medieval times, the catfish died out over much of its westernmost distribution area, around the 12th c. AD in The Netherlands (Brinkhuizen, 1979) and at the beginning of the postmedieval period in northern Germany (Heinrich, 1989). Relic populations persist today in southern Sweden, on the island of Sjælland in east Denmark, and in the north-western part of the Netherlands. These seem to be remnants of a wider post-Pleistocene distribution. Why the species survived in these areas remains to be investigated. The records of *Silurus glanis* from the 1970's onwards outside this distribution area do not reflect a natural expansion of the species. Instead, they correspond to specimens that were imported from Central Europe for breeding experiments and that escaped or were released intentionally.

ACKNOWLEDGEMENTS

REFERENCES

ANONYMOUS (1926). Chronique des Faits-divers. Pêche et Pisciculture, 37:173-178.

BAIGUSHEVA VS (1971). Fossil theriofauna of the Liventzovka sand-pit. Materialy po faunam Antropogena SSSR, 49:5-29.

BELYAEVA EI (1948). Catalogue of Tertiary fossil sites of the land mammals in the U.S.S.R. American Geological Institute, Alexandria.

BERG LS (1964). Freshwater fishes of the USSR and adjacent countries, volume 2, 4th edition. Israel Program for Scientific Translations Ltd, Jerusalem: 469-475. (Russian version published 1949).

BOESEMAN M (1975). De Nederlandse meerval, *Silurus glanis* Linnaeus. Zoölogische Bijdragen, 17:48-62.

BREINE J, SIMOENS I, STEVENS M & VAN THUYNE G (2007). Visbestandopnames op de Rupel en Durme (2007). INBO.R.2007.24 Instituut voor Natuur- en Bosonderzoek, Brussel.

BRINKHUIZEN DC (1979). On the finds of European catfish (*Siluris glanis* L.) in the Netherlands. In: KUBASIEWICZ M (ed), Archaeozoology I, Proceedings of the IIIrd International Archaeozoological Conference held 23-26th April 1978, Szczecin: 256-261.

BRINKHUIZEN DC (2006). Visresten van Albrandswaard-Koedood. Archeozoölogisch onderzoek van de laat-neolithische vindplaats. ArchaeoBone Rapport, 51. Leeuwarden.

BRULET R, COQUELET C, DEFGNÉE A, PIGIÈRE F & VERSLYPE L (2004). Les sites à «terres noires» à Tournai et l'étude des anciens cloîtres canoniaux. Etudes archéozoologique, palynologique et contextualisation. In: BRULET R & VERSLYPE L (eds), Terres noires. Actes de la table ronde de Louvain–la–Neuve. 09–10 novembre 2001, Département d'archéologie et d'Histoire de l'Art et Centre de Recherches d'Archéologie Nationale, Collection d'Archéologie Joseph Mertens XIV, Publications d'Histoire de l'Art et d'Archéologie de l'Université catholique de Louvain, Louvain: 152-172.

BRUYLANTS B, VANDELANNOOTE A & VERHEYEN RF (1989). De vissen van onze Vlaamse beken en rivieren. Hun ecologie, verspreiding en bescherming. WEL, Antwerpen.

BUISMAN J (1998). Weer, wind en water in de Lage Landen, volume III, 1450-1575. Uitgeverij Van Wijnen, Franeker.

BUISMAN J (2000). Weer, wind en water in de Lage Landen, volume III, 1575-1675. Uitgeverij Van Wijnen, Franeker.

CASIER E (1957). Sur la découverte d'épines pectorales de siluroïdes dans le Quaternaire de la Belgique. Société Royale Belge d'Etudes Géologiques et Archéologiques. Les Chercheurs de la Wallonnie, 16:343-347.

COOREMANS B, ERVYNCK A & VAN NEER W (1993). De voedselvoorziening in de Sint-Salvatorsabdij te Ename (stad Oudenaarde, prov. Oost-Vlaanderen) 2. De afvalput van de priorij (17de eeuw). Archeologie in Vlaanderen, 3:419-442.

DE CHARLEROY D & BEYENS J (1998). Het visbestand in het Demerbekken. Mededelingen 1998-2. Rapport Instituut voor Bosbouw en Wildbeheer IBW.Wb.V.R.96.043, Hoeilaart.

DE CUPERE B & VAN NEER W (1993). La faune du site de l'Hospice Saint-Gilles à Namur: résultats préliminaires. In: CORBIAU MH & PLUMIER J (eds), Actes de la Première Journée d'Archéologie Namuroise, Namur: 87-92.

DE NIE HW (1996). Atlas van de Nederlandse zoetwatervissen. Media Publishing, Doetinchem.

DEPÉRET C (1885). Description des vertébrés du pliocène d'eau douce du Roussillon. Masson, Paris.

DE SELYS-LONGCHAMPS E (1842). Classe IV, Poissons d'eau douce. Faune belge, 1. Indication méthodique des mammifères, oiseaux, reptiles et poissons observés jusqu'ici en Belgique. Dessain, Liège.

DUBROVO IA & NIGAROV AN (1990). Plio-Pleistocene fossil vertebrate localities of South-Western Turkmenia, U.S.S.R. Quatarpalaontologie, 8:35-45.

DUPONT E (1905) Notes sur Trou de Pont-à-Lesse. Manuscript deposited in the RBINS archives. Unpublished.

ENLOE JG (2001) Magdalenian Cultural Tradition. In: PEREGRINE PN & EMBER M (eds), Encyclopedia of Prehistory, Volume 4: Europe, Human Relations Area Files, Kluwer/Plenum Press, New York: 198-209.

ERVYNCK A (1994). L'archéozoologie de l'age du Fer: un bilan pour la Belgique. Lunula. Archaeologia protohistorica, 2:38-41.

ERVYNCK A & VAN NEER W (1992). De voedselvoorziening in de Sint-Salvatorsabdij te Ename (stad Oudenaarde, prov. Oost-Vlaanderen) I. Beenderen onder een keukenvloer (1450-1550 A.D.). Archeologie in Vlaanderen, 2:419-434.

ERVYNCK A, COOREMANS B & VAN NEER W (1994). De voedselvoorziening in de Sint-Salvatorsabdij te Ename (stad Oudenaarde, prov. Oost-Vlaanderen) 3. Een latrine bij de abtswoning (12de-begin 13de eeuw). Archeologie in Vlaanderen, 4:311-322.

ERVYNCK A, VAN NEER W & PIETERS M (2004). How the North was won (and lost again). Historical and archaeological data on the exploitation of the North Atlantic by the Flemish fishery. In: HOUSLEY RA & COLES GM (eds), Atlantic Connections and Adaptations: economies, environments and subsistence in lands bordering the North Atlantic, Symposia of the Association for Environmental Archaeology 21, Oxford: 230-239.

GAUTIER A & RUBBERECHTS V (1978). Animal remains of the Senecaberg fortification. Bulletin Musées royaux d'Art et d'Histoire, 48:51-84.

GILTAY L (1931). Note sur la présence, en Belgique, de *Silurus glanis* L., durant le Quaternaire. Bulletin de l'Institut Royal des Sciences Naturelles de Belgique, 7(21):1-7.

HEINRICH D (1989). Fischreste als archäozoologische Quellengattung – Probleme und Ergebnisse. Archäologische Informationen, 12 (2):172-179.

HEINRICH D (1994). Bemerkungen zur nordwestlichen Verbreitung des Welses, *Silurus glanis* L., unter Berücksichtigung subfossiler Knochenfunde. Zoologisches Jahrbuch für Systematik, 121:303-320.

HEINRICH D (2007). Some remarks on the postglacial immigration of catfish (*Silurus glanis*), pikeperch (*Stizostedion lucioperca*), asp (*Aspius aspius*) and other species into Scandinavia and northwestern Central Europe with special emphasis on Schleswig-Holstein, Germany. In: HÜSTER PLOGMANN H (ed), The role of fish in ancient time. Proceedings of the 13th Meeting of the ICAZ Fish Remains Working Group in October 4th-9th, Basel/Augst 2005. Verlag Marie Leidorf GmbH, Rahden/Westf.: 77-84.

LAMEERE A (1895). Manuel de la faune de Belgique. I Animaux non insectes. H. Lamertin, Bruxelles.

LEPIKSAAR J (2001). Die spät- und postglaziale Faunengeschichte des Süsswasserfische Schwedens. Übersicht der subfossilen Funde und Versuch einer faunengeschichtlichen Analyse der rezenten Artareale. Oetker-Voges Verlag, Kiel.

MAES L (1898). Notes sur la pêche fluviale et maritime en Belgique. Imprimerie scientifique Ch. Bulens, Bruxelles.

MCDERMOTT F, MATTEY DP & HAWKESWORTH C (2001). Centennial-scale Holocene climatic variability revealed by a high-resolution speleothem δ^{18}O record from SW Ireland. Science, 294:1328-1331.

MIGNOT PH (1994). Le Château de Montaigle. Fiche Patrimoine 94/12. Région wallonne, Service des Fouilles de la Direction Générale de l'Aménagement du Territoire, du Logement et du Patrimoine, Namur.

MOHR E (1957). Der Wels. Die Neue Brehm Bücherei, Wittenberg.

NIJSSEN H & DE GROOT SJ (1987). De vissen van Nederland. Natuurhistorische bibliotheek van de Koninklijke Nederlandse Natuurhistorische Vereniging, Utrecht.

PARENT JP, VAN DER PLAETSEN P & VANMOERKERKE J (1987). Prehistorische jagers en veetelers aan de Donk te Oudenaarde. VOBOV-info, 24-25:1-45.

PHILIPPART JC (2007). L'érosion de la biodiversité: les poissons. Rapport analytique 2006-2007 sur l'Etat de l'Environnement wallon. Ministère de la Région wallonne. Direction Générale des Ressources Naturelles et de l'Environnement, Namur.

PIGIÈRE F (2008). Approche archéozoologique de l'évolution socio-économique de l'Antiquité à la période mérovingienne sur les sites urbanisés de la zone limoneuse de la Moyenne Belgique et du sud des Pays-Bas. Doctoral thesis, UCL.

PIVETEAU J (1978). Un nouveau gisement de vertébrés dans le Chersonian Kurtchuk-Tchenkmedje Ouest (Thrace turque). Comptes Rendus Hebdomadaires des Séances de l'Academie des Sciences, Paris, Series D 287(5):455-458.

PRUMMEL W (1987). The faunal remains from the neolihtic site of Hekelingen III. Helinium, 27:190-258.

RAVERET-WATTEL C (1900). Atlas de poche des poissons d'eau douce de la France, de la Suisse Romande et de la Belgique avec leur description, moeurs et organisation; suivi d'un appendice sur les Crustacés, Mollusques, etc., les plus répandus dans les mêmes eaux. Bibliothèque de Poche du Naturaliste, 11. Paul Klincksieck, Paris.

ROUSSEAU E (1915). Les poissons d'eau douce indigènes et acclimatés de la Belgique. Station Biologique d'Overmeire, Imprimerie Scientifique Charles Bulens, Bruxelles.

SCHLUMBERGER O, SAGLIOCCO M. & PROTEAU JP (2001). Biogéographie du silure glane (*Silurus glanis*): causes hydrographiques, climatiques et anthropiques. Bulletin Français de la Pêche et de la Pisciculture, 357/360:533-547.

SHIKHSHABEKOV MM (1978). Sexual cycles of the catfish, *Silurus glanis*, the pike, *Esox lucius*, the perch, *Perca fluviatilis*, and the pikeperch, *Lucioperca lucioperca*. Journal of Ichthyology, 18:457-468.

SLECHTEN K (2004). Namen noemen. Het CAI-thesaurusproject. In: CAI-I. De opbouw van een archeologisch beleidsinstrument. IAP-Rapporten 14, CAI-I. Institute for the Archaeological Heritage of the Flemish Community, Brussels: 49-54.

STRAUSS LG (1999). Excavation of the basal Neolithic and Mesolithic levels at Abri du Pape (Freyr, Dinant, Namur province, Belgium), 1993-1994. In: LÉOTARD JM, STRAUS LG & OTTE M (eds), L'Abri du Pape. Bivouacs, enterrements et cachettes sur la Haute Meuse belge: du Mésolithique au Bas Empire Romain. Etudes et Recherches Archéologiques de l'Université de Liège (ERAUL) 88, Liège: 29-58.

STUIVER M & REIMER PJ (1986-2005). CALIB Radiocarbon Calibration Program (Internet address: www.calib.qub.ac.uk/calib).

STUIVER M & REIMER PJ (1993). Extended ^{14}C data base and revised CALIB 3.0 ^{14}C age calibration program. Radiocarbon, 35:215-230.

SZÉKELYHIDY I, TAKÁCS I & BARTOSIEWICZ L (1994). Ecological and diachronic variability in large-sized catfish (*Silurus glanis* L. 1758) and pike (*Esox lucius* L. 1758) in Hungary. Offa, 51:352-356.

VANDELANNOOTTE A, YSEBOODT R, BRUYLANTS B, VERHEYEN R, COECK J, BELPAIRE C, VAN THUYNE G, DENAYER B, BEYENS J, DE CHARLEROY D, MAES J & VANDENABEELE P (1998). Atlas van de Vlaamse Beek- en Riviervissen. WEL, Wijnegem.

VAN DER PLAETSEN P, VANMOERKERKE J & PARENT JP (1986). Mesolithische en neolithische sites aan de "Donk" te Oudenaarde. Archaeologia Belgica, 2 (1):15-18.

VAN HEERINGEN RM & LAUWERIER RCGM (1996). Bewoningssporen uit de Midden-Bronstijd en de Vroege IJzertijd in de Hoekse Waard, provincie Zuid-Holland. Westerheem, 45 (3):132-140.

VAN HEERINGEN RM, LAUWERIER RCGM & VAN DER VELDE HM (1998). Sporen uit de IJzertijd en de Romeinse tijd in de Hoeksche Waard; Een aanvullend archeologisch anderzoek te Westmaas-Maaszicht, gem. Binnenmaas, Rapportage Archeologische Monumentenzorg 56, Amersfoort.

VAN NEER W (1997). Fish remains from the Upper Magdalenian in the Grotte du Bois Laiterie. In: OTTE M & STRAUS LG (eds), La grotte du Bois Laiterie (Namur): La recolonisation magdalénienne de la Belgique. Etudes et Recherches Archéologiques de l'Université de Liège (ERAUL) 80, Liège: 205-213.

VAN NEER W (1999). Fish remains at Abri du Pape. In: LÉOTARD JM, STRAUS LG & OTTE M (eds), L'Abri du Pape. Bivouacs, enterrements et cachettes sur la Haute Meuse belge: du Mésolithique au Bas Empire Romain. Etudes et Recherches Archéologiques de l'Université de Liège (ERAUL) 88, Liège: 129-140.

VAN NEER W & LENTACKER A (1996). Restes fauniques provenant de trois fosses d'aisances du Grognon à Namur (XIIème, XVème-XVIème et XVIIème siècles). In: PLUMIER J & CORBIAU MH (eds), Actes de la Quatrième Journée d'Archéologie Namuroise, Namur: 89-104.

VAN NEER W & WOUTERS W (2007). Trooz/Forêt: La pêche attestée au Paléolithique moyen et supérieur dans la grotte Walou. Chronique de l'Archéologie Wallonne, 14:99-100.

VAN NEER W, WOUTERS W & GERMONPRÉ M (2007). Fish remains from three Upper Palaeolithic cave deposits in southern Belgium. Anthropologica et Praehistorica, 118:5-22.

VERBRUGGEN C, DENYS L & KIDEN P (1996). Belgium. In: BERGLUND BE, BIRKS HJB, RALSKA-JASIEWICZOWA M & WRIGHT HE (eds), Palaeoecological events during the last 15.000 years: regional syntheses of palaeoecological studies of lakes and mires in Europe. John Wiley & Sons Ltd, Chichester: 553-574.

VRIELYNCK S, BELPAIRE C, STABEL A, BREINE J & QUATAERT P (2003). De visbestanden in Vlaanderen anno 1840-1950. Een historische schets van de referentietoestand van onze waterlopen aan de hand van de visstand, ingevoerd in een databank en vergeleken met de actuele toestand. Rapport Instituut voor Bosbouw en Wildbeheer IBW.Wb.V.R. 2002.89, Hoeilaart.

ZEILER JT & BRINKHUIZEN DC (2005). Jachtwild, vis en vee uit Vrijenburg. Archeozoölogisch onderzoek van de Neolithische vindplaats 20-125 (Hazendonk-3) te Barendrecht – Vrijenburg. ArchaeoBone Rapport, 43. Leeuwarden.

SHORT NOTES

The killing technique of Eurasian lynx

Miha Krofel*, Tomaž Skrbinšek, Franc Kljun, Hubert Potočnik & Ivan Kos

Animal Ecology Research Group, Dept. for biology, University of Ljubljana, Večna pot 111, SI-1001 Ljubljana, Slovenia

*Corresponding author: M. Krofel, e-mail: miha.krofel@gmail.com

KEY WORDS : *Lynx lynx*, Felidae, killing behaviour, predation, Slovenia

Killing techniques differ among different groups of carnivores. Since felids are mostly solitary hunters, each bite must be made with precision, and must be positioned to kill the prey as soon as possible to avoid possible risks to the predator during the struggle (1). It has been previously reported that felids kill mainly by suffocation caused by a bite into the throat or muzzle, or by severing the spinal cord with a bite into the nape (2-5). Leyhausen (3) noted that the throat bites are more likely when killing larger prey.

Eurasian lynx (*Lynx lynx* Linnaeus, 1758) and the grey wolf (*Canis lupus* Linnaeus, 1758) are the main predators of ungulates in Europe. When attacking large prey, the lynx usually kills it with a neck bite, either from below, or from above into the nape (6; 7). So far the majority of authors have reported that when biting from below, the lynx suffocates its prey by biting its throat or windpipe (6-10). Suffocation by means of a bite on the larynx was also reported as a killing technique for the Iberian lynx (*Lynx pardinus* Temminck, 1827) when hunting ungulates (11).

In this paper we present preliminary results from an ongoing study on the ecology of the Eurasian lynx in the Dinaric Mountains in Slovenia. The lynx there hunt mainly roe deer (*Capreolus capreolus* Linnaeus, 1758), red deer (*Cervus elaphus* Linnaeus, 1758), fat dormouse (*Glis glis* Linnaeus, 1766) and to a lesser extent other rodents, chamois (*Rupicapra rupicapra* Linnaeus, 1758), red fox (*Vulpes vulpes* Linnaeus, 1758), and birds (KROFEL, unpublished data[1]). Two other species of large carnivore are also present in the study area; the brown bear (*Ursus arctos* Linnaeus, 1758) and the grey wolf.

We determined the method of killing through autopsy of lynx prey remains. We searched for wounds made by canines and claws inflicted premortem on the outer and inner side of the skin. We also inspected all deeper injuries and recorded their exact location using veterinary anatomical atlases (12; 13).

In 13 cases (ten roe deer, two red deer, and one chamois), the prey remains were found early enough for the bite marks to be studied. In all the cases lynx killed their prey with a bite in the neck region. In eight (62%) instances, the bite was from the ventral side of the neck only, in three (23%) cases only from the dorsal side, and in two (15%) cases bite marks could be distinguished on both sides of the neck.

In nine cases we performed a more detailed autopsy of the region with the bite marks. In five out of the six cases (83%) where the bite was delivered from the ventral side, we could find injuries in the region of the common carotid artery (a. carotis communis) and the truncus vagosympathicus (Fig. 1). In three out of these five cases the laryngeal cartilages and/or windpipe were damaged. In only one case the injuries inflicted by teeth were restricted to the windpipe.

Our observations indicate that, when biting from below, the bite into the throat causing suffocation might not always be crucial for the killing of a large prey by a lynx. The injuries observed in regions other than the throat could have been inflicted incidentally when the lynx missed the windpipe or larynx, but it is also possible that the lynx intentionally aimed for some other vulnerable points. The latter is not unlikely, as it is possible that the bites into the region of the common carotid artery and truncus vagosympathicus could accelerate death of the prey. It is known from forensic studies on humans that pressure on the carotid sinus (located at the origin of internal carotid artery near the end of lower jaw), which contains numerous baroreceptors, can result in bradycardia or in a total cardiac arrest and immediate death (14; 15). This mechanism of death is known as vagal inhibition, reflex cardiac arrest or carotid sinus reflex. Unfortunately, we could not find any data about this mechanism in other mammals, but we assume that it can also occur in other species, including lynx prey. If the lynx is indeed taking advantage of this reflex death in its killing technique, this would be beneficial for the predator, as it would shorten the struggle with the prey and in turn decrease the chances for injury. Such injuries may not be negligible, as was for example indicated by high mortality sustained by cougars during hunting (16).

---

[1] KROFEL, M. (2006). *Plenjenje in prehranjevanje evrazijskega risa (*Lynx lynx*) na območju Dinarskega krasa v Sloveniji, graduation thesis*. Dept. for Biology, University of Ljubljana, Ljubljana.

Fig. 1. – Female roe deer (*Capreolus capreolus*) killed by Eurasian lynx (*Lynx lynx*) in Dinaric Mountains, Slovenia. Arrows indicate the bite marks. (Photo: Miha Krofel)

Further research is needed to confirm the possible role of reflex death in lynx killings and to determine how often lynx really do kill their prey with a bite to the throat when gripping the underside of the victim's neck. This would also enable us to evaluate the general belief that lynx and other felids kill mainly using suffocation caused by a bite into the throat, and to resolve whether this might only be the consequence of inadequate inspection of prey remains in previous studies.

REFERENCES

1. BIKNEVICIUS AR & VAN VALKENBURGH B (1996). Design for killing: craniodental adaptations of predators. In: GITTLEMAN JL (ed), Carnivore behavior, ecology, and evolution, Volume 2, Cornell University Press, Ithaca and London: 393-428.

2. KRUUK H & TURNER M (1967). Comparative notes on predation by lion, leopard, cheetah and wild dog in the Serengeti area, East Africa. Mammalia, 31:1-27.

3. LEYHAUSEN P (1979). Cat behavior. Garland STPM Press, New York and London.

4. SCHALLER GB (1972). The Serengeti lion. The University of Chicago Press, Chicago and London.

5. LABISKY RF & BOULAY MC (1998). Behaviors of bobcats preying on white-tailed deer in the Everglades. American Midland Naturalist, 139:275-281.

6. KOS I, POTOČNIK H, SKRBINŠEK T, SKRBINŠEK MAJIĆ A, JONOZOVIČ M & KROFEL M (2005). Ris v Sloveniji, 2nd edition. Biotehniška fakulteta, Oddelek za biologijo, Ljubljana.

7. ČOP J (1988). Ris *Lynx lynx* Linnaeus, 1758. In: KRYŠTUFEK (ed), Zveri II: medvedi – Ursidae, psi – Canidae, mačke – Felidae, Lovska zveza Slovenije, Ljubljana: 233-292.

8. HUCHT-CIORGA I (1988). Studien zur Biologie des Luchses: Jagdverhalten, Beuteausnutzung, innerartliche Kommunikation und an den Spuren fassbare Körpermerkmale. Ferdinand Enke Verlag, Stuttgart.

9. HALLER H (1992). Zur Ökologie des Luchses *Lynx lynx* im Verlauf seiner Wiederansiedlung in den Walliser Alpen. Verlag Paul Parey, Hamburg and Berlin.

10. PEDERSEN VA, LINNELL JDC, ANDERSEN R, ANDRÉN H, LINDÉN M & SEGERSTRÖM P (1999). Winter lynx *Lynx lynx* predation on semi-domestic reindeer *Rangifer tarandus* in northern Sweden. Wildlife Biology, 5:203-211.

11. BELTRAN JF, SANJOSE C, DELIBES M & BRAZA F (1985). An analysis of the Iberian lynx predation upon fallow deer in the Coto Donana, SW Spain. XVIIth Congress of the International Union of Game Biologists, Brussels: 961-967.

12. HOFMANN R (1962). Zur Topographie der Eingeweide des Rehes (*Capreolus capreolus*). 1. Mitteilung: Die Topographie der Hals- und Burstorgane. Zeitschrift Jagdwissenschaft, 8/2:49-61.

13. POPESKO P (1980). Atlas topografske anatomije domaæih životinja. Prvi svezak: glava i vrat. Jugoslavenska medicinska naklada, Zagreb.

14. CAMPS FE & HUNT AC (1959). Pressure on the neck. Journal of Forensic Medicine, 6:116-135.

15. KNIGHT B (1996). Fatal Pressure on the Neck. In: KNIGHT B (ed), Forensic Pathology, 2nd edition, A Hodder Arnold Publication: 361-389.

16. ROSS PI, JALKOTZY MG & DAOUST P-Y (1995). Fatal trauma sustained by cougars, *Felis concolor*, while attacking prey in southern Alberta. Canadian Field-Naturalist, 109:261-263.

Diet composition of smooth-hound, *Mustelus mustelus* (Linnaeus, 1758), in Aegean Sea, Turkey

Halit Filiz

Mugla University, Faculty of Fisheries, Dept. of Hydrobiology, 48000, Kotekli, Mugla, Turkey

Corresponding author: sharkturk@yahoo.com

Elasmobranch fishes are among the top predators in the marine environment and thus play an important role in marine ecosystems, potentially regulating, through predation, the size and dynamics of their prey populations (1; 2). Since elasmobranchs are frequently apex predators in marine ecosystems, information on the composition of their diet is essential for understanding trophic relationships in these systems (1).

Sharks are often typified as opportunistic predators, with a wide trophic spectrum that ranges from plankton to marine mammals. In general, oceanic elasmobranch species feed on squid and big fishes (3), whereas the coastal and benthic species feed on crustaceans, molluscs and small or juvenile fishes (4; 5; 6). A few species feed on other elasmobranchs, birds, reptiles or marine mammals (7; 8; 9). Ontogenetic variation in diet is well known (10; 11), with a strong tendency to ingest larger and more mobile animals with increasing size. However, it is noteworthy that, while all sharks are higher-level predators they are not all true apex predators (12).

Demersal sharks occupy open habitats, including sandy, as well as more complex, closed habitats such as rocky areas and coral reefs (12). Those sharks living on or near the seafloor generally have ventral mouths containing relatively small teeth as is the case in *Mustelus mustelus*. Members of the *Mustelus* genus (Chondrichthyes, Triakidae) are common throughout the Mediterranean (except for the Black Sea) and the eastern Atlantic (13). The smooth-hound, *M. mustelus* (Linneaus, 1758), is a small, bottom-living shark, which occurs at depths between 3 and 150m (14). The species is common in the northeast Atlantic and in the Mediterranean (14; 15). Although there is no directed fishery for smooth-hound, it is captured as by-catch in the trawls in Sigacik Bay and landed.

Published information about feeding of this species is limited despite its abundance. Data on trophic ecology only mention that they feed mainly on crustaceans, but also cephalopods and bony fishes (15). SAUER & SMALE (16) provided some data on diet composition in the Atlantic, and MORTE et al. (17) quantified the diet in the Gulf of Valencia (Mediterranean). CONSTANTINI et al. (18) gave information about feeding habits in the northern Adriatic Sea (Mediterranean). However, similar studies from Turkey's coasts are scarce. The only information about feeding in this species comes from KABASAKAL (19) for the Aegean Sea. Yet, such information is necessary to understand the role that this species plays in the trophic structure of coastal marine communities in this area (20). To resolve this, this study presents data on the feeding activity of smooth-hound from the Aegean Sea.

All specimens were sampled by a commercial trawl (F/V Hapuloglu, 23m length and 550 HP), in Sigacik Bay (Fig. 1). *M. mustelus* specimens (forty males, 38.3–85.2cm TL and thirty-two females, 44.0–97.5cm TL) were sampled from 2006 autumn to 2007 autumn seasonally. A conventional bottom trawl net of 24mm cod-end mesh size was used and three hauls in the same day were carried out from dawn to dusk; haul durations ranged from 1 to 3h. The vessel speed was maintained at 2.2-2.5 knots. Depth range of the fishing ground was 100-213m. In total 12 hauls were carried out; all were made in nearly the same location (Fig. 1). The specimens were stored on ice until returned to the laboratory. Stomachs of the individuals were excised from the oesophageal region and individually preserved in 4% buffered formalin for 24 hours, stored in 70% ethanol in marked containers, and analyzed. Evidence of regurgitation was not observed in any of the fish. In order to designate condition of stomach content, a scale proposed by ALBERT (21) was applied (Table 1). The items were carefully separated, weighed (to the nearest 0.01g) and identified to group level. Diet composition was evaluated as described by SEVER et al. (22).
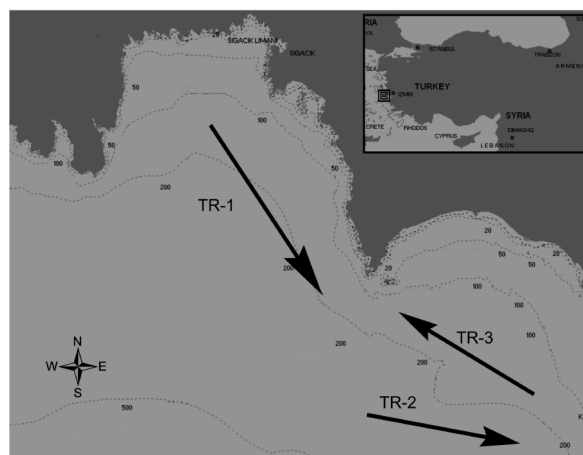
Fig. 1. – Map showing the location where sampling was carried out. Lines indicate true coordinates (TR: trawl).

TABLE 1

Definition of digestion status of prey

Status	Definition
I	Fresh; prey without signs of digestion.
II	Digestion just started; prey intact except for the more delicate parts
III	Moderately digested; prey clearly affected by digestion
IV	Severely digested; prey highly fragmented
V	Digestion almost complete; unidentifiable remains or indigestible parts only
VI	Digestion complete; stomach empty

In order to investigate the diet in the smooth-hound, I analysed the contents of seventy-two sharks. From these forty-three (59.7%) had food, twenty-nine (40.3%) were empty. According to the stomach content digestion scale (Table 1), the majority of the stomach contents (92.6%) was in category IV and higher, making it difficult to determine the prey items to low taxonomic levels. My data show that crustaceans and teleosts were the most important prey groups (MIP; IR≥137, and %IRI=75.29 and %IRI=21.98, respectively) in the diet. Cephalopods constituted the secondary prey group (SP; 137>IRI>15; %IRI=2.20), whereas polychaetes (%IRI=0.53) were an occasional prey group (OP; IR≤15) (Table 2). In order to determine whether any difference existed between seasons, stomach contents were examined for each season (Table 3). Generally, crustaceans and teleosts were found as important prey items in all seasons (Table 4).

TABLE 2

Percent number (%N), percent weight (%W), frequency of occurrence (%O), Index of Relative Importance (IRI) and percent Index of Relative Importance (%IRI) calculated for each prey item found in the stomachs of smooth-hound

Items	%N	%W	%O	IRI	%IRI
Polychaeta	4.12	0.79	2.56	12.58	0.53
Crustacea	76.47	31.77	16.67	1803.93	75.29
Cephalopoda	3.53	27.29	1.71	52.68	2.20
Teleostei	15.88	40.15	9.40	526.85	21.98
N	72				
% of empty stomachs	%40.3				

TABLE 3

Food items found for smooth-hound in Aegean Sea according to seasons.

Food Items	Spring		Summer		Autumn		Winter	
	IRI	%IRI	IRI	%IRI	IRI	%IRI	IRI	%IRI
Polychaeta	7.13	0.37	12.53	0.53	9.35	0.53	11.46	0.81
Crustacea	1324.77	68.27	1807.59	76.77	1392.93	79.13	1014.42	71.91
Cephalopoda	53.11	2.74	57.60	2.45	51.95	2.95	54.63	3.87
Teleostei	555.27	28.62	476.91	20.25	306.04	17.39	330.24	23.41
Total	1940.28	100.00	2354.63	100.00	1760.27	100.00	1410.75	100.00
N	22		14		18		18	
% of empty stomachs	38.89		42.86		38.89		38.89	

TABLE 4

Comparison of food prevalence of smooth-hound according to seasons

Food Items	Spring	Summer	Autumn	Winter
Polychaeta	OP	OP	OP	OP
Crustacea	MIP	MIP	MIP	MIP
Cephalopoda	SP	SP	SP	SP
Teleostei	MIP	MIP	MIP	MIP

The percentage of sharks with empty stomachs was 40.3%, which is somewhat higher than that found by CAPAPE (23), SAUER & SMALE (16), and SMALE & COMPAGNO (24) who reported 25.0, 13.3, and 8.7%, respectively. Both the percentage of empty stomachs and of the stomach contents in category IV (and higher categories) may be affected by long trawl hauls since the specimens were obtained from commercial trawl boats, and by the time interval that had elapsed between the field and the laboratory. In the lesser spotted dogfish, the time to evacuate food from the stomach varies according to the type of food and number of items consumed (25). For example, evacuation of 90% of the meal at 14ºC was completed in about 30h for one crustacean item with a thin exoskeleton, but evacuation took over 70h for two crustacean items with thicker, chitinous exoskeletons (25). The variety of prey items found in the diet of the smooth-hound implies that it may be a generalist. Smooth-hound prey on a wide range of items (polychaetes, crustaceans, cephalopods, fish); although crustaceans and fish are their main food groups (Table 2).

Some bottom-dwelling species, such as the *Mustelus* have teeth modified for crushing hard-shelled invertebrate prey such as crustaceans and molluscs (26). Since they have molariform teeth, the dominance of crustaceans in the diet of smooth-hound is expected and this finding agrees with previous studies. CAPAPE (23) found the diet of smooth-hound to consist of crustaceans (%O=59), fishes (%O=41), and cephalopods (%O=22). SMALE & COMPAGNO (24) noted that the diet was composed of crustaceans (%W=59.7), cephalopods (%W=27.4), fishes (%W=11.8), and invertebrates (%W=0.7). CORTES (1) recorded the diet as crustaceans (%IRI=54.7), cephalopods (%IRI=31.6), fishes (%IRI=13.1), and invertebrates (%IRI=0.6). In Sigacik Bay, commercial trawlers target deep-water shrimps such as *Parapaneus longirostris* (Lucas, 1846) and *Plesionika heterocarpus* (Costa, 1871). These and other crustaceans are caught in abundance, which may imply that smooth-hound may select these abundant and available food item.

In contrast, SAUER & SMALE (16) recorded that the diet consisted of cephalopods (%IRI=92.5), crustaceans (%IRI=6.5), and fishes (%IRI=0.1). KABASAKAL (19) found cephalopods in only 2 of 15 stomachs of smooth-hound but claimed that cephalopods are common prey items. However, it is an interesting finding that fishes are eaten by smooth-hounds as another main important prey item. Given that there is an intensive trawl fishery in the sampling area, this may suggest that the smooth-hound also feeds on wounded or dead animals in the fishing zone as an opportunist or scavenger.

In conclusion, this study indicates that the diet of smooth-hound is heterogenous and generalized. Crustaceans were consumed by most of the individuals, but teleosts represented a larger component of the total prey by mass. Cephalopods were less important numerically, but relatively more important gravimetrically. Polychaetes were relatively rare as prey. According to STERGIOU & KARPOUZI (27), fish that consume large decapods, cephalopods and fish (i.e. have a trophic level between 3.7 and 4.5) are considered as carnivores. With a trophic level of 3.8 (1), *M. mustelus* may also be considered as a carnivore.

ACKNOWLEDGEMENTS

REFERENCES

1. CORTES E (1999). Standardized diet composition and trophic levels of sharks. ICES Journal of Marine Science, 56:707-715.
2. WHETERBEE B & CORTÉS E (2004). Food consumption and feeding habits. In: CARRIER JF, MUSIK JA & HEITHAUS M (eds), Biology of sharks and their relatives, CRC press. USA.
3. SMALE MJ (1991). Occurrence and feeding of three shark species, *Carcharhinus brachyurus*, *C. obscurus* and *Sphyrna zygaena*, on the Eastern Cape coast of South Africa. South African Journal of Marine Science, 11:31-42.
4. CORTES E & GRUBER SH (1990). Diet, feeding habits, and estimates of daily ration of young lemon shark, *Negaprion brevirostris* (Poey). Copeia, 1:204-218.
5. CARRASÓN CM, STEFANESCU C & CARTES JE (1992). Diets and bathymetric distributions of two bathyal sharks of the Catalan deep sea (Western Mediterranean). Marine Ecology Progress Series, 82:21-30.
6. SIMPFENDORFER CA (1992). Diet of the Australian Sharpnose shark *Rhizoprionodon taylori*, from northern Queensland. Journal of Marine and Freshwater Research, 49:757-761.
7. WETHERBEE BM, LOWE CG & CROWE GL (1996). Biology of the Galapagos shark, *Carcharhinus galapagensis*, in Hawaii. Environmental Biology of Fishes, 45:299-310.
8. HEITHAUS MR (2001). The biology of tiger sharks, *Galeocerdo cuvier*, in Shark Bay, Western Australia: sex ratio, size distribution, diet, and seasonal changes in catch rates. Environmental Biology of Fishes, 61:25-36.
9. FILIZ H & TASKAVAK E (2005). Food of Lesser Spotted Dogfish, *Scyliorhinus canicula* (Linnaeus, 1758), in Foca (The Northeast Aegean Sea, Turkey) in Autumn 2002. In: BASUSTA N, KESKIN C, SERENA F & SERET B (eds), Workshop on Mediterranean Cartilaginous Fish with Emphasis on Southern and Eastern Mediterranean, Turkish Marine Research Foundation, 23:60-68, Istanbul, Turkey.
10. BRICKLE P, LAPTIKHOVSKY V, POMPERT J & BISHOP A (2003). Ontogenetic changes in the feeding habits and dietary overlap between three abundant rajoids species on the Falkland Island's shelf. Journal of the Marine Biological Association of the United Kingdom, 83:1119-1125.
11. BETHEA D, CARLSON JK, BUCKEL JA & SATTERWHITE M (2006). Ontogenetic and site-related trends in the diet of the atlantic sharpnose shark *Rhizoprionodon terraenovae* from the northeast gulf of Mexico. Bulletin of Marine Science, 78(2):287-307.
12. BENNETT M (2005). The role of sharks in the ecosystem (Internet address: http://affashop.gov.au-12995_roleshark_24feb05.pdf).
13. BRANSTETTER S (1986). Triakidae. In: WHITEHEAD PJP, BAUCHOT M-L, HUREAU J-C, NIELSEN J & TORTONESE E (eds), Fishes of the north-eastern Atlantic and Mediterranean, Vol. 1. UNESCO, Paris, pp. 117-121.
14. WHITEHEAD PJP, BAUCHOT ML, HUREAU JC, NIELSEN J & TORTONESE E (eds) (1984). Fishes of the North-eastern Atlantic and the Mediterranean. Unesco, Paris, 1, p. 510.
15. COMPAGNO LJV (1984). FAO species catalogue. Vol. 4. Sharks of the world. An annotated and illustrated catalogue of shark species known to date. Part 2 - Carcharhiniformes. FAO Fish. Synop., 125(4/2):251-655.
16. SAUER WHH & SMALE MJ (1991). Predation patterns on the inshore spawning grounds of the squid *Loligo vulgaris reynaudii* (Caphalopoda: Lologinidae) off the south-eastern Cape, South Africa. South African Journal of Marine Science, 11:513-523.
17. MORTE MS, REDON MJ & SANZ-BRAU A (1997). Feeding habits of juvenile *Mustelus mustelus* in the western Mediterranean. Cahiers de Biologie Marine, 38:103-107.
18. CONSTANTINI M, BERNARDINI M, CORDONE P, GIULIANNI PG & OREL G (2000). Observations on fishery, feeding habits and reproductive biology of *Mustelus mustelus* (Chondrichtyes, Triakidae) in northern Adriatic Sea. Biologia Marina Mediterranean, 7(1):427-432.
19. KABASAKAL H (2002). Cephalopods in the stomach contents of four Elasmobranch species from the northern Aegean Sea. Acta Adriatica, 43(1):17-24.
20. GELSLEICHTER J, MUSICK JA & NICHOLS S (1999). Food habits of the smooth dogfish, *Mustelus canis*, dusky shark, *Carcharhinus obscurus*, Atlantic sharpnose shark, *Rhizoprionodon terraenovae*, and the sand tiger, *Carcharias taurus*, from

the northwest Atlantic Ocean. Environmental Biology of Fishes, 54:205-217.

21. ALBERT OT (1995). Diel changes in food and feeding of small gadoids on a coastal bank. ICES Journal of Marine Science, 52:873-885.

22. SEVER TM, FILIZ H, BAYHAN B, TASKAVAK E & BILGE G (2008). Food habits of the hollowsnout grenadier, *Caelorinchus caelorhincus* (Risso, 1810), in the Aegean Sea, Turkey. Belgian Journal of Zoology, 138(1):81-84.

23. CAPAPE C (1975). Observations sur le régime alimentaire de 29 Selaciens pleurotêrmes des côtes tunisiennes. Archives de l'Institut Pasteur de Tunis, 52:395-414.

24. SMALE MJ & COMPAGNO LJV (1997). Life history and diet of two southern african smootnound sharks, *Mustelus mustelus* (Linnaeus, 1758) and *Mustelus palumbes* (Smith, 1957) (Pisces: Triakidae). South African Journal of Marine Science, 18:229-248.

25. MACPHERSON E, LLEONART J & SANCHEZ P (1989). Gastric emptying in *Scyliorhinus canicula* (L): a comparison of surface-dependent and non-surface dependent models. Journal of Fish Biology, 35:37-48.

26. STEVENS JD (ed). (1987). Sharks. Merehurst Press, London.

27. STERGIOU KI & KARPOUZI VS (2002). Feeding habits and trophic levels of Mediterranean fish. Reviews in Fish Biology and Fisheries, 11:217-254.